

NCD MOTOR TAIL DOMAIN INTERACTIONS WITH MICROTUBULES

by

Arzu Karabay

Dissertation submitted to the Faculty of the
Virginia Polytechnic Institute and State University
in partial fulfillment of the requirements for the degree of

Doctor of Philosophy

in

Biology

APPROVED:

Dr. Richard A. Walker, Chair

Dr. Brenda S. J. Winkel

Dr. Charles L. Rutherford

Dr. Asim Esen

Dr. Eric A. Wong

March 30th, 2000
Blacksburg, Virginia

NCD MOTOR TAIL DOMAIN INTERACTIONS WITH MICROTUBULES

by Arzu Karabay

(ABSTRACT)

Drosophila nonclaret disjunctional (Ncd) is a kinesin-like C-terminal motor protein that is involved in spindle assembly in oocytes during meiosis and in spindle maintenance in early embryos during mitosis. Ncd interacts with both “highway” and “cargo” microtubules (MTs) in meiotic and mitotic spindles through the action of ATP-dependent and ATP-independent MT binding sites in the head and tail domains, respectively. Through the action of these binding sites, Ncd bundles and, perhaps, slides MTs relative to each other. These functions are important for the *in vivo* role of Ncd in the formation of the bipolar spindle and maintenance of the spindle assembly.

Despite the high homology of the Ncd head domain to the kinesin head domain, the Ncd tail domain is unique among kinesin-like motor proteins. Characterization of ATP-independent interactions of Ncd with cargo MTs and identification of MT binding sites (located in amino acid residues 83-100 and 115-187) in the tail region by MT co-sedimentation assays revealed that the Ncd tail has functional similarities to microtubule-associated proteins, especially to tau and MAP2, that regulate MT assembly. Like tau MT binding motifs, MT binding sites of the tail domain are rich in basic amino acids that are flanked by proline residues. Cross-linking and MT co-sedimentation assays with subtilisin-digested MTs demonstrated that Ncd tail binding sites (located at the extreme C-terminus and in the H11-H12 loop / H12 helix of each tubulin monomer) on tubulin correspond to tau binding sites. Further, the Ncd tail domain, like tau, can promote and stabilize MT assembly under conditions that induce MT disassembly.

Taken together, these results suggest that the Ncd tail functions both in the transport of cargo MTs to spindle poles for the formation of the spindle assembly during meiosis, and in maintenance of spindle assembly during mitosis. How these different functions of Ncd are regulated still remains unknown, however further understanding of the regulation of Ncd function should contribute to our knowledge of cell cycle regulation in both meiotic and mitotic cells.

Acknowledgements

I would like to thank all the people who have helped to make this work possible, but some of these people deserve special mentioning.

First, I extend my special thanks to my advisor, Dr. Richard Walker for introducing me to the “ microtubule-world”. Thanks for everything, especially for encouraging me to be independent during my research and I will always value what you have taught me. I have spent about five years in your lab and I would happily do it again.

I thank to my committee members, Dr. Brenda S. J. Winkel, Dr. Charles Rutherford, Dr. Asim Esen and Dr. Eric A. Wong, for their support and encouragement. Their advice and comments were invaluable for my progress on my research.

I thank to Kalmia Phelps not only for being the best lab-mate with whom I had stimulating scientific discussions, but also for being my friend with endless enthusiasms, which made my life and being in the lab happier. I thank to Bill Zabaronick for patiently helping me when computers were not friendly to me.

I thank to Mr. Richard Alvarez and Mrs. Dale Alvarez for being a family and opening their home to me here. I was very fortunate to meet them.

My time away from home proved how true it was to be “ out of sight out of mind” , with only a few exceptions: My family and Cengiz, who only loved and thought of me more.

I am grateful to Cengiz for never ending support and believing in me. If you had kept the money you have spent for calling me, you would be a very rich person now ☺. I will always be indebted to you and you will always be at one of the few special places in my heart.

I am grateful to my dear brothers, Alper and Altug for constantly reminding me that I am the best sister any brother can ever have and for bragging about my achievements without having a clear idea (after all these years, still !) about I have been working on. By the way, you are almost ☺ the best brothers any sister can ever have.

My dearest father and mother ... I do not think words can ever be enough to express my gratitude to you. Without you this achievement could never be possible. Your love and unfailing understanding, support and belief in me made this possible. I love you very much and thanks for being my parents.

Table of Contents

	i
Title page	
Abstract	ii
Acknowledgements	iii
Table of Contents	iv
List of Figures	vi
List of Tables	vii

Chapter 1. Literature Review and Project Introduction

Literature Review	2
Project Introduction	16
Literature Cited	20

Chapter 2. Identification of Microtubule Binding Sites in the Ncd Tail Domain

Title Page	34
Abstract	35
Introduction	36
Materials and Methods	37
Results	41
Discussion	46
Literature Cited	73

Chapter 3. The Ncd Tail Domain Promotes Microtubule Assembly and Stability

Title Page	75
Abstract	76
Introduction	77
Materials and Methods	78
Results	80
Discussion	82
Literature Cited	93

Chapter 4. The Ncd Tail Domain Interacts with both α - and β -Tubulin

Title Page	94
Abstract	95

Introduction	96
Materials and Methods	98
Results	101
Discussion	104
Literature Cited	120
	122
Chapter 5. Conclusion	
	123
Curriculum vitae	

List of Figures

Chapter 1.

Figure 1. MT Structure	5
Figure 2. Structure of the conventional kinesin motor	12
Figure 3. Non-claret disjunctional (Ncd) spindle motor.	19

Chapter 2.

Figure 1. Schematic representation of TrxNT proteins.	52
Figure 2. Example purification of TrxNT proteins.	54
Figure 3. MT binding of Trx and TrxNT1-TrxNT4 proteins.	56
Figure 4. MT binding of TrxNT5-TrxNT12 proteins.	58
Figure 5. Interaction of tubulin with Trx-NT proteins in a blot overlay assay.	60
Figure 6. The effect of NaCl on TrxNT6 and TrxNT8 binding to MTs.	62
Figure 7. Competition of TrxNT proteins for binding to MTs.	64
Figure 8. MT binding affinity and stoichiometry of TrxNT6 protein.	66
Figure 9. MT binding of thrombin-cleaved NT6 and NT8 proteins.	68
Figure 10. MT bundling by selected TrxNT and NT proteins.	70

Chapter 3.

Figure 1. Effects of TrxNT6 and TrxNT8 on tubulin assembly as measured by a sedimentation assay.	84
Figure 2. Effects of TrxNT6 and TrxNT8 on tubulin assembly as measured by a turbidity assay.	86
Figure 3. TrxNT6-promoted MT assembly observed by VE-DIC microscopy.	88
Figure 4. EM images of TrxNT6 with tubulin and TMTs.	90
Figure 5. The effects of TrxNT6 and TrxNT8 on MT stability.	92

Chapter 4.

Figure 1. Amino acid sequences C-terminal domains of α - and β -tubulin.	109
Figure 2. Cross-linking of NT6 to α -MTs.	111
Figure 3. Western blot analysis of the α -MTs-NT6 cross-linked products.	113
Figure 4. Binding affinity and stoichiometry of NT6 protein to MTs and subtilisin-digested- MTs.	115
Figure 5. Western blot analysis of α - and/or β -tubulin C-terminal fragment-NT6	117

cross- linked products.

Figure 6. Western blot analysis of the subtilisin-digested-MTs and subtilisin-digested-MTs-NT6 cross-linked products.

119

List of Tables

Chapter 2.

Table 1. Physical Properties of Ncd Tail Proteins	71
Table 2. Summary of MT Binding and Bundling Assays	72

CHAPTER 1
LITERATURE REVIEW AND PROJECT INTRODUCTION

LITERATURE REVIEW

INTRODUCTION

The cytoskeleton of eukaryotic cells is a complex network providing an architectural framework with three major structural elements: microtubules, microfilaments and intermediate filaments. Cytoskeletal elements give cells strength and rigidity, hence enable them to assume and maintain their shape, but contrary to the meaning that the term “skeleton” conveys, the cytoskeleton of the cells is highly dynamic and changeable in nature. Cytoskeletal elements also control movements within the cells and provide anchoring points for other cellular structures.

MICROTUBULES

Among the structural elements of the cytoskeleton, the microtubules (MTs) are thought to be the fundamental organizers of a variety of cellular processes, such as generation of cell shape and polarity, cell growth, chromosome segregation during mitosis, intracellular organelle positioning and transport. Like the other structural elements, MTs are highly dynamic and labile, and these properties are crucial in MT-dependent cellular processes that require rapid reorganization of MTs. MTs are polymers of α - and β -tubulin heterodimers, and each tubulin monomer has approximately 450 amino acids and a molecular weight of about 50 kDa. Tubulin dimers self-assemble into long protofilaments and, because of the asymmetry of tubulin subunits, MTs have intrinsic polarity, such that α -tubulin is exposed at one end and β -tubulin is exposed at the opposite end. The two ends of MTs are distinguished by the differences in rate of assembly. *In vitro*, MTs self-nucleate and grow from both ends, while *in vivo*, MTs nucleate from the MT organizing center (MTOC). The end that remains attached to the MTOC is named the minus end, and the distal end to MTOC is named the plus end. The plus end grows 2-3 times faster than the minus end (Mitchison and Kirschner, 1984). It has been shown that the MT minus ends can be labeled with a phage-derived antibody specific to β -tubulin, indicating that the minus end is comprised of β -tubulin; hence the α -tubulin is the terminal subunit at the plus end (Fan et al., 1996) (Figure 1).

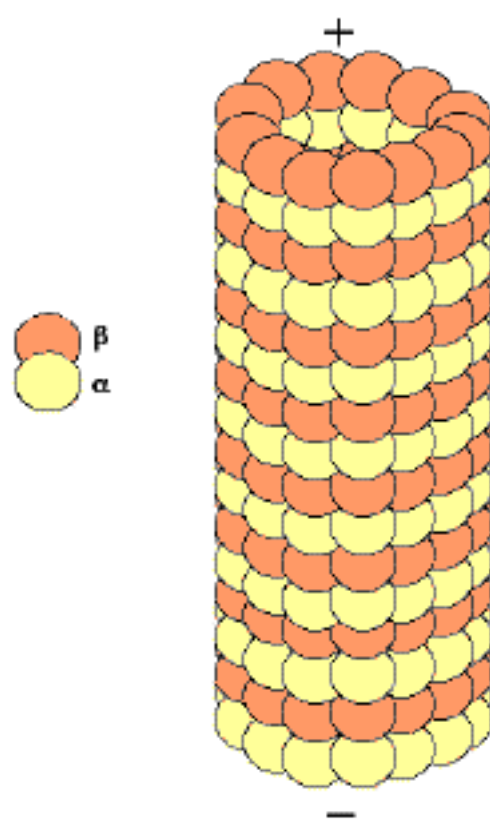
Dynamic instability is the major pathway of MT turnover in living cells (Cassimeris et al., 1988). This process, which can be defined as alternating phases of elongation and rapid shortening, is a function of GTP hydrolysis (Mitchison and Kirschner, 1984). During the elongation phase of dynamic instability, MTs increase in length before a catastrophe occurs. With the catastrophe, MTs switch to a rapid shortening phase until a rescue occurs and then convert back to an elongation phase (Walker et al., 1988, 1991; Tran et al., 1997).

While dynamic instability is an inherent property of tubulin, MTs assembled from pure tubulin *in vitro* are much less dynamic than MTs *in vivo*, indicating the presence of

other factors modulating dynamic instability in the cells. Indeed, many of the functions of MTs are carried out by associated proteins. Research has led to the identification and characterization of two classes of proteins that co-purify with MTs. One group of these proteins interacts with MTs in a nucleotide-independent manner and is co-purified with MTs through several cycles of polymerization and depolymerization. This group of proteins is involved in polymerization of tubulin and stabilization of MTs and named “microtubule-associated proteins” (MAPs) (reviewed in Desai and Mitchison, 1997). The second group of proteins interacts with MTs in a nucleotide-dependent manner and shares the ability to couple the energy from ATP hydrolysis to force generation and movement; hence these proteins are named “MT-dependent motor proteins” (reviewed in Hirokawa et al., 1998).

FIGURE 1: MT structure

MTs are polymers of α - and β -tubulin heterodimers and have intrinsic polarity such that β -tubulin is exposed at the minus end and α -tubulin is exposed at the plus end.



MICROTUBULE-ASSOCIATED PROTEINS (MAPs)

In vivo, MTs grow about five times faster than *in vitro* for an equivalent concentration of tubulin (Sammak and Borisy, 1988). This enhancement of growth rate *in vivo* is due to MAPs, which stabilize MTs by binding to the walls of MTs. The stimulation of MT growth can also be mimicked *in vitro* by addition of MAPs to pure tubulin (Pryer et al., 1992). The best-characterized MAPs, MAP1, MAP2 and tau, are particularly highly expressed in mammalian brain tissue, which is the most abundant source for MTs, and are distributed along the lengths of MTs in neurons. Recent research has led to the identification of several new non-neuronal MAPs, including E-MAP-115 in human HeLa cells, XMAP215, XMAP230, and XMAP310.

Neuronal MAPs and regulation of MT dynamic instability in non-dividing cells

MAP1 and MAP2 are high molecular weight MAPs, 277 and 200 kDa, respectively, whereas tau isoforms range from 50 to 68 kDa. MAP1a, the adult isoform of MAP1, is found in axons, dendrites and neuronal cell bodies, as well as in many glial cells (Huber and Matus, 1984; Bloom et al., 1984; Matus, 1988), while the embryonic isoform MAP1b is expressed only in growing axons (Garner et al., 1990; Mansfield et al., 1991; Avila et al., 1994). MAP2 is a heat-stable protein, and occurs as four primary isoforms, MAP2a, MAP2b, MAP2c and MAP2d (Chapin et al., 1995). MAP2c and MAP2d are the predominant isoforms in embryonic and postnatal brain, but disappear from most of the brain during adulthood when MAP2a and MAP2b become the major isoforms (Matus, 1988; Garner and Matus, 1988). All four isoforms of MAP2 are located in the cell bodies and dendrites, but are not present in axons (Matus 1988); only MAP2d is found in glial cells (Doll et al., 1993). Human tau occurs in six main isoforms ranging from 352 to 441 amino acid residues in size (Lee et al., 1988). The only isoform present in the fetal brain corresponds to the smallest isoform in the adult brain, which contains all six isoforms (Goedert et al., 1989). Like MAP2, tau is also a thermostable protein (Cleveland et al., 1977) and found mainly in the axons where it maintains the axonal transport (Binder et al., 1985).

The neuronal MAPs weakly increase the rate of MT polymerization and rescue frequency, but also strongly inhibit the catastrophe frequency and reduce the shortening rate (Pryer et al., 1992; Drechsel et al., 1992; Kowalski and Williams, 1993). This mechanism of regulation of dynamic instability in neurons by MAPs is different than that observed in proliferating cells. In neurons, MTs are resistant to MT depolymerizing drugs and are less dynamic; this increased stability is believed to be necessary for neuronal morphogenesis. MAP1, MAP2 and tau have been shown to promote tubulin assembly into MTs by stimulating rates of MT nucleation and elongation, and the MT binding property of neuronal MAPs is associated with the stabilization of MTs, a reduction in dynamic instability, and an

increase in MT rescue events (Pedrotti and Islam, 1994; Takemura et al., 1992; Itoh and Hotani, 1994; Gamblin et al., 1996).

Tau and MAP2 have homologous MT binding sites located at the C-terminus, containing a set of 3 (MAP2a-c and fetal tau isoform) or four (MAP2d, adult tau isoforms) imperfect repeats. Each repeat represents a MT binding site and is composed of 31-32 amino acids including several basic residues. In each MT binding site, an 18 amino acid imperfect repeat with a distinctive Pro-Gly/Lys-Gly-Gly motif is separated by a 13 or 14 amino acid inter-repeat region (Lewis et al., 1988; Joly et al., 1989; Ludin et al., 1996; Ennulat et al., 1989; Goode et al., 1997).

Although the mechanisms of binding of tau and MAP2 to MTs have been shown to involve an ionic interaction between the basic MT binding domain of these MAPs and the acidic C-terminus of tubulin (Chau et al., 1998; Paschal et al., 1989), MAP1a has a unique MT binding site that is acidic rather than basic (Cravchik et al., 1994). The acidic MT binding domain of MAP1a lies in the middle of the primary amino acid sequence, and unlike the other MAPs, has no identifiable sequence repeats. Based on experiments indicating that MAP1a and MAP2 do not compete for binding to MTs, MAP1a is believed to bind a region of tubulin distinct from the C-terminus (Pedrotti and Islam, 1994). The MT binding domain of MAP1b is associated with a region near the N-terminus consisting multiple copies of the motifs KKEE or KKE(I/V) (Noble et al., 1989). Although this MT binding domain of MAP1b is also basic, it bears no sequence relationship to MAP2 or tau.

Non-neuronal MAPs and regulation of MT dynamic instability in dividing cells

Knowledge about how MT dynamics are regulated *in vivo* has been greatly enhanced by studies of the neuronal MAPs, however these proteins are not found in dividing cells where MTs undergo dramatic rearrangements. Formation of the mitotic spindle in dividing cells requires depolymerization of the interphase MT network, followed by MT growth around chromosomes. This reorganization of MTs at the onset of mitosis involves drastic changes in MT dynamics. This would require modulators that would promote elongation and rescue frequency and also increase catastrophe frequency. Apparently, the characteristics of neuronal MAPs, which strongly inhibit catastrophe frequency and only weakly increase elongation, are not suitable for dividing cells. The *Xenopus* egg-extract system has been invaluable in the identification of non-neuronal MAPs with the functions that would be needed for dividing cells, and the best-characterized non-neuronal MAPs, XMAP215, XMAP230, and XMAP310 have been isolated from *Xenopus* eggs. Like neuronal tau and MAP2, XMAP230 is also thermostable, and with the exception of prophase it is localized to spindle MTs throughout the cell cycle (Faruki and Karsenti, 1994; Andersen et al., 1994). XMAP215 is found to localize to spindle MTs with the exception of astral MTs (Gard and Kirschner, 1987; Vasquez et al., 1994), and XMAP310 is localized to the nucleus during

interphase and to spindle MTs during mitosis (Andersen and Karsenti, 1997). XMAP230 is a MT polymerization stimulator and stabilizer; it increases MT growth rate, decreases shortening rate and eliminates catastrophes (Anderson et al., 1994). Unlike XMAP230, XMAP310 has no effect on the growth rate or catastrophe frequency of MTs; but instead acts as a MT stabilizer by increasing the rescue frequency (Andersen and Karsenti, 1997). In contrast to XMAP230 and XMAP310, XMAP215 does not affect catastrophe or rescue frequency, but dramatically increases MT elongation at the plus ends of MTs (Gard and Kirschner, 1987).

Another well characterized MAP is MAP4, which is a ubiquitous protein found from *Drosophila* to humans in both neuronal and non-neuronal cells (Bulinski and Borisy, 1980; Goldstein et al., 1986). MAP4 is thermostable and shares sequence homology in the basic domain with tau and MAP2 (Olmsted et al., 1989). MAP4 promotes MT polymerization by increasing the rescue frequency (Ookata et al, 1995).

MICROTUBULE-DEPENDENT MOTOR PROTEINS

Most of the cellular functions of MTs are carried out by MT-dependent motor proteins. In contributing to these cellular functions, MTs serve as roadways for these mechanochemical motors capable of using the energy of ATP hydrolysis to drive movements in the cells. There are two major motor protein families, the dynein family and the kinesin family. Members of these two families share certain structural and functional features. All motor proteins recognize the asymmetry of MTs and move along these tracks with a defined polarity. MTs provide a navigational system for motor proteins that move towards either the minus ends (minus end-directed motor proteins) or the plus ends (plus end-directed motor proteins) of MTs. Motor proteins are composed of three structural domains: head/motor, stalk and tail domains. The motor domain consists of 2-3 large globular heads and contains an ATP-binding site and a nucleotide-dependent MT binding site. The head domain is responsible for the mechanochemical function of the motor protein. The rod-like stalk domain forms an α -helical coiled-coil and is responsible for dimerization. The globular tail domain is involved in binding of the motor to the specific cargo, such as organelles, various vesicles or MTs. Tails that bind MTs as cargo contain a nucleotide-independent MT binding site.

Dynein Family

Dynein was first discovered in cilia (axonemal dynein) in the early 1960s (Gibbons, 1963) and later shown to be present in the cytoplasm (cytoplasmic dynein) of all eukaryotic cells (Porter and Johnson, 1989). Axonemal dynein is responsible for the beating movements of cilia and flagella in eukaryotes (Gibbons and Rowe, 1965) and cytoplasmic dynein is

involved in retrograde axonal transport, mitosis and organelle positioning (Paschal and Vallee, 1987; Echeverri et al., 1996; Vaisberg et al., 1993 and 1996; Heald, 1996).

All dyneins discovered so far are minus end-directed motor proteins. Dyneins are very large motor proteins and have a subunit composition of 2 or 3 heavy chains (470-530 kDa each), 2 or 3 intermediate chains (69-130 kDa) and 4-6 light chains (8-30 kDa). The heavy chains form the head and stalk domains of the dynein and are responsible for ATPase activity and force production. Intermediate chains form the tail domain of dynein and are involved in subcellular targeting (Paschal and Vallee, 1987). Light chains are thought to have roles in regulation of motility and tail domain interactions with cargo (Vale and Toyoshima, 1988).

Kinesin Family

Conventional kinesin, the founding member of the family, was first detected (Allen et al., 1982 and 1985) and identified (Brady, 1985; Vale et al., 1985a) in the axoplasm of the squid. Conventional kinesin moves towards the plus ends of MTs and is involved in organelle transport along MTs (Vale et al., 1985b). For five years after its discovery, kinesin was thought to be the only member of its class. However, the determination of the kinesin heavy chain sequence (KHC) (Yang et al., 1989) facilitated the identification of proteins related to kinesin, resulting in an explosion in the number of new kinesin-like proteins that are either plus end- or minus end-directed motors. The methodologies used for identification of these proteins have ranged from analysis of mutant phenotypes to the use of conserved kinesin motor domain degenerate primers for PCR screening and antipeptide antibodies directed against conserved regions of the kinesin motor domain. Currently, there are 215 sequences containing the kinesin motor domain present in the databases; of these, 166 entries contain a complete motor domain. Based on sequence similarities and/or functional roles, many of these proteins can be assigned to one of ten subfamilies: KHC, KRP85/95, Unc104, Kar3/Ncd, BimC, MKLP1, Chromokinesin/KIF4, MCAK/KIF2, KIP3 or Ce1 subfamily (Kinesins home-page: <http://www.blocks.fhcrc.org/kinesin/>). It should be noted that there are many kinesin-related motors that have been identified by sequence homology, but for which motor function has not been directly tested and confirmed.

Conventional kinesin: The N-terminal 340 amino acids of the conventional kinesin heavy chain constitute the catalytic core of the motor domain, which contains the ATP and MT binding sites (Huang and Hackney, 1994). This domain is highly conserved throughout the kinesin superfamily (Goodson et al., 1994). The adjacent 45-50 amino acids are termed the neck domain, which is thought to be important for kinesin mechanics. Following the neck domain is an extended coiled-coil domain, identified the stalk (Huang et al., 1994). The globular tail domain is involved in light chain and/or cargo binding interactions.

Conventional kinesin is a heterotetramer of approximately 360 kDa molecular weight. Two kinesin heavy chains (105-130 kDa, each) form a homodimer via the alpha helical coiled-coil stalk region, giving rise to an elongated molecule with two globular heads and a fan-shaped tail (Bloom and Wagner, 1988). Two highly conserved light chains (60-75 kDa, each) associate with the kinesin heavy chains at the tail region (Kuznetsov and Vaisberg, 1988; Gauger and Goldstein, 1993) (Figure 2).

Kinesin is a highly processive enzyme, able to take approximately 100 steps along a MT without detaching. This property makes kinesin a highly efficient organelle transport motor (Howard, 1989). The kinesin step size has been shown to be 8 nm (Svoboda et al., 1993), which corresponds to the length of an α -tubulin dimer. Kinetic experiments revealed a coordination of the ATPase cycles in the two heads of the kinesin dimer (Hackney, 1994; Ma and Taylor, 1997). Most models for kinesin movement are consistent with two head domains operating by a hand-over-hand mechanism. In this mechanism of movement, one head of the kinesin binds to a MT and undergoes a conformational change as a result of ATP hydrolysis. This conformational change brings the other head forward to its binding site on the MT, releasing the first head for binding to a new site.

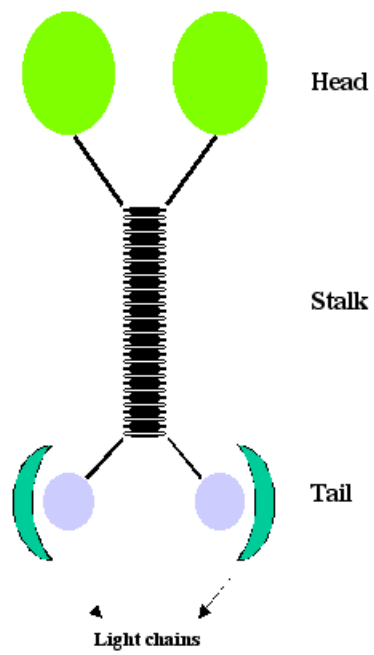
Kinesin is a MT-activated ATPase that generates movements on the MTs in a nucleotide-dependent manner. In the ATP-bound state kinesin binds to MTs very strongly with positive cooperativity between two heads; hydrolysis of ATP to ADP+Pi and then the release of the phosphate convert the binding to a weak state (Romberg and Vale, 1993; Hackney, 1994 and 1995; Gilbert and Webb, 1995; Hirose et al., 1995).

Kinesin has been extensively studied for its role in neuronal cells where it has been shown to be associated with various membrane vesicles (Hirokawa et al., 1991). In neurons, kinesin has been implicated as the anterograde axonal transporter (Brady et al., 1990; Amaratunga et al., 1993; Elluru et al., 1995; Hurd et al., 1996). In non-neuronal cells, kinesin has been localized to the Golgi complex and suggested to have a role in the Golgi to ER recycling of vesicles (Lipponcott-Schwartz et al., 1995; Marks et al., 1994; Johnson et al., 1996). Conventional kinesin has also been implicated in lysosomal movement, mitochondrial distribution, and delivery of secretion vesicles (Nakata and Hirokawa, 1995; Hollenbeck and Swanson, 1990; Jellali et al., 1994; Bi et al., 1997; Meng et al., 1997; Tanaka et al., 1998).

Regulation of kinesin activity is still not well understood. The kinesin heavy chain is targeted to different cargos by the activity of kinesin light chains, which are regulated by phosphorylation and dephosphorylation (Khodjakov et al., 1998). Control of kinesin motor activity by phosphorylation has also been reported (Lindesmith et al., 1997).

FIGURE 2: Structure of the conventional kinesin motor.

The conventional kinesin is a heterotetramer composed of two dimerized heavy chains and two light chains. The heavy chains have three structural domains: head, stalk and tail. The light chains are associated with the heavy chains at the tail region.



Kinesin-like proteins: The number of identified kinesin-like proteins has expanded enormously in recent years. The membership card for belonging to the kinesin superfamily is amino acid identity within the motor domain. Each kinesin-like protein shares a putative motor domain of approximately 340 amino acids, which is usually 35-45% identical among all kinesin superfamily members. Based on the location of the motor domain, kinesin-like proteins can be divided into three major groups: N-terminal, C-terminal and internal. There are two subclasses of C-terminal motors and seven subclasses of N-terminal motors. Many kinesin-like proteins, however, do not belong to any identified class of motors at present and are termed “orphans”.

N-terminal kinesin-like proteins:

I. The BimC subfamily: N-terminal-bipolar kinesin-like proteins

The BimC subfamily of proteins are plus-end directed motors that move ten-fold slower than the conventional kinesin (Sawin et al., 1992; Cole et al., 1994). Immunolocalization experiments showed that these proteins are located on the spindle MTs near the centrosomes (Enos and Morris, 1990; Hagan and Yanagida, 1992). Biochemical and genetic analysis have indicated that these proteins are needed for the separation of centrosomes during early prophase and for the maintenance of the metaphase spindle at the later stages of mitosis and meiosis (Samejima et al., 1993; Blangy et al., 1995). BimC, one of the first kinesin-like proteins identified, was isolated from *Aspergillus nidulans*. *Homo sapiens* Eg5, *Xenopus laevis* Eg5 and *Drosophila melanogaster* Klp61F are the other well-characterized members of this subfamily.

II. The Chromokinesin/KIF4 subfamily: N-terminal chromokinesins

The chromokinesin subfamily includes recently discovered kinesin-like proteins that are associated with chromosome arms during mitosis (Wang and Adler, 1995; Vernos and Karsenti, 1995). This group of motors contains what is termed the chromokinesin functional domain composed of a nuclear localization signal in the stalk, a zinc-finger like domain and a cdc2 site in the tail (Wang and Adler, 1995). Among the chromokinesins, only *Mus musculus* KIF4 has been characterized and found to move towards the plus ends of MTs (Sekine et al., 1994). Other well-studied members of this family are *X. laevis* klp and *Gallus gallus* Chrkin.

III. The KRP85/95 subfamily: N-terminal heteromeric kinesin-like proteins

Members of this subfamily move towards the plus ends of MTs and consist of two distinct heterodimerized kinesin subunits (Cole et al., 1993; Scholey, 1996). Well-characterized members of this subfamily include *D. melanogaster* Klp68, *M. musculus* Kif 3a

and 3b, which are involved in anterograde axonal vesicle transport, and *Chlamydomonas* rFla10, which is involved in flagellar assembly (Aizawa et al., 1992; Pesavento et al., 1994; Yamazaki et al., 1995).

IV. The UNC-104/KIF1 subfamily: N-terminal monomeric kinesin-like proteins

The *M. musculus* Kif 1a and 1b members of this subfamily move towards the plus ends of MTs and are involved in intracellular transport of membranous organelles such as synaptic vesicle precursors and mitochondria, respectively (Nangaku et al., 1994; Okada et al., 1995). Another member of this family, *Caenorhabditis elegans* UNC-104, is involved in anterograde transport of synaptic vesicles (Otsuka et al., 1991; Hall and Hedgecock, 1991).

V. The KHC subfamily: N-terminal conventional kinesin proteins

All conventional kinesins move towards the plus ends of MTs. This group of proteins shares an amino acid sequence identity extending beyond the motor domain region. The best-characterized members of this family, *H. sapiens* KHC and *Lytechinus pictus* KHC, have been implicated in the transport of synaptic vesicles in axons (Vale et al., 1985a; Niclas et al., 1994). *D. melanogaster* KHC is involved in neuromuscular function (Hurd et al., 1996). The other members of KHC subfamily are involved in organelle transport and positioning (Lipponcott-Schwartz et al., 1995).

VI. The KIP3 subfamily: N-terminal

The founding member of this subfamily, the *Saccharomyces cerevisiae* KIP3 motor protein, is involved in spindle positioning (Miller et al., 1998). The polarity of this motor protein has not yet been determined.

VII. The MKLP1 subfamily: N-terminal

C. griseus CHO1 and *H. sapiens* MKLP1 have been shown to localize to spindle, midbody and poles, and suggested to be involved in spindle pole separation (Sellitto and Kuriyama, 1988; Kuriyama et al., 1994). *H. sapiens* MKLP1 moves towards the plus ends of MTs (Nislow et al., 1992).

Internal kinesin-like proteins:

I. The MCAK/KIF2 subfamily:

All internal motor domain kinesin-like proteins are homodimers. *M. musculus* KIF2 is associated with synaptic vesicles and a plus end-directed motor protein (Aizawa et al., 1992). MCAK and *X. laevis* XKCM1 localize to the centrosomes of the mitotic spindle and

centromeres of mitotic chromosomes, and have been shown to depolymerize MTs (Wordeman and Mitchison, 1995; Walczak et al., 1996).

C-terminal kinesin-like proteins:

I. The Ce1 (*C. elegans* 1) subfamily:

This subfamily was formed based on the sequence homology of *C. elegans* motor proteins (Kinesins home-page: <http://www.blocks.fhcrc.org/kinesin/>). The subcellular localization and motor properties of these proteins have not yet been determined.

II. Kar3/Ncd subfamily:

Members of this subfamily move towards the minus ends of MTs. The best-characterized members of this subfamily, *S. cerevisiae* Kar3 and *D. melanogaster* Ncd, localize to spindles and centrosomes (Meluh and Rose, 1990; Hatsumi and Endow, 1992). Kar3 is required for karyogamy and associated with a centomere-binding complex, indicating a role for the motor in mitotic chromosome movement (Endow et al., 1994). Ncd is required for normal chromosome segregation during meiosis in oocytes and for spindle formation and maintenance in mitosis in early embryos (Endow and Komma, 1996). The Ncd protein will be discussed in detail in the project introduction section of this dissertation.

PROJECT INTRODUCTION

NON-CLARET DISJUNCTIONAL (NCD) MOTOR PROTEIN

The *claret* (*ca*) locus in *Drosophila* has been studied intensively since Sturtevant (1929) reported that the *ca* mutations in *D. simulans* caused females to produce very few offspring, many of which were abnormal and recessive phenotypes of claret eye color in both females and males. A *D. melanogaster* mutant produced by X-radiation (Lewis and Gencarella, 1952) was recovered with the same phenotype and named claret non-disjunctional (*cand*). Later, the discovery of an allele, non-claret disjunctional (Ncd) that causes abnormal chromosome segregation but does not affect the eye color suggested that there were two genes present at the *ca* locus (O'Tousa and Szauter, 1980). *Drosophila* females carrying mutations in the chromosome segregation gene of this locus showed high frequency of non-disjunction and loss of chromosomes in meiosis. Embryos produced by mutant females also showed loss of chromosomes in early embryonic mitotic divisions. Because loss of either the X or the fourth chromosome is non-lethal in *Drosophila*, offspring that have lost these chromosomes can be recovered as gynandromorphs (X/X, X/0 mosaics) or as haplo-4, diplo-4 mosaics (Yamamoto et al., 1989).

Subsequent DNA sequence analysis of the Ncd gene revealed a high degree of homology to the motor domain of kinesin (Endow et al., 1990). The homology of the Ncd gene to kinesin heavy chain was also determined by McDonald and Goldstein (1990) using PCR primers derived from the conserved region of the *Drosophila* kinesin heavy chain with *Drosophila* embryonic cDNA. Ncd encodes a protein of approximately 700 amino acids in length with a predicted molecular weight of 77 kDa. Unlike the kinesin heavy chain, the motor domain (residues 356-700) of Ncd is located at the C-terminus of the protein. The Ncd motor domain shares 41% sequence identity with the kinesin motor domain, and the region of similarity includes the putative ATP binding site (residues 428-448) and MT binding site (residues 516 to 668). The tail domain (residues 1-200) of Ncd is located at the N-terminal region of the protein and is rich in basic amino acids and prolines. The central stalk region of the protein includes heptad repeats and is involved in subunit dimerization (Endow et al., 1990; McDonald and Goldstein, 1990a and b; Chandra et al., 1993).

Despite the high homology to the kinesin heavy chain, Ncd is a minus end-directed motor protein (Walker et al., 1990; McDonald and Goldstein, 1990b). Recent research has identified that polarity determinants, the residues that contribute to the direction of movement, are present in the neck region of Ncd, while the polarity determinants of kinesin are located in the motor core of the kinesin heavy chain (Endow and Waligora, 1998; Sablin et al., 1998; Henningsen and Schliwa, 1997).

The motor properties (ATP and MT binding sites in the head domain), the directionality of movement of the Ncd protein, and abnormal chromosome distribution in mutant oocytes and embryos have implicated the Ncd protein in spindle function and

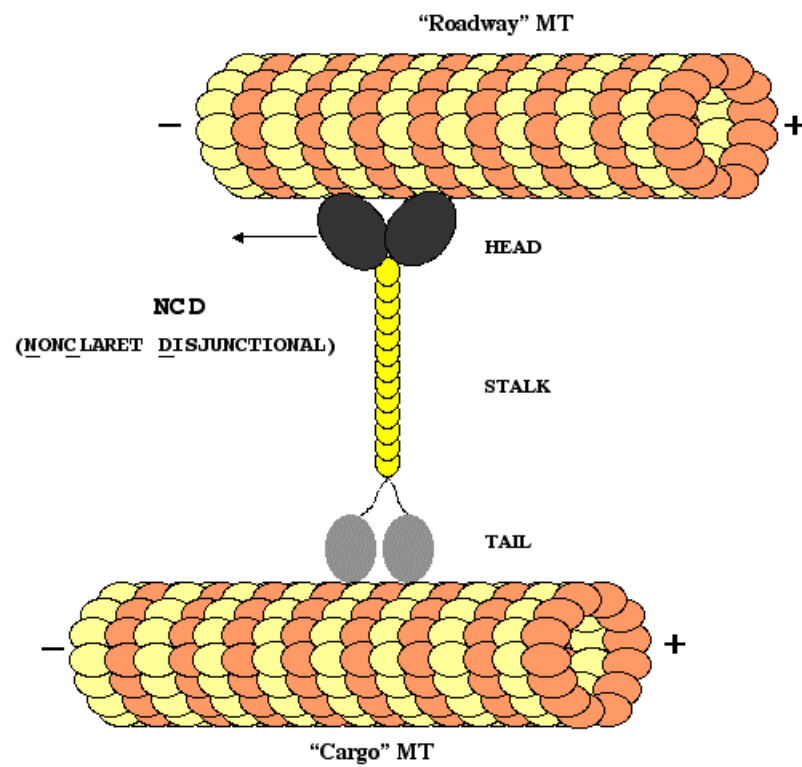
chromosome segregation during meiosis and mitosis (Endow et al., 1990; McDonald et al., 1990; Komma et al., 1991; Hatsumi and Endow, 1992a). Immunolocalization of Ncd to the meiotic spindle in all stages of meiosis suggested that the Ncd motor is required for chromosome segregation during meiosis in oocytes, where it has been proposed to function in assembly of bipolar meiotic spindles (Hatsumi and Endow, 1992a and b; Matthies et al., 1996). These experiments have also led to the hypothesis that the Ncd motor functions at the spindle poles in mitosis in early embryos and acts to maintain centrosome attachment to poles and prevent centrosome separation until late anaphase (Endow et al., 1994; Endow and Komma, 1996 and 1997). The Ncd motor also acts to prevent chromosome loss, possibly by maintaining attachment of chromosomes to spindle fibers during metaphase/anaphase transition and facilitating poleward movement of the chromosomes (Endow and Komma, 1996 and 1997).

Based on the sequence homology to the kinesin heavy chain, the motor domain of Ncd has been known to contain an ATP-dependent MT binding site. Experiments in which bacterially-expressed full-length Ncd bundled MTs (McDonald et al., 1990b) and Ncd tail proteins (Chandra et al., 1993) bound and bundled MTs suggest that the Ncd tail domain contains an ATP-independent MT binding site. The ability of Ncd to bind and bundle MTs is likely to be important for Ncd function *in vivo* in the formation of bipolar spindles and maintenance of spindle assembly (Figure 3).

Since the discovery of the Ncd motor protein, most research has focused on the motor domain and there has been little known about the tail domain. In order to learn more about Ncd function, I chose to focus on the tail domain and characterization of interactions of the Ncd with cargo MTs. My first objective was to identify MT binding sites in the Ncd tail domain. Characterization of the MT binding sites in the tail region revealed similarities between the Ncd tail and MAPs and this led to the analysis of the role of the Ncd tail domain in MT assembly and stability. Finally, sequence and functional similarities led to the identification of the Ncd tail binding sites on tubulin.

FIGURE 3: Non-claret disjunctional (Ncd) spindle motor.

Ncd is a minus end-directed motor protein. Ncd binds to “roadway” and “cargo” MTs via ATP-dependent and ATP-independent MT binding sites in the head and tail domains, respectively.



LITERATURE CITED

Aizawa, H., Sekine, Y., Takemura, R., Zhang, Z., Nangaku, M., and Hirokawa, N. (1992). Kinesin family in murine central nervous system. *J. Cell Biol.* 119, 1287-1296

Allen, R. D., Metuzals, J., Tasaki, I., Brady, S. T., and Gilbert, S. P. (1982). Fast axonal transport in squid giant axon. *Science* 218, 1127-1129

Allen, R. D., Weiss, D. G., Hayden, J. H., Brown, D. T., Fujiwake, H., and Simpson, M. (1985). Gliding movement of and bidirectional transport along single native microtubules from squid axoplasm: evidence for an active role of microtubules in cytoplasmic transport. *J. Cell Biol.* 100, 1736-1752

Amaratunga, A., Morin, P. J., Kosik, K. S., and Fine, R. E. (1993). Inhibition of kinesin synthesis and rapid anterograde axonal transport *in vivo* by an antisense oligonucleotide. *J. Biol. Chem.* 268, 17427-17430.

Andersen, S., Buendia, B., Dominguez, J. E., Sawyer, A., and Karsenti, E. (1994). Effect on microtubule dynamics of XMAP230, a microtubule-associated protein present in *Xenopus laevis* eggs and dividing cells. *J. Cell Biol.* 127, 1289

Andersen, S. S., and Karsenti, E. (1997). XMAP230: a *Xenopus* rescue-promoting factor localized to the mitotic spindle. *J. Cell Biol.* 139, 975-983

Avila, J., Dominguez, J., and Diaz-Nido, J. (1994). Regulation of microtubule dynamics by microtubule-associated protein expression and phosphorylation during neuronal development. *Int. J. Dev. Biol.* 38 13-25

Bi, G. Q., Morris, R. L., Liao, G., Alderton, J. M., Scholey, J. M., and Steinhardt, R. A. (1997). Kinesin- and myosin-driven steps of vesicle recruitment for Ca²⁺-regulated exocytosis. *J. Cell Biol.* 138, 999-1008

Binder, L. I., Frankfurter, A., and Rebhun, L. (1985). The distribution of tau in the mammalian central nervous system. *J. Cell Biol.* 101, 1371-1378

Blangy, A., Lane, H. A., d'Herin, P., Harper, M., Kress, M., and Nigg, E. A. (1995). Phosphorylation by p34cdc2 regulates spindle association of human Eg5, a kinesin-related motor essential for bipolar spindle formation *in vivo*. *Cell* 83, 1159-1169

Bloom, G. S., Schoenfeld, T. A., and Vallee, R. B. (1984). Widespread distribution of the major polypeptide component of MAP (microtubule-associated protein 1) in the nervous system. *J. Cell Biol.* 98, 320-330

Bloom, G. S., and Wagner, M. C. (1988). Native structure and physical properties of bovine brain kinesin and identification of the ATP-binding subunit polypeptide. *Biochemistry* 27, 3409-3416

Bulinski, J. C., and Borisy, G. G. (1980). Widespread distribution of a 210,000 mol wt microtubule-associated protein in cells and tissue of primate. *J. Cell Biol.*, 87, 802-808

Brady, S. T. (1985). A novel brain ATPase with properties expected for the fast axonal transport motor. *Nature* 317, 73-75

Brady, S. T., Pfister, K. K., and Bloom, G. S. (1990). A monoclonal antibody against kinesin inhibits both anterograde and retrograde fast axonal transport in squid axoplasm. *Proc. Natl. Acad. Sci. USA* 87, 1061-1065

Cassimeris, L., Pryer, N.K., Salmon, E.D. (1988). Real time observation of microtubule dynamic instability in living cells. *J. Cell Biol.* 107, 2223-2231

Chandra, R., Salmon, E. D., Erickson, H. P., Lockhart, A., and Endow, S. A. (1993). Structural and functional domains of the *Drosophila* Ncd microtubule motor protein. *J. Biol. Chem.* 268, 9005-9013

Chapin, S. J., Lue, C.-M., Yu, M.T., and Bulinski, J. C. (1995). Differential expression of alternatively spliced forms of MAP4: a repertoire of structurally different microtubule binding domains. *Biochem.* 34, 2289-2301

Chau, M-F., Radeke, M.J., Ines, C. de, Barosain, I., Kohlstaedt, L.A., and Feinstein, S. C. (1998) The microtubule-associated protein tau cross-links to two distinct sites on each and tubulin monomer via separate domains. *Biochemistry* 37, 17692-17703

Cleveland, D. W., Hwo, S. Y., and Kirschner, M. W. (1977). Purification of tau, a microtubule-associated protein that induces assembly of microtubules from purified tubulin. *J. Mol. Biol.* 116, 207-225

- Cole, D. G., Chinn, S. W., Wedaman, K. P., Hall, K., Vuong, T., and Scholey, J. M. (1993). Novel heterotrimeric kinesin-related protein purified from sea urchin eggs. *Nature* 366, 268-270
- Cole, D. G., Saxton, W. M., Sheehan, K. B., and Scholey, J. M. (1994). A "slow" homotetrameric kinesin-related motor protein purified from *Drosophila* embryos. *J. Biol. Chem.* 269, 22913-22916
- Cravchik, A., Reddy, D., and Matus, A. (1994). Identification of a novel microtubule binding domain in microtubule-associated protein 1A (MAP1A). *J. Cell Sci.* 107, 661-672
- Desai, A. and Mitchison, T. J. (1997) Microtubule polymerization dynamics. *Ann. Rev. Cell Dev. Biol.* 13, 83-117
- Doll, T., Meichsner, M., Riederer, B. M., Honegger, P., Matus, A. (1993). An isoform of microtubule-associated protein-2 (MAP2) containing 4 repeats of the tubulin-binding motif. *J. Cell. Sci* 106, 633-640
- Drechsel, D. N., Hyman, A. A., Cobb, M. H., and Kirschner, M. W. (1992). Modulation of the dynamic instability of tubulin assembly by the microtubule-associated protein tau. *Mol. Biol. Cell* 3, 1141-1154
- Echeverri, C. J., Paschal, B. M., Vaughan, K. T., and Vallee R. B. (1996). Molecular characterization of the 50-kD subunit of dynactin reveals function for the complex in chromosome alignment and spindle organization during mitosis. *J. Cell Bio.*, 132, 617-633
- Elluru, R. G., Bloom, G. S., and Brady, S. T. (1995). Fast axonal transport of kinesin in the rat visual system: functionality of kinesin heavy chain isoforms. *Mol. Biol. Cell* 6, 21-40
- Endow, S. A., Henikoff, S., Soler-Niedziela, L. (1990). Mediation of meiotic and early mitotic chromosome segregation in *Drosophila* by a protein related to kinesin. *Nature* 345, 81-83
- Endow, S. A., Chandra, R., Komma, D. J., Yamamoto, A. H., and Salmon, E. D. (1994). Mutants of the *Drosophila* ncd microtubule motor protein cause centrosomal and spindle pole defects in mitosis. *J. Cell Sci.* 107, 1-9

Endow, S. A., and Komma, D. (1996). Centrosome and spindle function of the *Drosophila* Ncd microtubule motor visualized in live embryos using Ncd-GFP fusion proteins. *J. Cell Sci.* 109, 2429-2442

Endow, S. A., and Komma, D. (1997). Spindle dynamics during meiosis in *Drosophila* oocytes. *J. Cell Biol.*, 137,13321-1336

Endow, S. A., and Waligora, K. W. (1998). Determinants of kinesin motor polarity. *Science* 281, 1200-1202

Ennulat, D. J., Liem, R.K.H., Hashim, G. A., and Shelanski, M. L. (1989). Two separate 18-amino acid domains of tau promote the polymerization of tubulin. *J. Biol. Chem.* 264, 5327-5330.

Enos, A. P., and Morris, N. R. (1990). Mutations of a gene that encodes a kinesin-like protein blocks nuclear division in *A. nidulans*. *Cell* 60-1019-1027

Fan J., Griffiths A. D., Lockhart A., Cross R. A., Amos L. A. (1996). Microtubule minus ends can be labelled with a phage display antibody specific to γ -tubulin. *J. Mol. Biol.* 259, 325-330

Faruki, S., and Karsenti, E. (1994). Purification of microtubule proteins from *Xenopus* egg extracts: identification of a 230 K MAP4-like protein. *Cell Motil. Cytoskel.* 28, 108

Gamblin, T. C., Nachmanoff, K., Halpain, S., and Williams, R. (1996). Recombinant microtubule-associated protein 2c reduces the dynamic instability of individual microtubules. *Biochemistry* 35 12576-12586

Gard, D. L., and Kirschner, M. W. (1987). Microtubule assembly in cytoplasmic extracts of *Xenopus* oocytes and eggs. *J. Cell Biol.*, 105, 2191-2201

Gard, D. L., and Kirschner, M. W. (1987). A microtubule-associated protein from *Xenopus* eggs that specifically promotes assembly at the plus-end. *J. Cell Biol.*, 105, 2203-2215

Garner, C. C., and Matus, A. (1988). Different forms of microtubule-associated protein 2 are encoded by separate mRNA transcripts. *J. Cell. Biol.* 106, 779-783

- Garner, C. C., Garner, A., Huber, G., Kozak, C., and Matus, A. (1990). Molecular cloning of microtubule-associated protein 1 (MAP1a) and microtubule-associated protein 5 (MAP1b): identification of distinct genes and their differential expression in developing brain. *J. Neurochem.* 55, 146-154
- Gauger, A. K. and Goldstein, L. S. (1993). The *Drosophila* kinesin light chain. Primary structure and interaction with kinesin heavy chain. *J. Biol. Chem.* 268, 136657-13666
- Gee, M. A., Heuser, J E., and Vallee, R. B. (1997) An extended microtubule binding structure within the dynein motor domain. *Nature*, 390, 636-639
- Gibbons, I. R. (1963). Studies on the protein components of cilia from *Tetrahymena pyriformis*. *Proc. Natl. Acad. Sci. USA* 50, 1002-1010
- Gibbons, I. R., and Rowe, A. J. (1965). Dynein: a protein with adenosine triphosphatase activity from cilia. *Science* 149, 424-426
- Gibbons, I. R., Gibbons, B. H., Mocz, G., and Asai, D. J. (1991). Multiple nucleotide binding sites in the sequence of dynein beta heavy chain. *Nature* 352, 640-643
- Gilbert, S. P., and Webb, M. R. (1995) Pathway of processive ATP hydrolysis by kinesin. *Nature* 373, 671-676
- Goedert, M., Spillantini, M., Jakes, R., Rutherford, D., and Crowther, R. A. (1989). Multiple isoforms of human microtubule-associated protein tau: sequences and localization in neurofibrillary tangles of Alzheimer's disease. *Neuron* 3, 519-526
- Goldstein, L. S. B., Laymon, R. A., McIntosh, J. R. (1986). A microtubule-associated protein in *Drosophila melanogaster*: identification, characterization, and isolation of coding sequences. *J. Cell Biol.* 107, 2076-2087
- Goode, B. L., Denis, P. E., Panda, D., Radeke, M. J., Miller, H. P., Leslie Wilson, and Feinstein, S.C. (1997). Functional interactions between the proline-rich and repeat regions of tau enhance microtubule binding and assembly. *Mol. Biol. Cell* 8, 353-365
- Goodson, H. V., Kang, S. J., and Endow, S. A. (1994). Molecular phylogeny of the kinesin family of microtubule motor proteins. *J. Cell Sci.* 107, 1875-1884

- Hackney, D. D. (1994). Evidence for alternating head catalysis by kinesin during microtubule-stimulated ATP hydrolysis. *Proc. Natl. Acad. Sci. USA*, 91, 6865-6869
- Hackney, D. D. (1994). The rate-limiting step in microtubule-stimulated ATP hydrolysis by dimeric kinesin head domains occurs while bound to the microtubule. *J. Biol. Chem.* 269, 16508-16511
- Hackney, D. D. (1995). Highly processive microtubule stimulated ATP hydrolysis by dimeric kinesin head domains. *Nature* 377, 448-450
- Hagan, I., and Yanagida, M. (1992). Kinesin-related cut7 protein associates with mitotic and meiotic spindles in fission yeast. *Nature* 356, 74-76
- Hatsumi, M., and Endow, S. A. (1992a). Mutants of the microtubule motor protein, nonclaret disjunctional, affect spindle structure and chromosome movement in meiosis and mitosis. *J. Cell Sci.* 101, 547-559
- Hatsumi, M., and Endow, S. A. (1992b). The *Drosophila* microtubule motor protein is a spindle-associated in meiotic and mitotic cells. *J. Cell Sci.* 103, 1013-1020
- Hall, D., and Hedgecock, E. M. (1991). Kinesin-related gene unc-104 is required for axonal transport of synaptic vesicles in *C. elegans*. *Cell* 65, 837-847
- Heald, R. (1996). Self-organization of microtubules into bipolar spindles around artificial chromosomes in *Xenopus* egg extracts. *Nature* 382, 420-425
- Henningsen, U., and Schliwa, M. (1977). Reversal in the direction of movement of a molecular motor. *Nature* 389, 93-96
- Hirokawa, N., Sato, Y. R., Kobayashi, N., Pfister, K. K., Bloom, G. S., and Brady, S. T. (1991). Kinesin associates with anterograde transported membranous organelles *in vivo*. *J. Cell Biol.* 114, 295-302
- Hirokawa, N., Noda, Y., and Okada Y. (1998) Kinesin and dynein superfamily proteins in organelle transport and cell division. *Curr Opin. Cell Biol* 10, 60-73

- Hirose, K., Lockhart, A., Cross, R. A., and Amos, L. A. (1995). Nucleotide-dependent angular change in kinesin motor domain bound to tubulin. *Nature* 376, 277-279
- Hollenbeck, P. J., and Swanson, J. A. (1990). Radial extension of macrophage tubular lysosomes supported by kinesin. *Nature*, 346, 864-866
- Howard, J., Hudspeth, A. J., and Vale, R. D. (1989). Movement of microtubules by single kinesin molecules. *Nature* 342, 154-158
- Huang, T. G., and Hackney, D. D. (1994). *Drosophila* kinesin minimal motor domain expressed in Escherichia coli: purification and characterization. *J. Biol. Chem.* 269, 16502-16507
- Huang, T. G., Suhan, J., and Hackney, D. D. (1994). *Drosophila* kinesin minimal motor domain extending to amino acid position 392 is dimeric when expressed in Escherichia coli. *J Biol Chem.* 269, 32708
- Huber, G., and Matus, A. (1984). Differences in the cellular distributions of two microtubule-associated proteins, MAP1 and MAP2, in rat brain. *J. Neurosci.* 4, 151-160
- Hurd, D. D., Stern, M., and Saxton, W. M. (1996). Mutation of the axonal transport motor kinesin enhances paralytic and suppresses Shaker in *Drosophila*. *Genetics* 142, 195-204.
- Itoh, T., and Hotani, H. (1994). Microtubule-stabilizing activity of microtubule-associated proteins (MAPs) is due to increase in frequency of rescue in dynamic instability: shortening length decreases with binding of MAPs onto microtubules. *Cell Struc. Funct.* 19 279-290
- Jellali, A., Metz-Boitugue, M. H., Surgucheava, I., Jancsik, V., Schawartz, C., Filliol, D. (1994). Structural and biochemical properties of kinesin heavy chain associated with rat brain mitochondria. *Cell Motil. Cytoskel.* 28, 79-93
- Johnson, K. J., Hall, E. S., and Boekelheide, K. (1996). Kinesin localizes to the trans-Golgi network regardless of microtubule organization. *Eur. J. Cell Biol.* 69, 276-287
- Joly, C. J., Flynn G., and Purich, D. (1989). The microtubule binding fragment of microtubule-associated protein-2: Location of the protease-accessible site and identification of an assembly-promoting peptide. *J. Cell Biol.* 109 2289-2294

- Khodjakov, A. L., Lizunova, E. M., Minin, A. A., Koonce, M. P., and Gyoeva, F. K. (1998). A specific light chain of kinesin associates with mitochondria in cultured cells. *Mol. Biol. Cell* 9, 333-343
- Komma, D. J., Horne, A. S., and Endow, S. A. (1991). Separation of meiotic and mitotic effects of claret non-disjunctional on chromosome segregation in *Drosophila*. *EMBO J.* 10, 419-424
- Kowalski, R. J., and Williams, R. C. (1993). Microtubule-associated protein 2 alters the dynamic properties of microtubule assembly and disassembly. *J. Biol. Chem.* 268, 9847-9855
- Kuriyama, R., Dragas-Granoic, S., Maekawa, T., Vasillev, A., Khodjakov, A., and Kobayashhi, H. (1994). Heterogeneity and microtubule interaction of the CHO1 antigen, a mitosis-specific kinesin-like protein. *J. Cell Sci.* 107, 3485-3499
- Kuznetsov, S. A., and Vaisberg, E. A. (1988). The quaternary structure of bovine brain kinesin. *EMBO J.* 7, 353-356
- Langkopf, A., Hammarback, J. A., Muller, R., Vallee, R. B. and Garner, C. C. (1992). Microtubule-associated protein 1A and LC2. Two proteins encoded in one messenger RNA. *J. Biol. Chem.* 267, 16561-16566
- Lee, G., Cowan, N., and Kirschner, M. (1988). The primary structure and heterogeneity of tau protein from mouse brain. *Science* 239, 285-288.
- Lewis, E. B., and Gencarella, W. (1952). Claret and nondisjunction in *Drosophila melanogaster*. *Genetics* 37, 600-601
- Lewis, S. A., Wang, D., Cowan, N. J. (1988). Microtubule-associated protein MAP2 shares a microtubule binding motif with tau protein. *Science* 242, 936-939
- Lindesmith, L., McIlvain, J. M., Argon, Y., and Sheetz, M. P. (1997). Phosphotransferases associated with the regulation of kinesin motor activity. *J. Biol. Chem.* 272, 22929-22933
- Lipponcott-Schwartz, J., Cole, N. B., Marotta, A., Conrad, P. A., and Bloom, G. S. (1995). Kinesin is the motor for microtubule-mediated Golgi-to-ER membrane traffic. *J. Cell Biol.* 128, 293-306

- Ludin, B., Ashbridge, K., Funfschilling, U., and Matus, A. (1996). Functional analysis of the MAP2 repeat domain. *J. Cell Sci.* 109, 91-99
- Ma, Y-Z., and Taylor, E. W. (1997). Interacting head mechanism of microtubule-kinesin ATPase. *J. Biol.Chem.* 272, 724-730
- Mann, S. S., and Hammarback, J. A. (1994). Molecular characterization of light chain 3. A microtubule binding subunit of MAP1A and MAP1B. *J. Biol. Chem.* 269, 11492-11497
- Mansfield, S. G., Diaz-Nido, J., Gordon-Weeks, P. R., and Avila, J. (1991). The distribution and phosphorylation of the microtubule-associated protein MAP 1B in growth cones. *J. Neurocytol.* 21 1007-1022
- Marks, D. L., Larkin, J. M., and McNiven, M. A. (1994). Association of kinesin with the Golgi apparatus in rat hepatocytes. *J. Cell Sci.*, 107, 2417-2426
- Matthies, H. J., McDonald, H. B., Goldstein, L. S. B., and Theurkauf, W. E. (1996). Anastral meiotic spindle morphogenesis: role of non-claret disjunctional kinesin-like protein. *J. Cell Biol.* 134, 455-464
- Matus, A., (1988). Microtubule-associated proteins in the developing brain. *Ann. NY Acad. Sci.* 466, 167-179
- Matus, A., (1988). Microtubule-associated proteins: their potential role in determining neuronal morphology. . *Ann. Rev. Neurosci.* 11, 29-44
- McDonald, H. B., and Goldstein, L. S. B. (1990a). Identification and characterization of a gene encoding a kinesin-like protein in *Drosophila*. *Cell* 61, 991-1000
- McDonald, H. B., Stewart, R. J., Goldstein, L. S. B. (1990b). The kinesin-like Ncd protein of *Drosophila* is a minus end-directed microtubule motor. *Cell* 63, 1159-1165
- Meluh, P. B. and Rose, M. D. (1990). Kar3, a kinesin-related gene required for yeast nuclear fusion. *Cell* 60, 1029-1041.
- Meng, Y. X., Wilson, J. W., Avery, M. C., Varden, J. H., and Balczon, R. (1997). Suppression of the expression of a pancreatic beta-cell form of the kinesin heavy chain by

antisense oligonucleotides inhibits insulin secretion from primary cultures of mouse beta-cells. *Endocrinology* 138, 1979-1987

Miller, R. K., Heller, K. K., Frisen, L., Wallack, D. L., Loayza, D., Gammie, A. E., and Rose, M. D. (1998). The kinesin-related proteins, Kip2p and Kip3p, function differently in nuclear migration in yeast. *Mol. Biol. Cell* 9, 2051-2068.

Mitchison, T., and Kirschner, M. (1984). Dynamic instability of microtubule growth. *Nature* 312, 237-242

Nangaku, M., Sato-Yoshitake, R., Okada, Y., Noda, Y., Takemura, R., Yamazaki, H., and Hirokawa, N. (1994). KIF1B, a novel microtubule plus end-directed monomeric motor protein for transport of mitochondria. *Cell* 79, 1209-1220

Nakata, T., and Hirokawa, N. (1995). Point mutation of adenosine triphosphate-binding motif generated rigor kinesin that selectively blocks anterograde lysosome membrane transport. *J. Cell Biol.* 131, 1039-1053.

Niclas, J., Navone, F., Hom-Booher, N., and Vale, R. D. (1994). Cloning and localization of a conventional kinesin motor expressed exclusively in neurons. *Neuron* 12, 1059-1072

Nislow, C., Lombillo, V. A., Kuriyama, R., and McIntosh, J. R. (1992). A plus-end-directed motor enzyme that moves antiparallel microtubules *in vitro* localizes to the interzone of mitotic spindle. *Nature*, 359, 543-547

Noble, M., Lewis, S. A., and Cowan, N. J. (1989). The microtubule binding domain of microtubule-associated protein MAP1b contains a repeated sequence motif unrelated to that of MAP2 and tau. *J. Cell Biol.* 109, 3367-3376

Okada, Y., Yamazaki, H., Sekine-Aizawa, Y., and Hirokawa, N. (1995). The neuron-specific kinesin superfamily protein KIF1A is a unique monomeric motor for anterograde axonal transport of synaptic vesicle precursors. *Cell* 81, 769-780

Olmsted, J. B., Stemple, D. L., Saxton, W. M., Neighbors, B. W., and McIntosh, J. R. (1989). Cell cycle-dependent changes in the dynamics of MAP 2 and MAP 4 in cultured cells. *J. Cell Biol.* 109, 211-223

Otsuka, A.J., Jeyapragash, A., Garcia-Anovereros, J., Tang, L. Z., Fisk, G., Hartshorne, T. (1991). The *C. elegans* unc-104 gene encodes a putative kinesin heavy chain-like protein. *Neuron* 6, 113-122

O'Tousa, J., and Szauter, P. (1980). The initial characterization of nonclaret disjunctional (*ncd*): evidence that ca^{nd} is the double mutant, *ca ncd*. *Dros. Inf. Serv.* 55, 119

Ookata, K., Hisanaga, S., Bulinski, J.C., Murofushi, H., Aizawa, H., Itoh, T.J., Hotani, H., Okumura, E., Tachibana, K., Kishimoto, T. (1995). Cyclin B interaction with microtubule-associated protein 4 (MAP4) targets p34cdc2 kinase to microtubules and is a potential regulator of M-phase microtubule dynamics. *J. Cell Biol.* 128, 849-862

Paschal, B. M., and Vallee, R. B. (1987). Retrograde transport by the microtubule-associated protein MAP1C. *Nature* 330, 181-183

Paschal, B. M., Obar, R. A., and Vallee, R. B. (1989). Interaction of brain cytoplasmic dynein and MAP2 with a common sequence at the C-terminus of tubulin. *Nature* 342, 569-572

Pedrotti, B., and Islam, K. (1994). Purified native microtubule associated protein MAP1A: kinetics of microtubule assembly and MAP1A/tubulin stoichiometry. *Biochemistry* 33 12463-12470

Pesavento, P. A., Stewart, R. J, and Goldstein, L. S. B. (1994). Characterization of the KLP68D kinesin-like protein in *Drosophila*: possible roles in axonal transport. *J. Cell Biol.* 127, 1041-1048

Porter, M. E. and Johnson, K. A. (1989). Dynein structure and function. *Annu. Rev. Cell Biol.* 5, 119-151

Pryer, N. K., Walker, R. A., Skeen, V. P., Bourns, B. D., Soboeiro, M. F., and Salmon, E.D. (1992). Brain microtubule-associated proteins modulate dynamic instability in vitro. *J. Cell Sci.* 103, 965

Romberg, L., and vale, R. D. (1993). Chemomechanical cycle of kinesin differs from that of myosin. *Nature* 361, 168-170

Sablin, E. P., Case, R. B., Dai, S. C., Hart, C. L., Ruby, A., Vale, R. D., and Fletterick, R. J. (1998). Direction determination in the minus-end-directed kinesin motor Ncd. *Nature* 395, 813-816

Samejima, I., Matsumoto, T., Nakaseko, Y., Beach, D., and Yanagida, M. (1993). Identification of seven new cut genes involved in *Schizosaccharomyces pombe* mitosis. *J. Cell Sci.* 105, 135-143.

Sammak, P.J., and Borisy, G. G. (1988). Direct observation of microtubule dynamics in living cells. *Nature* 332, 724.

Sawin, K. E., LeGuellec, K., Philippe, M., and Mitchison, T. J. (1992). Mitotic spindle organization by a plus-end-directed microtubule motor. *Nature* 359, 540-543

Scholey, J. M. (1996). Kinesin-II, a membrane traffic motor in axons, axonemes, and spindles. *J. Cell Biol.* 133, 1-4

Sekine, Y., Okada, Y., Noda, Y., Kondo, S., Aizawa, H., Takemura, R., and Hirokawa, N. (1994). A novel microtubule-based motor protein (KIF4) for organelle transports, whose expression is regulated developmentally. *J. Cell. Biol.*, 127, 187-201

Sellitto, C. and Kuriyama, R. (1988). Distribution of a matrix component of the midbody during the cell cycle in Chinese hamster ovary cells. *J. Cell Biol.* 106, 431-439

Sturtevant, A. H. (1929). The claret mutant type of *Drosophila simulans* study of chromosome elimination and of cell lineage. *Z. Wiss. Zool.* 13, 323-356

Svoboda, K., Schmidt, C. F., Schnapp, B. J., and Block, S. M. (1993). Direct observation of kinesin stepping by optical trapping interferometry. *Nature* 365, 721-727

Tanaka, Y., Kanai, Y., Okada, Y., Nonaka, S. (1998). Targeted disruption of mouse conventional kinesin heavy chain, kif5B, results in abnormal perinuclear clustering of mitochondria. *Cell* 93, 1147-1158

Takemura, R., Okabe, S., Umeyama, T., Kanai, Y., Cowan, N. J., Hirokawa, N. (1992). Increased microtubule stability and alpha tubulin acetylation in cells transfected with microtubule-associated proteins MAP1B, MAP2 or tau. *J. Cell Sci.* 103, 953-964

- Tran, P. T., Walker, R. A., and Salmon, E. D. (1997). A metastable intermediate state of microtubule dynamic instability that differs significantly between plus and minus ends. *J. Cell Biol.* 138, 105-117
- Vaisberg, E. A., Koonce, M. P., and McIntosh, J. R. (1993). Cytoplasmic dynein plays a role in mammalian mitotic spindle formation. *J. Cell Biol.* 123, 849-858
- Vaisberg, E. A., Grissom, P. M., and McIntosh, J. R. (1996). Mammalian cells express three distinct dynein heavy chains that are localized to different cytoplasmic organelles. *J. Cell Biol.* 133, 831-842
- Vale, R. D., Reese, T. S., and Sheetz, M. P. (1985a). Identification of a novel force-generating protein, kinesin, involved in microtubule-based motility. *Cell* 42, 39-50
- Vale, R. D., Schnapp, B. J., Mitchison, T., Stuer, E., Reese, T. S., and Sheetz, M. P. (1985b). Different axoplasmic proteins generate movement in opposite directions along microtubules *in vitro*. *Cell* 43, 623-632
- Vale, R. D., and Toyoshima, Y. Y. (1988). Rotation and translocation of microtubules *in vitro* induced by dyneins from *Tetrahymena* cilia. *Cell* 52, 459-469
- Vasquez, R. J., Gard, D. L., and Cassimeris, L. (1994). XMAP from *Xenopus* eggs promotes rapid plus end assembly of microtubules and rapid microtubule polymer turnover. *J. Cell Biol.* 127, 985-993
- Walker, R. A., O'Brien, E. T., Pryer, N.K., Soboeiro, M.F., Voter, W. A., and Erickson, H.P. (1988). Dynamic instability of individual microtubules analyzed by video light microscopy: rate constants and transition frequencies. *J. Cell Biol.* 107: 1437-1448
- Vernos, I., Raats, J., Hirano, T., Heasman J., Karsenti, E., and Wylie, C. (1995). Xklp1, a chromosomal *Xenopus* kinesin-like protein essential for spindle organization and chromosome positioning. *Cell* 81, 117-127
- Walczak, C. E., Mitchison, T. J., and Desai, A. (1996). XKCM1: a *Xenopus* kinesin-related protein that regulates microtubule dynamics during mitotic spindle assembly. *Cell* 84, 37-47
- Walker, R. A., Salmon, E. D., and Endow, S. A. (1990). The *Drosophila* claret segregation protein is a minus end-directed motor molecule. *Nature* 347, 780-782

- Walker, R. A., Pryer, N. K., and Salmon E. D. (1991) Dilution of individual microtubules observed in real time *in vitro*: evidence that cap size is small and independent of elongation rate. J. Cell Biol. 114: 73-81
- Wang, S. -Z., and Adler, R. (1995). Chromokinesin: a DNA-binding, kinesin-like nuclear protein. J. Cell. Biol., 128, 761-768
- Wordeman, L., and Mitchison, T. J. (1995). Identification and partial characterization of mitotic centomere-associated kinesin, a kinesin-related protein that associates with centromeres during mitosis. J. Cell Biol. 128, 95-105
- Yamamoto, A. H., Komma, D. J., Shaffer, C. D., Pirrotta, V., and Endow, S. (1989). The claret locus in *Drosophila* encodes products required for eye color and for meiotic chromosome segregation. EMBO 8, 3543-3552
- Yamazaki, H., Nakata, T., Okada, Y., and Hirokawa, N. (1995). KIF3A/B: a heterodimeric kinesin superfamily protein that works as a microtubule plus end-directed motor for membrane organelle transport. J. Cell. Biol. 130, 1387-1399.
- Yang, J. T., Laymon, R. A., and Goldstein, L. S. B. (1989). A three-domain structure of kinesin heavy chain revealed by DNA sequence and microtubule binding analyses. Cell 56, 879-889

CHAPTER 2

IDENTIFICATION OF MICROTUBULE BINDING SITES IN THE NCD TAIL DOMAIN

This work was previously published as:

A. Karabay and R. A. Walker* (1999) **Biochemistry**, 38 (6), 1838-1849

Department of Biology, Virginia Polytechnic Institute and State University, Blacksburg, VA

* Corresponding author: Dr. Richard A. Walker

Department of Biology

Virginia Polytechnic Institute and State University

Blacksburg, VA 24061-0406

Phone: (540) 231-3803

Fax: (540) 231-9307

E-mail: rawalker@vt.edu

Running Title: Ncd Tail Domain Binding To Microtubules

ABSTRACT

Non-claret disjunctional (Ncd) is a minus end-directed, C-terminal motor protein that is required for spindle assembly and maintenance during meiosis and early mitosis in *Drosophila* oocytes and early embryos. Ncd has an ATP-independent MT binding site in the N-terminal tail domain and an ATP-dependent MT binding site in the C-terminal motor domain. The ability of Ncd to cross-link MTs through the action of these binding sites may be important for Ncd function *in vivo*. In order to identify the region(s) responsible for ATP-independent MT interactions of Ncd, 12 cDNAs coding various regions of Ncd tail domain were expressed in *E. coli* as C-terminal fusions to thioredoxin (Trx). Ncd tail fusion proteins (TrxNT) were purified by ion exchange (S-sepharose) and/or Talon metal affinity chromatography. Purified TrxNT and NT proteins were analyzed in microtubule (MT) co-sedimentation and bundling assays to identify which tail proteins were able to bind and bundle MTs. Based on the results of these experiments, all TrxNT and NT proteins that showed MT binding activity also bundled MTs, and there are two ATP-independent MT interaction sites in the tail region: one within amino acids 83-100 that exhibits conformation-independent, high affinity MT binding activity, and another within amino acids 115-187 that exhibits conformation-dependent, lower affinity MT binding activity. It is possible that both of these MT interacting sites combine in the native protein to form a single MT binding site that allows the Ncd tail to bind cargo MTs *in vivo*.

INTRODUCTION

The kinesin-like microtubule (MT) motor Non-claret disjunctional (Ncd) is involved in spindle assembly and maintenance during meiosis in *Drosophila* oocytes and early mitosis in *Drosophila* embryos (1-6). Ncd translocates towards the minus ends of MTs (7, 8) and is a member of the C-terminal motor group of kinesin superfamily motors (1, 2). Like other kinesin superfamily motors, Ncd is composed of three distinct domains: a conserved motor domain (residues 356-700) that contains the ATP-dependent MT binding site responsible for the force-generating activity of the motor that drives movement; a central stalk region (residues 200-356) of heptad repeats thought to be involved in subunit dimerization; and a tail domain (residues 1-200) thought to be involved in cargo binding and/or regulation of motor activity (1, 2, 8, 9).

To date, most research on Ncd and MT motors in general has focused on the motor domain and the mechanisms by which motor proteins move along MTs. In comparison, relatively little is known about the tail domains of these proteins. In the case of Ncd, the sequence of the N-terminal tail domain is unique among kinesin superfamily motors, although like many others, is positively charged and proline-rich (1, 2, 9). Based on experiments in which full-length Ncd was found to bundle MTs *in vitro* (8), and in which bacterial expressed Ncd tail proteins both bound and bundled MTs *in vitro* (9), it has been suggested that the tail of Ncd contains an ATP-independent MT binding site (8, 9). The ability of the tail region to bind MTs and of Ncd to bundle MTs may be important for Ncd function *in vivo*, and several *in vivo* observations are consistent with this hypothesis (3, 5, 6, 8).

To further define and characterize the region(s) responsible for ATP-independent MT binding of Ncd, we have generated 12 cDNAs encoding various portions of the Ncd tail (NT) domain and expressed the corresponding proteins in *E. coli*. Since previous work with bacterial-expressed Ncd tail proteins found limited solubility (9), the tail proteins were produced as fusions with thioredoxin (Trx) in an effort to increase protein solubility. The purified, bacterial- expressed Ncd tail proteins were then analyzed for the ability to bind and bundle MTs both with and without attached Trx (TrxNT and NT proteins respectively). Based on the results of these experiments, Ncd amino acid sequences 83-100 and 115-187 contain domains that exhibit ATP-independent MT binding activity with high and lower affinity, respectively. The MT interaction site present in the 83-100 sequence is able to interact with tubulin even when the Ncd tail protein is denatured, while the site present in 115-187 appears to be much more sensitive to protein conformation. It is possible that both sequences contribute to MT binding activity in the full-length Ncd motor.

MATERIALS AND METHODS

Construction of NT Plasmids

DNA fragments encoding different regions of the Ncd tail domain were amplified by PCR from the pET-N2 plasmid (9). NT1-NT4 were generated by pairing a T7 promoter primer (5'-TAA TAC GAC TCA CTA TAG GG-3') with specific reverse primers that contained a *Hind* III site: P2 (5'-AAG CTT GTT GAG GTC CCT TGA GAG GG-3'); P3 (5'-AAG CTT AAT GCT GGG CAA TGA AGG AGC-3'); P4 (5'-AAG CTT TGT TGC TGT TAT TGA CGA AGG-3'); and P5 (5'-AAG CTT AGC AGC AGC CGC GGC TCC TGA-3'), respectively. NT5-NT9 were produced by pairing specific forward primers that contained an *Eco*R I site: P6 (5'-TCA AGG GAA TTC AAC AAT CTG CCC CAG GTG-3'); P7 (5'-GCC TCC CCA GAA TTC ATG AAG TTG GGC CAC-3'); P8 (5'-AGC GCT GAA TTC ATC AAC GAA CTG CGT GGT-3'); P9 (5'-GCT GCT GAA TTC TTG CCC AGC ATT CCC AGC-3'), and P10 (5'-GCG CCT GAA TTC ATA ACA GCA ACA GCT GTC-3'), respectively, with the P5 reverse primer. Finally, NT10-NT12 were generated by pairing the P6, P7, and P8 forward primers with the P4 reverse primer. Amplified DNA fragments were digested with *Eco*R I and *Hind* III and cloned into pET-32 (pET-32c for NT1-NT4; pET-32a for NT5-NT12 (Novagen)). NT proteins were expressed as fusions with Trx and contained two 6X His tags, one between Trx and the NT protein and one at the C-terminus of the fusion protein. For all constructs, sequence analysis of both strands confirmed that the inserts were in-frame and of the correct sequence.

Expression and Purification of the NT Proteins

pET-NT plasmid constructs were transformed into BL21 (DE3) pLysS host cells for protein expression. Overnight cultures of BL21 (DE3) pLysS cells containing pET-NT constructs were diluted 1:100 into LB media supplemented with ampicillin (100 µg/ml) and chloramphenicol (34 µg/ml), grown at 37°C until $A_{550} = 0.5-0.7$, and then expression was induced with the addition of 0.25 mM IPTG. After 4 hours at 22°C, cells were pelleted, washed with AB buffer (20 mM Pipes, pH 6.9, 1 mM MgCl₂, 1 mM EGTA) and kept frozen at -70°C. TrxNT proteins were purified by either ion exchange chromatography (S-sepharose (Pharmacia)) or metal affinity chromatography (Talon, (Clontech)), or a combination of both. For purification on S-sepharose resin, frozen cells were thawed and resuspended in lysis buffer (20 mM Pipes, pH 6.9, 1 mM MgCl₂, 1 mM EGTA, 100 mM NaCl, 1 mM DTT, 1 mM PMSF) including 10 mM MgCl₂ and 40 µg/ml DNase I (Boehringer Mannheim). After 30 minutes on ice, cell lysates were clarified by centrifugation at 20,000 x g for 15 minutes at 4°C, and the supernatants were further centrifuged at 100,000 x g for 15 minutes at 4°C. The resulting high-speed supernatants

were loaded onto 1 ml S-sepharose columns pre-equilibrated with lysis buffer. After washing the column with lysis buffer, bound proteins were eluted with lysis buffer containing 250 mM NaCl (final concentration). Trx, TrxNT1, TrxNT9, and TrxNT12 did not bind to S-sepharose. Whenever metal affinity chromatography was used, alone or in combination with S-sepharose chromatography, EGTA was omitted from all buffers, and 0.5 mM β -mercaptoethanol was substituted for DTT; hence, the Talon lysis buffer was composed of 20 mM Pipes, pH 6.9, 1 mM $MgCl_2$, 100 mM NaCl, 1 mM PMSF, and 0.5 mM β -mercaptoethanol. For purification by metal affinity chromatography, high-speed supernatants were prepared using Talon lysis buffer as above and loaded on 1 ml Talon columns. After washing the column with Talon lysis buffer containing 10 mM imidazole, proteins were eluted with Talon lysis buffer supplemented with 150 mM imidazole. In some cases, eluates from S-sepharose were subjected to further purification with metal affinity resin. After proteins were bound to the Talon resin and the column was washed with Talon lysis buffer containing 250 mM NaCl and/or Talon lysis buffer containing 250 mM NaCl (final concentration) plus 10 mM imidazole, bound proteins were eluted from the Talon resin with Talon lysis buffer containing 250 mM NaCl (final concentration) and 150 mM imidazole. Eluates were dialyzed against AB buffer plus 1 mM DTT. After dialysis the proteins were stored on ice or quick frozen in liquid nitrogen and stored at $-70^{\circ}C$. Proteins were concentrated with Centriprep-30 concentrators (Amicon) as needed.

As appropriate, TrxNT fusion proteins were incubated with 1 U of thrombin per mg of fusion protein (2 hours at $22^{\circ}C$ in AB buffer supplemented with 2.5 mM $CaCl_2$) to cleave the Trx fusion partner (13.8 kDa) from TrxNT proteins to generate non-fusion NT proteins. Thrombin was inactivated by addition of EDTA to 5 mM and PMSF to 1 mM, and cleaved proteins were either used immediately or frozen at $-70^{\circ}C$.

MT Binding and Bundling Assays

MT co-sedimentation assays were performed in AB buffer containing 40 μM taxol (Calbiochem) and 100 $\mu g/ml$ bovine serum albumin (BSA). In a reaction volume of 100 μl , TrxNT or NT proteins (typically 5 - 50 μM final) were mixed with taxol-stabilized MTs (5 μM tubulin final). Control reactions contained no MTs. After incubation for 20 minutes at $22^{\circ}C$, reactions were centrifuged at $100,000 \times g$ for 30 minutes at $25^{\circ}C$ through 25% sucrose in AB buffer plus 10 μM taxol. The supernatants were transferred into tubes containing equal amounts of 2X SDS sample buffer and the pellets were resuspended in 100 μl of 1X SDS sample buffer. Supernatant and pellet fractions were then analyzed by SDS-PAGE or tricine-PAGE (10). For quantitative analysis, the amount of supernatant and pellet samples loaded onto the gels was optimized to ensure a linear relationship between the amount of protein loaded and the intensity of the Coomassie blue stained protein bands. The amount of

TrxNT and NT proteins in the supernatant and the pellet fractions was quantified by measuring the protein band intensities relative to standards with AlphaImager™ 2000 Documentation and Analysis System controlled by AlphaEase™ version 3.3 software (Alpha Innotech Corporation).

Prior to performing MT binding competition experiments, we determined whether the 20 minute incubation time used in the co-sedimentation experiments described above was sufficient to allow the binding reaction to reach equilibrium. The TrxNT6 protein (20 μ M final) was mixed with taxol-stabilized MTs (5 μ M tubulin final) and incubated at 22°C for up to 120 minutes. Samples were taken at various times (10, 20, 30, 45, 60, 90 and 120 minutes) and each sample was subjected to centrifugation as described above except that no sucrose gradient was used. SDS-PAGE and densitometry of Coomassie blue stained proteins were then used to determine the relative amounts of TrxNT6 in the supernatant and pellet fractions for each sample. At each time point, the relative amounts of TrxNT6 in the supernatant and pellet fractions were identical (data not shown), indicating that the binding reaction reached equilibrium within 10 minutes. For the actual competition experiments, TrxNT proteins were mixed (see Figure 7 for final concentrations) either simultaneously or sequentially with taxol-stabilized MTs (5 μ M tubulin final). For simultaneous addition, two different TrxNT proteins were added and the reaction was centrifuged after 20 minutes at 25°C. For sequential addition, one TrxNT protein was incubated with taxol-stabilized MTs for 20 minutes and then a second TrxNT protein was added (diluting the reaction 5%) and the reaction centrifuged after an additional 20 minute incubation at 22°C.

A MT co-sedimentation assay was also used to determine the binding affinity (K_d) and stoichiometry (B_{max}) of selected TrxNT and NT proteins to MTs. In these experiments, the taxol-stabilized MT concentration was kept constant (5 μ M tubulin) and the TrxNT or NT protein concentration was varied to obtain different molar ratios of TrxNT or NT to tubulin (from 1:1 to 10:1). The reactions were incubated for 20 minutes at 22°C then subjected to centrifugation (no sucrose gradient was used) and SDS-PAGE as described above. For each protein, the concentration of tail protein in the supernatant and pellet fractions was determined by densitometry of Coomassie blue stained proteins, and K_d and B_{max} were obtained by fitting the data with a rectangular hyperbola.

TrxNT and NT proteins were assayed for their ability to bundle MTs by mixing taxol-stabilized MTs (5 μ M tubulin) with TrxNT or NT proteins at indicated molar ratios (see Figure 10). After 20 minutes, a 10 μ l sample was removed and prepared for observation by video-enhanced differential interference contrast (VE-DIC) microscopy (11).

Blot Overlay Assay

TrxNT1-TrxNT8 proteins were used in blot overlay assays to examine interactions with tubulin. The TrxNT proteins used in blot overlay assay were purified by metal affinity chromatography as described above except that 20 mM Tris-HCl, pH 8.0, 100 mM NaCl and 8 M urea was used as a denaturing lysis buffer, and proteins were eluted with the same buffer containing 100 mM imidazole. Eluates were further purified by SDS-PAGE using a Mini Prep Cell 491 (BioRad).

Purified TrxNT proteins were separated by SDS-PAGE, transferred to nitrocellulose membranes, and then processed for blot overlay assay as described previously (12, 13) except that AB buffer containing 0.1 % (v/v) Tween 20, 0.1 % (w/v) gelatin, and 1 mM DTT was used as overlay buffer. After washing with Tris-buffered saline the blots were processed for immunodetection as described previously (14).

Estimation of Native Molecular Weights

Sedimentation coefficients ($S_{20,w}$) were determined by sucrose density gradient centrifugation on a 2.5% to 10% linear sucrose gradient in AB buffer containing 1 mM DTT. Gradients were centrifuged at 41,000 rpm for 20 hours at 4°C in a Beckman SW 41 Ti rotor. Bovine pancreas trypsin inhibitor (aprotinin) (1 S), horse heart cytochrome c (1.9 S), chicken egg albumin (3.66 S), bovine serum albumin (4.3 S) were used as standards.

Stokes radii (R_s) were determined by gel filtration chromatography using a 90 cm SR-200 gel filtration resin equilibrated with AB buffer containing 200 mM NaCl and 0.02 % Tween-20. The column was calibrated with standard proteins of known Stokes radii (horse heart cytochrome c (1.2 nm), bovine erythrocyte carbonic anhydrase (2.15 nm), chicken egg albumin (3.05 nm), bovine serum albumin (3.55 nm)). TrxNT and NT proteins were assayed at a concentration of approximately 50 μ M. To determine if these proteins would form oligomers at higher concentrations, a concentration of approximately 120 μ M was used. Native molecular weights were calculated as described by Siegel and Monty (15) using the equation: $M = (6 \pi N R_s S_{20,w}) / (1 - \rho v)$.

RESULTS

Expression and Purification of TrxNT Proteins

In order to identify and characterize the region(s) responsible for ATP-independent MT binding of Ncd, cDNAs coding various portions of the Ncd tail domain were expressed as fusion proteins with Trx (Figure 1). Upon induction with IPTG, all 12 TrxNT constructs produced proteins of the expected molecular weight. TrxNT1-TrxNT4 were only slightly soluble (10-20 %) after lysis, and showed increasing aggregation during attempts at purification by ion exchange or metal affinity chromatography. However, these proteins could be purified to near homogeneity by a denaturing protocol (see Materials and Methods, Blot Overlay Assay). The other TrxNT proteins remained soluble (80-90 %) after lysis and were purified with ion exchange chromatography and/or metal affinity chromatography (Figure 2).

Interaction of TrxNT Proteins with MTs

A MT co-sedimentation assay was used to evaluate the ability of the expressed TrxNT proteins to bind MTs (Figure 3 and 4). TrxNT proteins, either partially purified as high-speed supernatants (Figure 3: TrxNT1-TrxNT4) or further purified by column chromatography (Figure 4: TrxNT5-TrxNT12), were combined with MTs and subjected to centrifugation to separate unbound protein in the supernatant from MT-bound protein in the pellet. Although the exact molar ratio of TrxNT:tubulin in the experiments with high speed supernatant samples was unknown (Figure 3), it was clear that Trx and TrxNT1 were absent from the MT-containing pellet fractions, indicating that these proteins were unable to bind MTs. In contrast, TrxNT2-TrxNT4 were present in the MT-containing pellet fractions and were completely depleted from the high speed supernatants, indicating the ability to bind MTs. With column-purified proteins (Figure 4), binding experiments were performed at TrxNT:tubulin molar ratios of 2:1 (TrxNT5, TrxNT6, TrxNT9-TrxNT12) or 4:1 (TrxNT7 and TrxNT8). At these molar ratios, TrxNT5 and TrxNT6 were found entirely in the pellet fraction, small amounts of TrxNT7, TrxNT8 and TrxNT10 were present in the supernatant fractions, and TrxNT11 was distributed equally between the supernatant and pellet fractions. TrxNT9 and TrxNT12 did not show binding to MTs under the same conditions. In control reactions performed in the absence of MTs, little TrxNT protein was found in any pellet fraction. Addition of 5 mM ATP had no effect on the MT binding ability of TrxNT1-TrxNT6.

Binding of TrxNT5, TrxNT6 or TrxNT11 to MTs was unaffected by storage of the protein on ice (1.5 months) or at -70°C (for as long as 4 months), and was consistent across 4 separate preparations. In contrast, the MT binding activity of TrxNT7, TrxNT8, and TrxNT10 was unstable with prolonged storage at -70°C (2.5 months) or storage on ice (1.5

months), and there was complete (TrxNT7 and TrxNT8) or substantial (TrxNT10) loss in MT binding activity under these conditions. There was also significant variability (from binding to complete loss of binding) in the MT binding activity of TrxNT7 and TrxNT8 among 7 different preparations, and the binding activity of TrxNT10 showed variability (from binding to reduced binding) only with prolonged storage. All results reported in this paper were obtained with proteins that were stored at -70°C for no longer than three weeks.

The interaction of Trx and TrxNT1-TrxNT8 with unassembled tubulin subunits was examined using a blot overlay assay (12, 13). In these experiments, tubulin subunits were used to probe purified TrxNT proteins (see Materials and Methods) that had been separated by SDS-PAGE and transferred to nitrocellulose (Figure 5). Tubulin interacted with TrxNT2 and TrxNT6, but showed no interaction with Trx, TrxNT1, or in most cases, with TrxNT7. Tubulin was also able to bind TrxNT3-TrxNT5, but generally not to TrxNT8; although occasionally preparation-dependent weak interactions were observed with TrxNT7 and TrxNT8 (data not shown).

To investigate the effect of ionic conditions on the MT binding ability of TrxNT proteins, 0-1 M NaCl was added to reactions containing TrxNT and MTs, and binding was evaluated by a MT co-sedimentation assay. Comparative MT binding experiments using 0 and 500 mM NaCl with high speed supernatants of TrxNT2-TrxNT4 proteins showed that bound TrxNT2-TrxNT4 proteins were almost completely released from MTs in the presence of 500 mM NaCl (data not shown). Comparative MT binding experiments using a greater range of NaCl concentrations (0, 250, 500, 750 mM, and 1 M) with TrxNT6 and TrxNT8 resulted in almost complete release of bound TrxNT8 at 250 mM NaCl (Figure 6b), whereas 500 mM NaCl was required to completely release bound TrxNT6 (Figure 6a).

MT binding of selected TrxNT proteins was compared in competition experiments in which two different TrxNT proteins (each at a 4:1 molar ratio to tubulin) were mixed either simultaneously or sequentially with MTs and then subjected to centrifugation (Figure 7). Competition experiments between TrxNT5 and TrxNT6 indicated that if these proteins were added simultaneously, or if either protein was added prior to the other, similar amounts of each protein bound to MTs, suggesting that TrxNT5 and TrxNT6 have similar affinities to MTs. In contrast, TrxNT5 inhibited binding of TrxNT11 to MTs, either when TrxNT5 was added before or simultaneously with TrxNT11. Some binding of TrxNT11 was observed if this protein was added prior to TrxNT5, but the amount of TrxNT11 in the pellet was reduced compared to binding in the absence of competing protein. The competition experiment results with TrxNT5 and TrxNT11 therefore suggested that TrxNT5 has a greater affinity for MTs when compared to TrxNT11. Competition experiments between TrxNT5 and TrxNT9 demonstrated that TrxNT5 was able to bind MTs without interference from TrxNT9, as expected given the earlier result that TrxNT9 did not bind MTs (data not shown).

To obtain a quantitative measure of the binding of Ncd tail proteins to MTs, various concentrations (5 - 50 μ M final) of representative TrxNT proteins (TrxNT6, TrxNT7, TrxNT8, or TrxNT11) were mixed with MTs (5 μ M tubulin) to generate binding reactions at different molar ratios (1:1 to 10:1) of TrxNT to tubulin (Figure 8). After centrifugation to separate supernatants containing unbound TrxNT protein from pellets containing bound TrxNT protein, densitometry of fractions separated by SDS-PAGE was used to determine the concentration of TrxNT protein in both supernatants and pellets (with known amounts of the appropriate TrxNT protein as standards). This data was plotted (Figure 8c) and fit with a rectangular hyperbola to calculate affinity (K_d) and stoichiometry (B_{max}) values. Using TrxNT6 as an example (Figure 8a, b), almost no TrxNT6 was observed in supernatant fractions at TrxNT6:tubulin ratios of 2:1, but TrxNT6 was observed in increasing amounts in the supernatant fractions as the TrxNT6:tubulin ratio was increased from 3:1 to 10:1 (Figure 8a). In comparison, TrxNT6 increased in the pellet fractions as the TrxNT6:tubulin ratio was increased to 3:1 and then remained relatively constant at that ratio as the total TrxNT6:tubulin ratio was increased to 10:1 (Figure 8b). A plot of TrxNT6 in the pellet vs. TrxNT6 in the supernatant and subsequent fitting of the data with a rectangular hyperbola generated a calculated K_d of 0.13 ± 0.03 μ M and a B_{max} of 15.88 ± 0.48 μ M (Figure 8d). Since tubulin was held constant at 5 μ M, the calculated B_{max} corresponded to a maximum binding stoichiometry of 3:1 TrxNT6:tubulin. Using identical methods, K_d and B_{max} values for TrxNT7, TrxNT8, and TrxNT11 were also calculated (data not shown) and the resulting values are presented in Figure 8d. Based on the calculated K_d values, the relative order of MT affinity for the proteins examined was: TrxNT6 > TrxNT11 > TrxNT8 > TrxNT7. This order was consistent with the effects of NaCl observed in Figure 6 and the results of the competition experiments described in Figure 7. The calculated B_{max} values for TrxNT11, TrxNT7 and TrxNT8 indicated that each bound to tubulin at a maximum stoichiometry of 4:1 (Figure 8d).

To evaluate the ability of NT proteins without attached Trx to bind MTs, thrombin was added to MT-bound TrxNT proteins to cleave and release the Trx partner, and the effect of cleavage on MT binding was determined. Thrombin treatment of bound TrxNT6 protein had no effect on the ability of NT6 to remain bound to MTs (Figure 9a). When MT-bound TrxNT5, TrxNT10 and TrxNT11 were treated with thrombin, the corresponding released NT proteins also retained MT binding activity. In contrast, thrombin digestion of MT-bound TrxNT8 resulted in loss of NT8 binding to MTs (Figure 9b). Digestion of MT-bound TrxNT7 to generate NT7 gave similar results to those observed for TrxNT8 and NT8. As expected from previous experiments with Trx (Figure 3), the cleaved Trx protein did not bind MTs as indicated by its presence in the supernatant fractions and absence from pellet fractions. TrxNT6 and TrxNT8 were also incubated with thrombin to cleave the Trx partner prior to incubation with MTs in a co-sedimentation assay (Figure 9c). After enzymatic

treatment, NT6 retained the ability to bind MTs, whereas NT8 lost MT binding activity. Again, Trx showed no MT binding activity and was released to the supernatant fraction. When the binding of NT6, NT7, and NT8 to MTs was quantified as described in Figure 8, K_d and B_{max} values were obtained only for NT6 because NT7 or NT8 did not bind MTs even in the 10:1 reaction. However, the K_d calculated for NT6 (Figure 8d) was similar to that of TrxNT6, and the calculated B_{max} was slightly greater than that of TrxNT6 but the same as the B_{max} determined for TrxNT11, TrxNT7, and TrxNT8 (yielding a NT6:tubulin maximum stoichiometry of 4:1).

Since full-length Ncd and the N-terminal 204 residues of Ncd (N2) were previously found to bundle MTs *in vitro* (8, 9), video-enhanced DIC microscopy was used to examine the ability of the TrxNT proteins to bundle MTs (Figure 10). Reactions were prepared as described in Materials and Methods. High speed supernatants containing TrxNT1 did not bundle MTs (Figure 10b), while high speed supernatants containing TrxNT2, TrxNT3 (data not shown), and TrxNT4 (Figure 10c) produced bundles. Column purified TrxNT6 (Figure 10d), TrxNT7 (Figure 10g), TrxNT5, TrxNT8, TrxNT10, and TrxNT11 (data not shown) were also able to bundle MTs. At a molar ratio of 1:1 (TrxNT:tubulin), all of the TrxNT proteins that exhibited MT binding activity in the co-sedimentation assay (Figure 4), except TrxNT5 and TrxNT10, showed MT bundling activity. TrxNT5 and TrxNT10 started to show MT bundling activity at a 2:1 (TrxNT:tubulin) molar ratio, and at this molar ratio the extent of bundling with TrxNT5 was higher than TrxNT10 based on the presence of single MTs in TrxNT10-containing samples. At very high TrxNT: tubulin molar ratios (4:1), it was possible to detect bundling by eye as a fiber-like precipitate in the sample tube. Two main types of bundles were observed: TrxNT7 and TrxNT8 generated linear, cable-like bundles, while the other MT binding TrxNT proteins produced more compact, matted bundles. Based on the number of single MTs observed, TrxNT10 and TrxNT11 were less effective at bundling MTs compared to TrxNT5 and TrxNT6.

To evaluate the ability of NT proteins to bundle MTs, thrombin-treated TrxNT and NT proteins were used in MT bundling assay. Cleavage of MT-bound TrxNT6 (Figure 10e) did not change its bundling activity, whereas cleavage decreased the MT bundling activity of MT-bound TrxNT5 and TrxNT10. Addition of thrombin-released NT6 (Figure 10f) to MTs showed the same extent of bundling as the TrxNT6 fusion protein, although the appearance of the bundles changed from matted structures to long cable-like structures. Based on the number of single MTs, thrombin-released NT5 showed greater bundling activity than released NT10, but not as high as NT6 (data not shown). Cleavage of MT-bound TrxNT7 (Figure 10h) and TrxNT8 resulted in complete loss of bundling activity, and addition of thrombin-released NT7 (Figure 10i) or NT8 to MTs did not produce MT bundling.

To determine whether TrxNT- and NT-induced MT bundling was due to the formation of dimers or oligomers, the sedimentation coefficients and Stokes radii of the MT

binding TrxNT and NT proteins were determined and used to estimate native molecular weights (Table I). When compared to molecular weights predicted from amino acids sequences, the calculated molecular weights indicated that TrxNT and NT proteins exist as monomers. Running TrxNT or NT proteins in the presence of DTT, or at concentrations in excess of those used in MT co-sedimentation assays (see Materials and Methods) had no effect on the estimated molecular weights.

DISCUSSION

In order to identify the region(s) in the Ncd tail domain that are involved in ATP-independent binding to MTs, 12 TrxNT proteins corresponding to different regions of the tail domain were expressed in *E. coli*. MT co-sedimentation and bundling assays were used to determine the ability of purified TrxNT and thrombin-released NT proteins to interact with MTs. The results (summarized in Table II) indicate that two sites of MT interaction exist in the Ncd tail domain: one in the sequence from amino acid 83-100 and the other in the sequence from 115-187.

Evidence in support of amino acids 83-100 containing a MT interaction site is based on the findings that TrxNT2-TrxNT6, TrxNT10 and TrxNT11, as well as the thrombin-released NT5, NT6, NT10, and NT11 proteins, bind and bundle MTs. A lower limit of 83 is indicated since this represents the N-terminal amino acid of NT6 and NT11, while an upper limit of 100 is based on the fact that NT12 does not show MT binding. Consistent with this assignment, blot overlay experiments indicated that TrxNT2-TrxNT6, which contain the 83-100 sequence, interact with tubulin, while those that lack this sequence either have no interaction (TrxNT1) or interact only weakly (TrxNT7 and TrxNT8) with tubulin. The finding that TrxNT2-TrxNT6 proteins purified in the presence of urea and separated by SDS-PAGE were still able to interact with tubulin suggests that the interaction with MTs is not dependent on correct folding of the polypeptide chain to create the binding site. This conclusion is supported by the consistent MT binding activity of TrxNT2-TrxNT6, TrxNT10, and TrxNT11 across multiple protein preparations and varied storage conditions. However, the finding that not all proteins that contain this site bind and/or bundle MTs equally (Figure 7 and 8; Table II) suggests that, in some of these proteins, the site may either be masked by incorrect folding or that binding may be enhanced by a second MT interaction site.

A second site involved in MT binding is present within the Ncd region spanning amino acids 115-187. This conclusion is based on the findings that TrxNT7 and TrxNT8 show MT binding and bundling activity. However, the situation is more complicated than that described previously for the 83-100 sequence. As discussed above, TrxNT7 and TrxNT8 do not interact significantly with tubulin in the blot overlay assay. In addition, TrxNT7 and TrxNT8 showed significant variability in MT binding activity across different protein preparations and after various storage conditions. Further, cleavage of TrxNT7 and TrxNT8 to generate NT7 and NT8 resulted in complete loss of MT binding and bundling activity. Taken together, these results suggest the presence of a conformation-dependent MT interaction site within the Ncd sequence from 115-187. The ability of this site to bind MTs is clearly dependent on conditions that affect protein conformation (urea, SDS) and is unstable over time. It is likely that the Trx fusion partner, although unable to bind MTs itself, may aid in stabilizing the NT7 and NT8 conformations and thereby the MT binding activity of these proteins. Thus, cleavage of Trx may trigger a conformational change in NT7 and NT8 that

leads to loss of the interaction site and therefore loss of MT binding activity. The presence of aggregated and denatured protein in Figure 10i, in which NT7 had been released by thrombin and then stored at -70°C prior to the experiment, supports this conclusion. Interestingly, denaturation may be enhanced by freezing and storage since cleaved NT7, when viewed immediately after digestion, does not appear denatured and aggregated (Figure 10h).

The mechanism by which TrxNT7 and TrxNT8 bind MTs is also complicated by the fact that neither TrxNT9 nor TrxNT12, which together contain the same sequence as TrxNT7 (100-187), bind MTs. One possible explanation for these results is that the conformation-dependent MT interaction site is located in either NT9 or NT12 but is not correctly folded. Alternatively, a bipartite site may be involved in which amino acids in the sequence spanned by NT9 may need to be brought together with amino acids in NT12 by correct folding. Competition experiments (Figure 7) in which TrxNT5 and TrxNT6 showed equivalent affinity for MTs, but TrxNT5 showed greater affinity than TrxNT11, are consistent with either of these possibilities. TrxNT5 and TrxNT6 contain the 83-100 and 115-187 sequences, while TrxNT11 contains the 83-100 sequence but ends at amino acid 149. Thus it is possible that TrxNT11 is missing either part or all of the conformation-dependent site and that this is the reason for its lower affinity (Figure 7 and 8).

The K_d and B_{max} values obtained for representative Ncd tail proteins (Figure 8) also support the concept of two MT interaction sites. Proteins that contain the 83-100 sequence, and hence the conformation-independent MT interaction site (TrxNT6, NT6, TrxNT11), have a higher affinity for MTs than proteins that contain only the conformation-dependent MT interaction site present in the 115-187 sequence (TrxNT7, TrxNT8). In addition, proteins that contain both sequences (TrxNT6, NT6) have a higher affinity than TrxNT11, which has only the 83-100 sequence. The fact that TrxNT7 and TrxNT8 exhibited reasonably tight binding to MTs, while NT7 and NT8 did not show any MT binding (even at 10:1 molar excess over tubulin) also supports the conclusion that the 115-187 sequence MT interaction site is conformation-dependent. The K_d values calculated for TrxNT6, NT6 and TrxNT11 are similar to or lower than the K_d values reported for the AMP-PNP or apyrase-induced tight binding of kinesin and Ncd motor domains to MTs (14, 16, 17,) and the K_d values reported for the binding to MTs of full length tau and tau fragments that contain the MT-binding site (18, 19), and therefore support the concept of a tight, specific interaction. A more surprising result was the B_{max} values and the corresponding NT:tubulin maximum binding stoichiometries of 3:1 to 4:1. Based on these numbers, it appears that there are 4 potential binding sites per tubulin dimer (presumably 2 each per α - and β -tubulin) and that TrxNT6, perhaps due to steric-hindrance, cannot fill all possible binding sites. The fact that all proteins for which B_{max} was calculated bind at a 4:1 stoichiometry suggests that all are binding to the same sites on tubulin (albeit with different affinities). Further, there was no evidence of cooperative binding and the data was best fit with a rectangular hyperbola,

suggesting that all 4 sites on the dimer are identical in terms of affinity (Figure 8c). Given the ionic nature of binding (see following paragraph) and the large number of acidic residues in the C-terminal domains of α - and β -tubulin that are exposed on the outer surface of a MT, it is likely that each of the binding sites on tubulin represents a cluster of acidic residues. Two such clusters are present in both tubulin monomers; one precedes the H12 helix and the other is present at the extreme C-terminus (20). These stoichiometries are higher than reported for other MT binding proteins: motor domains typically saturate at 1 per tubulin dimer (see reference 14), while tau saturates at 0.5 per tubulin dimer (19). This raises the issue of how 4 separate protein molecules may pack along the dimer. Given the relatively large number of proline residues in the Ncd tail, it is possible that the MT interaction sites protrude from the bulk of the tail domain and that this may allow 4 proteins to bind to one tubulin dimer without significantly interfering with each other. In addition, if the acidic clusters present in the C-terminal domains of α - and β -tubulin are involved in binding the Ncd tail, the distance between the two clusters in each monomer could be nearly the length (4 nm) of the monomer (20), while the distance between clusters on adjacent monomers may vary depending on the flexibility of these regions, and these two factors could allow access to all four sites simultaneously. One final point in considering these stoichiometry values is that Ncd exists as a dimer and this structure may force constraints on the distance between tail domains, making it is unlikely that full length Ncd could fill all possible binding sites on the dimer. Future binding experiments with a stalk-tail dimer of Ncd should help address this issue.

Given the high percentage (17%) of basic amino acids in the 200 amino acids of the Ncd tail domain and the large number of acidic amino acids exposed on the outer surface of MTs (21, 22), it is reasonable to expect that the Ncd tail interaction with MTs is ionic in nature. The effect of NaCl on the MT binding of TrxNT proteins is consistent with this hypothesis (Figure 6). Further, the finding that a higher concentration of NaCl is required to inhibit the MT binding of TrxNT6 as compared to TrxNT8 is consistent with two MT interaction sites (with TrxNT6 having both and TrxNT8 having one). EDC cross-linking between TrxNT7 or TrxNT8 and MTs also supports an ionic interaction (A. Karabay and R. A. Walker, unpublished observations).

In addition to a large number of basic amino acids, the Ncd tail is also rich in proline (22 of 200 or 11%). The abundance of basic amino acids and prolines is a property shared by many MT-associated proteins (MAPs), such as MAP2 and tau, that bind and regulate MT assembly (see references 23 and 24 for review). MAP2 and tau share 3-4 imperfect amino acid repeats that are involved in binding to MTs. Each repeat is composed of 31 amino acids and contains several basic residues as well as a distinctive Pro-Gly/Lys-Gly-Gly motif (25, 26). A recent study also demonstrated the involvement of the proline-rich region of tau (and by inference, MAP2) in MT binding and provided clear evidence for the importance of

specific basic residues (²¹⁵K, ²¹⁶K and ²²¹R) and adjacent proline residues in MT interactions (24). Although no repeats are obvious in the Ncd tail, there are clusters of basic residues flanked by proline residues. Analysis of the Ncd 83-100 sequence (⁸³MKLGHRAKLRRSRSA¹⁰⁰) indicates that this region contains 6 basic residues (or 33% of the region) and has 2 adjacent proline residues (⁸⁰PEP⁸²). Additional basic clusters are also present in the Ncd sequence from 115-187 in the following regions: ¹⁰⁴RGNKR¹⁰⁸, ¹²¹KVSR¹²⁴, ¹³⁵RLVR¹³⁹, and ¹⁵⁰VKRPPVTRPAPRAAGGAAKKPAGTG¹⁷⁵. The nearest proline residues to the 104-108 and 121-124 clusters are ¹¹⁶PSIP¹¹⁹, while ¹³⁹PAAP¹⁴² are closest to the 135-139 cluster. The largest cluster, residues 150-175, contains 6 basic residues as well as 2 adjacent (¹³⁹PAAP¹⁴²) and 4 internal proline residues (¹⁵³PPVTRPAP¹⁶⁰). The internal proline residues are part of a sequence in Ncd (¹⁵¹KRPPVTR¹⁵⁷) that is similar to the MT binding sequence in the proline-rich region of tau (²¹⁵KKVAVVR²²¹) (19). The relationship between the basic and proline clusters in Ncd and tau/MAP2 is unclear and awaits further characterization of the specific amino acids involved in MT binding. However, in preliminary experiments using video microscopy and co-sedimentation assays, we have found that TrxNT6 and NT6 promote MT assembly (A. Karabay and R.A. Walker, unpublished observations). Of related interest, Kar3, another C-terminal kinesin superfamily motor, may also interact with MTs via the tail domain (22). The tail region of Kar3 resembles that of Ncd in terms of the percentage of prolines (8.2%) and basic (16.4%) amino acids, and similar regions of basic residue clusters with adjacent proline residues are present within amino acids 5-80 of the Kar3 tail (27).

As implied above, and consistent with TrxNT1's failure to bind MTs, amino acids 27-63 do not appear to contain a MT binding site. However, this region does appear to affect the solubility of expressed NT proteins. Fusion to Trx did not substantially improve the solubility of the constructs that contained amino acids 27-63 (TrxNT1-TrxNT4). TrxNT2-TrxNT4 were consistently insoluble in different preparations, while TrxNT1 showed variable solubility in different preparations. In comparison, TrxNT proteins, which did not contain this region, showed greater solubility. Protein sequence analysis showed that this region is rich in hydrophobic and polar-uncharged amino acids and has only three charged amino acids (R²⁸, R⁵⁹, and D⁶⁰).

All TrxNT proteins that bound MTs also bundled MTs, and all NT proteins that retained MT binding ability after thrombin cleavage were also able to bundle MTs (Table II). The differences in the structure (cable-like with TrxNT7 and TrxNT8, matted with all other TrxNT and NT proteins that showed MT binding activity) and extent (more free MTs with TrxNT7, TrxNT8, TrxNT10, TrxNT11, NT10, and NT11 than TrxNT5, TrxNT6, NT5, and NT6) of MT bundling may be an indication of differences in the stability and/or accessibility of MT interaction sites. Alternatively, these differences may be a function of having one versus two of the MT interaction sites.

How do TrxNT and NT proteins induce MT bundling? One possible mechanism could be dimerization of the proteins to form cross-bridges between MTs. However, based on the results of gel filtration and sedimentation experiments (Table I), TrxNT and NT proteins appear to exist as monomers. Although this does not exclude the possibility that TrxNT and NT proteins may form dimers or oligomers in the presence of MTs, it is also possible that the proteins form bundles by shielding charges. As discussed above, it is likely that the positively-charged MT binding sites in the Ncd tail interact with the negatively-charged C-terminus of α - and/or β -tubulin. It has been proposed that MT bundling could result from the neutralization of acidic carboxyl terminal region of tubulin, which can be achieved by binding of MAPs including tau (28, 29). Consistent with this hypothesis, binding of the monomeric motor domain of Ncd to MTs can also induce MT bundling (K. Phelps and R. A. Walker, unpublished results). Hence it is possible that TrxNT and NT proteins form bundles not by physically connecting separate MTs, but rather by masking tubulin domains that otherwise inhibit MT bundling. Although bundles could be formed *in vitro* by charge neutralization, it is likely that MT bundling as part of spindle organization *in vivo* would occur through a mechanism in which the motor domains of Ncd interact with one MT and the tail domains interact with a second MT, and thereby cross-link the two filaments.

In conclusion, there appear to be two regions in the Ncd tail that can interact with MTs. Given the importance of protein conformation in one of these regions, it is likely that MT binding is not simply due to nonspecific charge interactions, but rather that structural complexity is important for MT binding. Intramolecular interactions between basic and proline-rich regions may bring these two MT interaction sites together in the folded protein to form a single MT binding site. Thus, determination of the 3D structure of the Ncd tail region should help elucidate the interactions of the tail domain with MTs. In the future, site directed mutagenesis experiments will also be needed to determine the amino acid residues essential for MT binding. Finally, since Ncd has not yet been purified from native cells, it is conceivable that the MT interaction of the tail region could be regulated by non-motor subunits or associated proteins.

FIGURE 1: Schematic representation of TrxNT proteins.

Full length Ncd consists of 700 amino acids (1). N2 corresponds to the tail region and encodes amino acids 1-204 of Ncd (9). The region encompassed by NT proteins in this study corresponds to amino acids 27-187. TrxNT1-TrxNT4 start from amino acid 27 and include different lengths of deletions at the C-terminus. TrxNT5-TrxNT9 include different lengths of N-terminal deletions in the region starting from amino acid 27. TrxNT10-TrxNT12 contain combined N- and C-terminal deletions. The expected molecular weights (kDa) are: 23,116 (TrxNT1); 29,132 (TrxNT2); 32,122 (TrxNT3); 34,459 (TrxNT4); 31,977 (TrxNT5); 29,805 (TrxNT6); 27,838 (TrxNT7); 26,258 (TrxNT8); 23,243 (TrxNT9); 28,641 (TrxNT10); 26,469 (TrxNT11); 24,501 (TrxNT12). Trx from pET32 is 20,401 kDa.

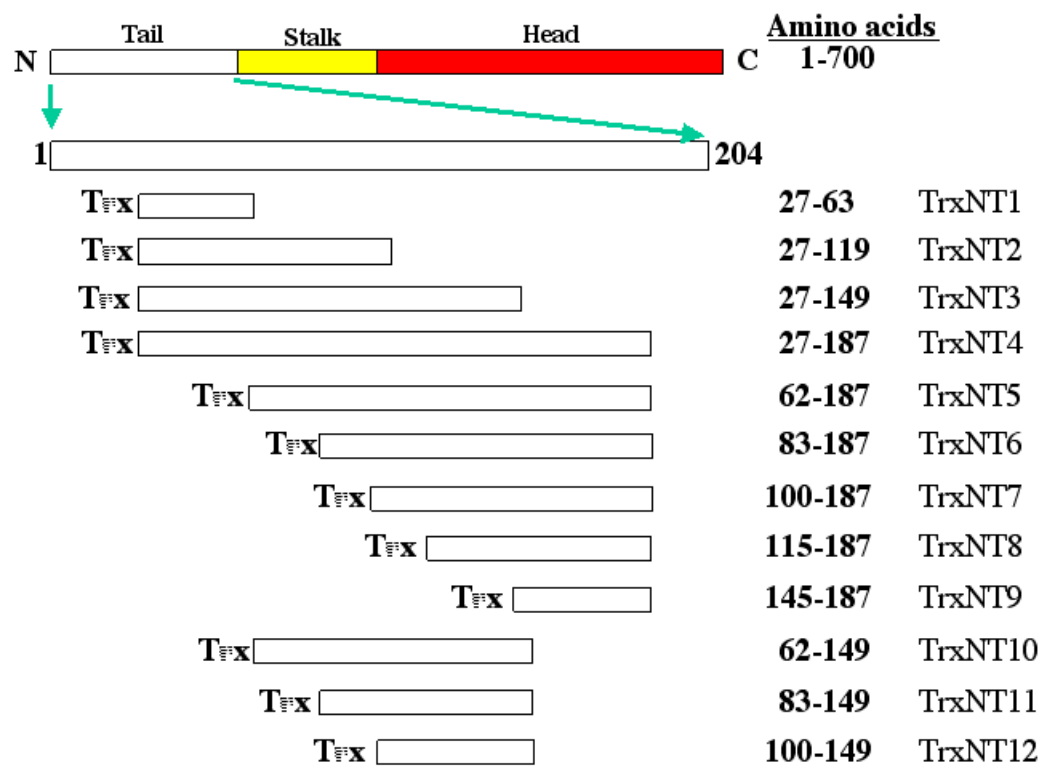


FIGURE 2: Example purification of TrxNT proteins.

Bacterial cell lysate (lane 1) induced to express TrxNT6 was centrifuged to produce low speed (lane 2) and high speed (lane 3) supernatants as described in Materials and Methods. The high speed supernatant was then passed over an S-sepharose column (lane 4 shows proteins that did not bind the resin), and the column was then washed with lysis buffer (lane 5). Bound proteins were eluted (lane 6 and 7, peak elution fractions), then combined (lane 8), and passed over Talon metal affinity resin (lane 9, flow through). After washing the column (lane 10), bound proteins were eluted with Talon elution buffer (lane 11 and 12, peak elution fractions). Final eluates from Talon resin were concentrated 50-fold relative to the lysate. Samples were run on a 9% SDS-polyacrylamide gel, and stained with Coomassie Blue. M: Molecular weight marker (indicated in kDa).

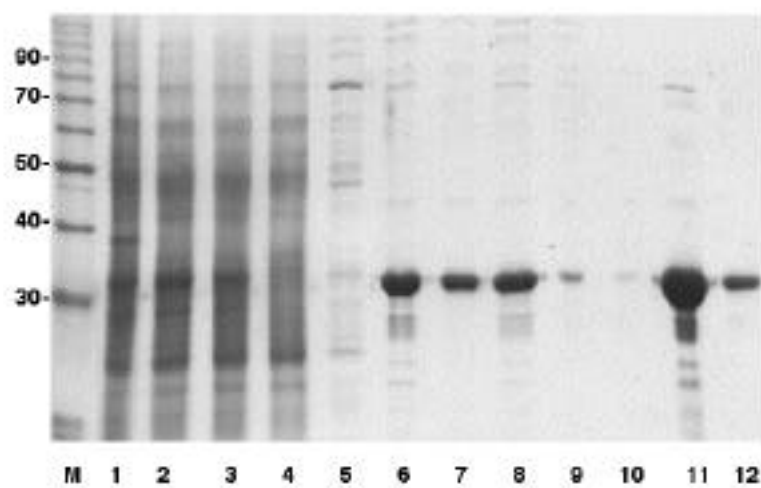


FIGURE 3: MT binding of Trx and TrxNT1-TrxNT4 proteins.

High speed supernatant samples of Trx and TrxNT1-TrxNT4 proteins were divided into two reactions, and taxol and taxol-stabilized MTs were added to one (+MTs), while AB was added to the other (-MTs). After 20 minutes, the reactions were centrifuged as described in Materials and Methods, and supernatant (Panel a) and pellet (Panel b) fractions were separated by SDS-PAGE and proteins stained with Coomassie Blue. Lanes 1-4 indicate corresponding TrxNT protein. The positions of thioredoxin (T) and TrxNT1 (horizontal line) are indicated in Panel a, and the positions of TrxNT2-TrxNT4 proteins are indicated (horizontal lines) in Panel b. TrxNT2-TrxNT4 bands in Panel a supernatant fractions were obscured by endogenous *E. coli* proteins. Tubulin is indicated by an asterisk. Molecular weight markers (M) are indicated in kDa.

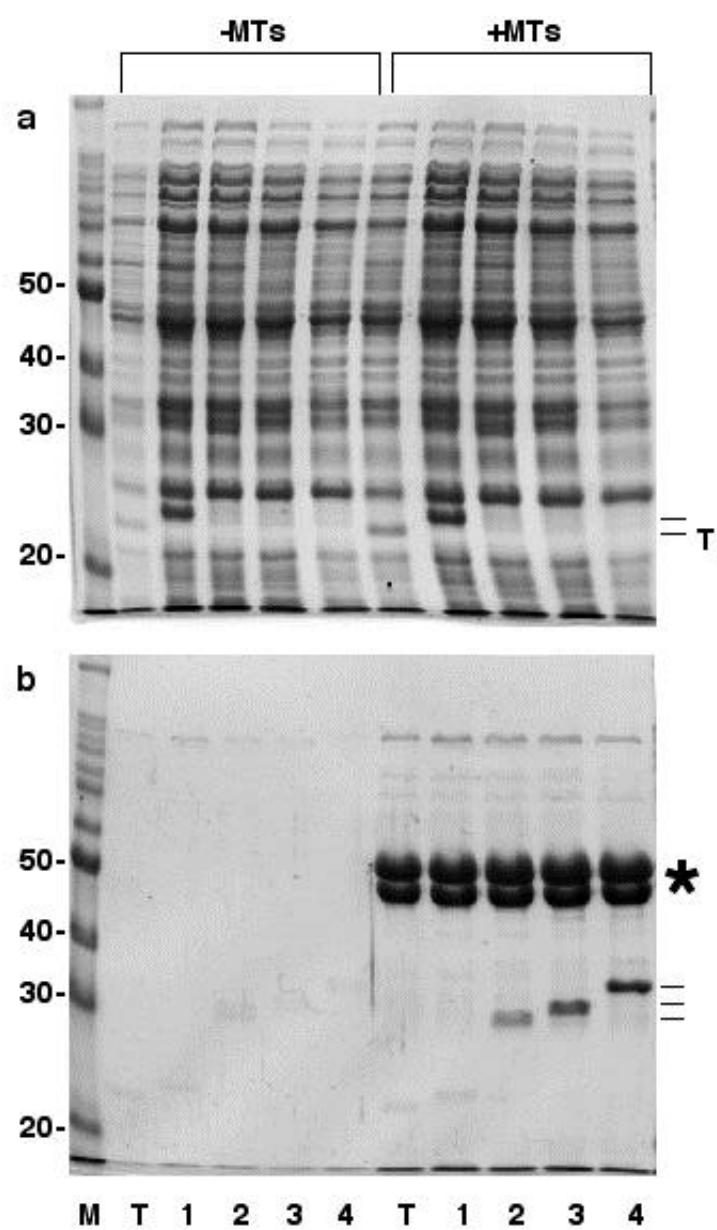


FIGURE 4: MT binding of TrxNT5-TrxNT12 proteins.

Column purified TrxNT proteins were used at 2:1 (TrxNT5, TrxNT6, and TrxNT9-TrxNT12) or 4:1 (TrxNT7 and TrxNT8) molar ratios in a MT co-sedimentation assay as described in the Materials and Methods. Panel numbers indicate corresponding TrxNT protein. Supernatant (S) and pellet (P) fractions in the absence (left column of each panel), and presence (right column of each panel) of MTs were separated on 8% (5-8, and 11), 9% (9 and 12), or 10% (10) SDS- polyacrylamide gels. The location of tubulin in each panel is indicated by an asterisk.

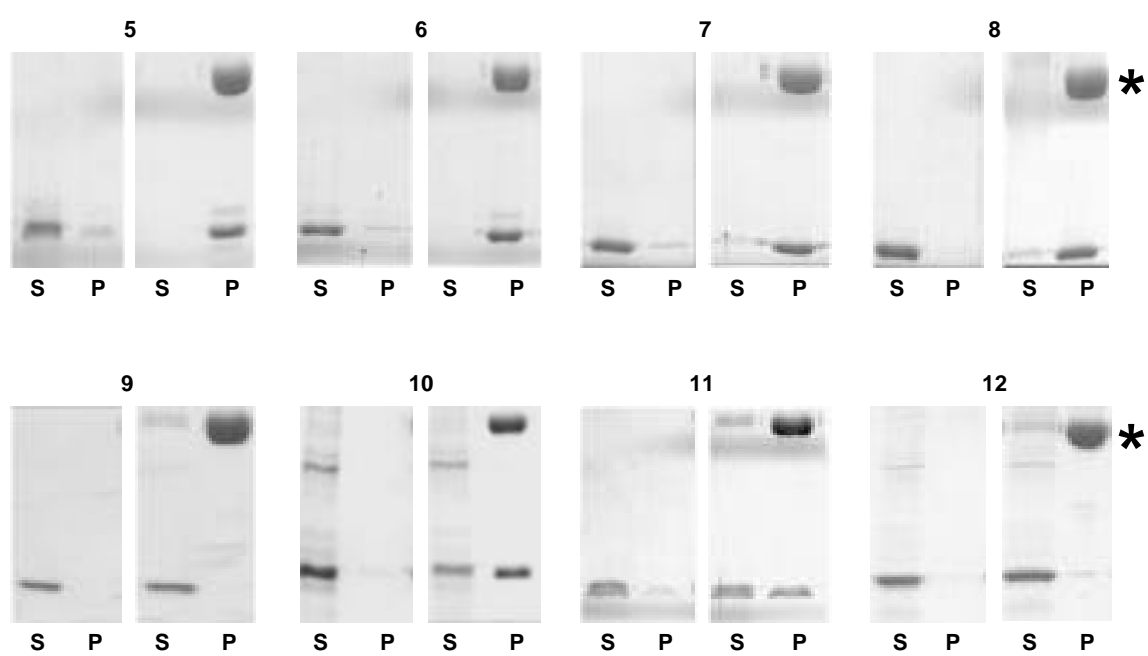


FIGURE 5: Interaction of tubulin with Trx-NT proteins in a blot overlay assay.

Column purified TrxNT proteins were separated by SDS-PAGE, transferred onto nitrocellulose membranes, and processed for overlay with tubulin and subsequent immunodetection as described in the Materials and Methods. T: Thioredoxin. Lane numbers indicate the corresponding TrxNT protein, and the dots indicate positions of transferred proteins as detected by Ponceau-S red staining.

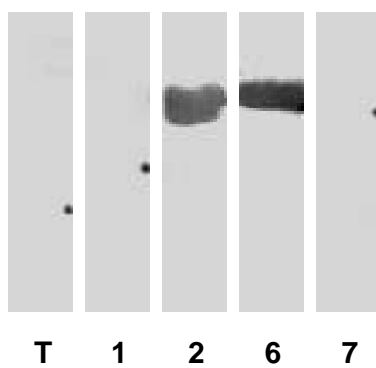


FIGURE 6: The effect of NaCl on TrxNT6 and TrxNT8 binding to MTs.

MT co-sedimentation assay was carried out as described in the Materials and Methods, and the pellets were resuspended with AB buffer containing 40 μ M taxol and the indicated NaCl concentration (mM). After 15 minutes, samples were centrifuged as previously described and supernatant (S) and pellet (P) fractions were analyzed by SDS-PAGE. Panel a: TrxNT6. Panel b: TrxNT8. The positions of tubulin (asterisk), TrxNT6 (arrowhead) and TrxNT8 (solid arrow) are indicated.

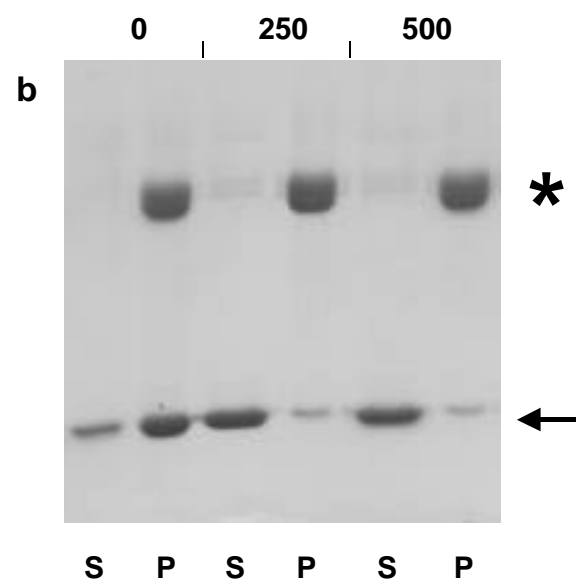
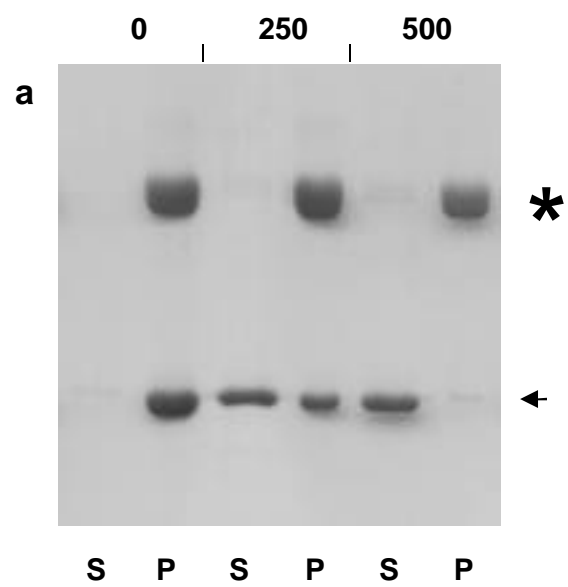


FIGURE 7: Competition of TrxNT proteins for binding to MTs.

Column purified TrxNT5 was added either simultaneously or sequentially with TrxNT6 or TrxNT11, and the binding of each protein was evaluated by MT co-sedimentation assay. All proteins were added at 4:1 TrxNT:tubulin molar ratio. Upper row (panel a-e) shows competition between TrxNT5 and TrxNT6, and lower row (panel f-j) shows competition between TrxNT5 and TrxNT11. Supernatant (first lane of each panel) and pellet (second lane of each panel) fractions in the presence of MTs are shown. Panel a and f: TrxNT5 alone. Panel b and g: TrxNT6 and TrxNT 11 alone respectively. Panel c: TrxNT5 and TrxNT6 were added simultaneously. Panel h: TrxNT5 and TrxNT11 were added simultaneously. Panel d and i: TrxNT5 was added prior to TrxNT6 or TrxNT11 respectively. Panel e and j: TrxNT6 or TrxNT11 was added prior to TrxNT5 respectively. The positions of tubulin (asterisk), TrxNT5 (arrowhead), TrxNT6 (open arrow), and TrxNT11 (solid arrow) are indicated.

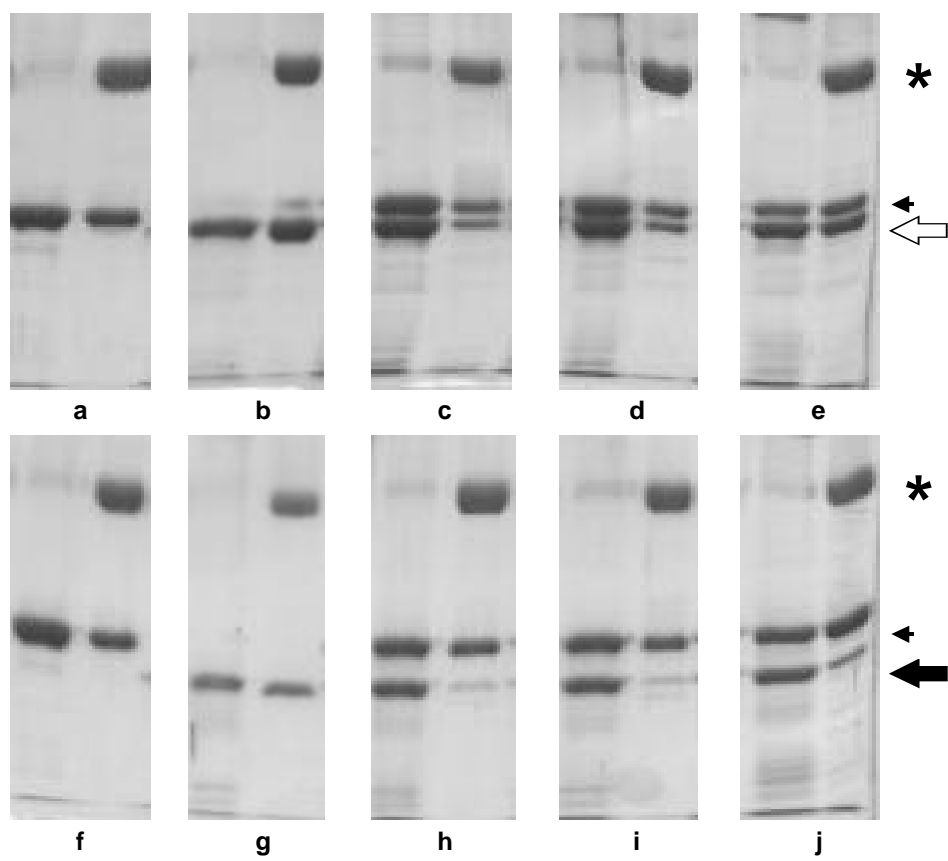


FIGURE 8: MT binding affinity and stoichiometry of TrxNT6 protein.

TrxNT6 (5-50 μ M final) was mixed with taxol-stabilized MTs (5 μ M final) and centrifuged after a 30 minute incubation at 22°C (see Materials and Methods). Supernatant (a) and pellet (b) fractions were then separated on 10% SDS-polyacrylamide gels and the amount of TrxNT6 in each fraction was determined. The TrxNT6:tubulin ratio is indicated below Panel b for both supernatant and pellet fractions. Tubulin (asterisk) and TrxNT6 (arrowhead) bands are indicated. The bands adjacent to the a and b labels are BSA. The data were plotted as shown in (c) and fit with a rectangular hyperbola to determine K_d and B_{max} values (d). TrxNT7, TrxNT8, TrxNT11 and NT6 (see Figure 9) were examined using the same approach (data not shown), and the calculated K_d and B_{max} values for those proteins are also presented in (d).

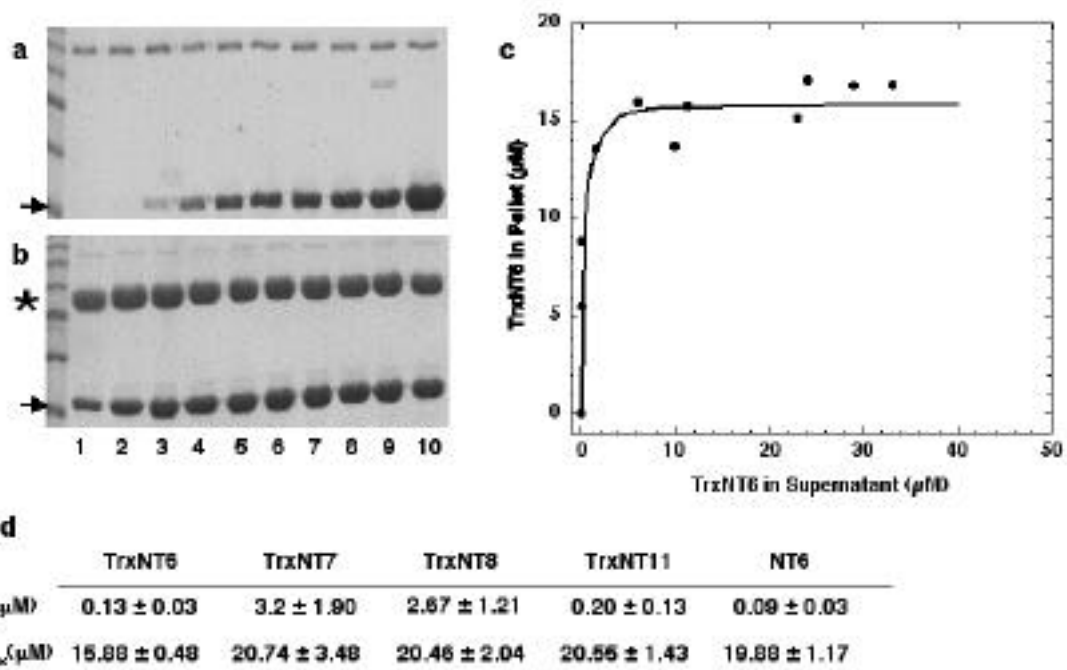


FIGURE 9: MT binding of thrombin-cleaved NT6 and NT8 proteins.

To evaluate the binding of NT proteins to MTs, TrxNT6 and TrxNT8 were treated with thrombin either while bound to MTs (a) or prior to incubation with MTs (b). The numbers above the sections of each panel denote the corresponding TrxNT or NT protein (6 or 8) shown. For each protein in Panel a, lane 1 shows the pre-thrombin mixture of the TrxNT6 or TrxNT8 protein bound to MTs; lane 2 shows the results of thrombin cleavage of each MT-bound TrxNT protein; lane 3 shows the supernatant fraction of each cleaved TrxNT protein after centrifugation; and lane 4 shows the pellet fraction of each cleaved TrxNT protein after centrifugation. In Panel b, lanes 1 and 4 show the initial samples of cleaved NT6 and NT8; lanes 2 and 5 show the supernatant fractions of cleaved NT6 and NT8 after incubation with MTs and subsequent centrifugation; lanes 3 and 6 show the pellet fractions of cleaved NT6 and NT8 after incubation with MTs and subsequent centrifugation. Samples were separated by tricine-PAGE and stained with Coomassie Blue. The position of tubulin is indicated by an asterisk. The TrxNT proteins (TrxNT6 or TrxNT8) are indicated by solid arrows, and NT6 (dotted line), NT8 (arrowhead) and thioredoxin (dashed line) are also indicated.

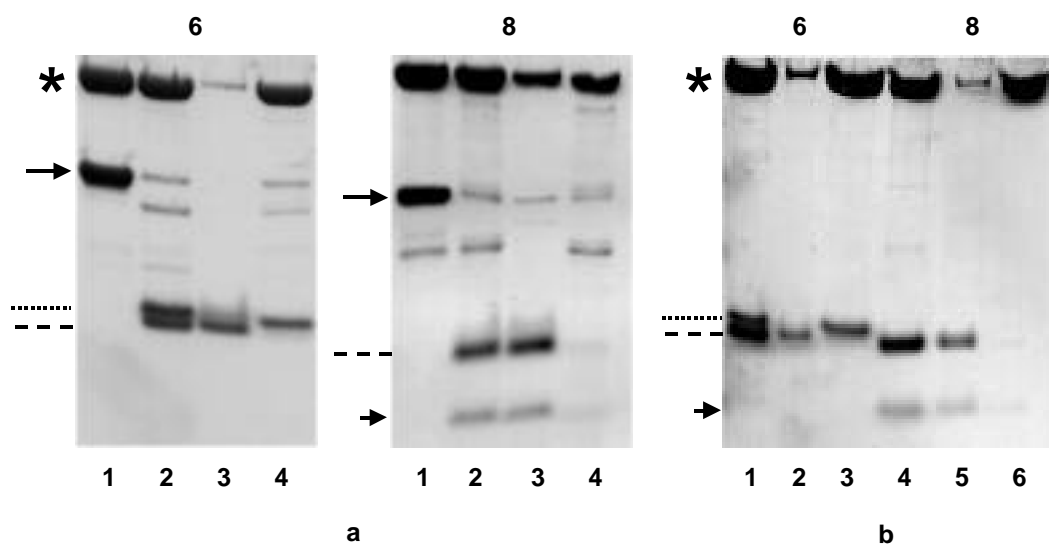


FIGURE 10: MT bundling by selected TrxNT and NT proteins.

Panel a: MTs. Panel b: TrxNT1. Panel c: TrxNT4. Panel d: TrxNT6 . Panel e: cleavage of MT-bound TrxNT6. Panel f: NT6. Panel g: TrxNT7. Panel h: cleavage of MT-bound TrxNT7. Panel i: NT7 protein at 2:1 molar ratio. High speed supernatant samples of TrxNT1 and TrxNT4 were used for MT bundling assay, and samples shown in the upper row were diluted tenfold before observation. Middle row shows MT bundling ability of TrxNT6 and NT6 used at 2:1 molar ratio to tubulin. Lower row shows MT bundling ability of TrxNT7 (panel g) and NT7 (panel h and i) used at 1:1 and 2:1 molar ratios to tubulin respectively. Each panel is 25 μm wide.

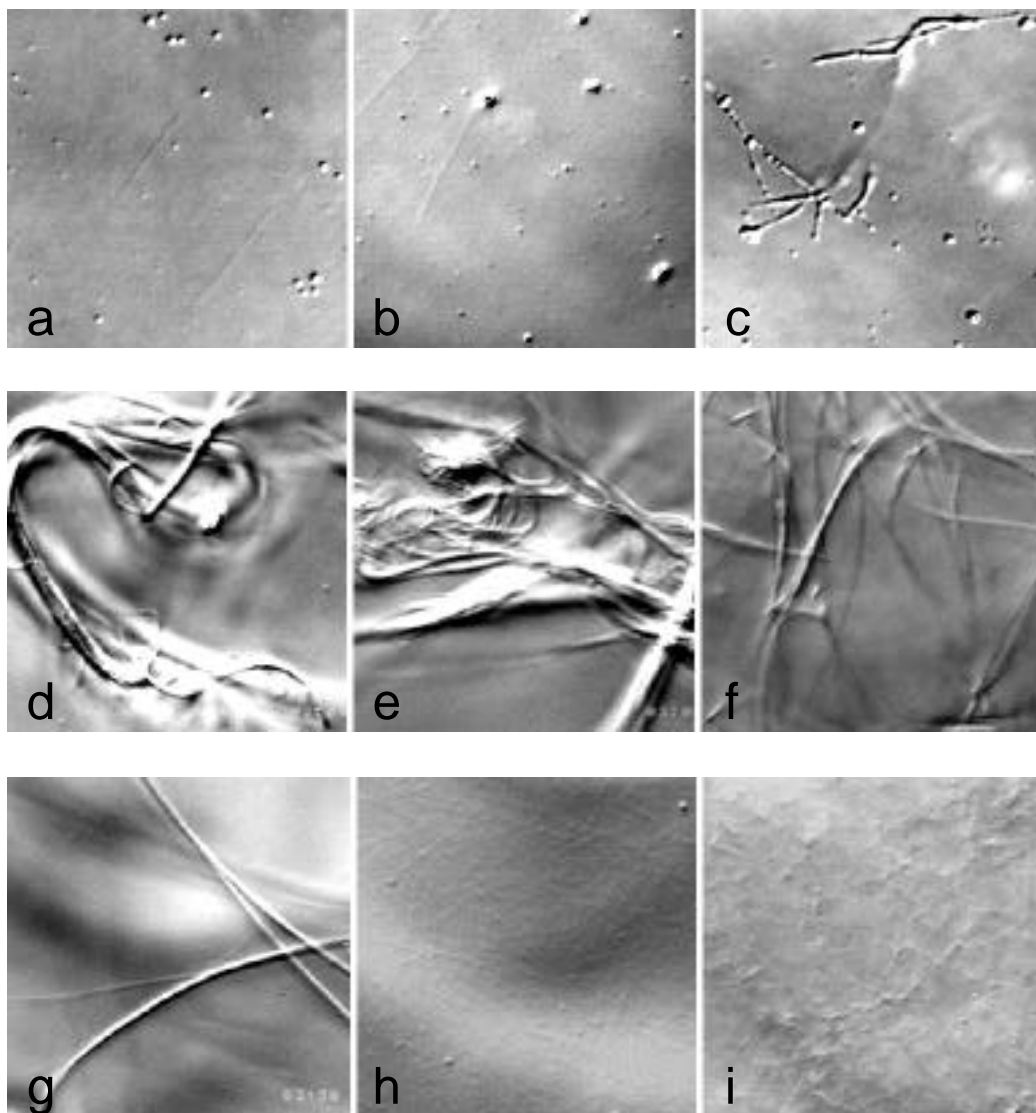


TABLE 1: Physical Properties of Ncd Tail Proteins

	<u>TrxNT</u>				<u>NT</u>			
	Polypeptide MW	R _s	S _{20,w}	Calculated MW	Polypeptide MW	R _s	S _{20,w}	Calculated MW
NT5	31977	35.2	1.9	27597	18209	*<12	1.7	**
NT6	29805	33.8	1.9	26499	16037	*<12	1.5	**
NT7	27838	32.7	1.9	25637	14069	*<12	1.3	**
NT8	26258	32.2	1.9	25245	12489	*<12	1.3	**
NT10	28641	30.1	1.9	23599	14872	*<12	1.3	**
NT11	26469	28.9	ND	ND	12701	*<12	ND	**

Polypeptide MW was determined from the protein sequence.

R_s: Stokes radius (A°), S_{20,w}: sedimentation coefficient.

Calculated MW was determined as described in Materials and Methods.

*: Stokes radii of NT proteins were smaller than that of the lowest standard used (horse heart cytochrome, 12 A°); therefore precise calculated MW (**) of NT proteins could not be determined. TrxNT6 and NT6 proteins were each run twice, and other proteins were run once. ND: not determined.

TABLE 2: Summary of MT Binding and Bundling Assays

a)	<u>TrxNT</u>	
	<u>Binding</u>	<u>Bundling</u>
Trx	–	–
NT1	–	–
NT2	+	+
NT3	+	+
NT4	+	+
NT5	+	+
NT6	+	+
NT7	+	+
NT8	+	+
NT9	–	–
NT10	+	+
NT11	+	+
NT12	–	–

b)	<u>Thrombin-cleaved</u>		<u>Thrombin-cleaved</u>	
	<u>MT-bound TrxNT</u>		<u>NT</u>	
	<u>Binding</u>	<u>Bundling</u>	<u>Binding</u>	<u>Bundling</u>
NT5	+	+	ND	+
NT6	+	+	+	+
NT7	–	–	ND	–
NT8	–	–	–	–
NT10	+	+	ND	+
NT11	+	ND	ND	ND

Panel a indicates MT binding and bundling activities of all TrxNT proteins. Panel b, right column indicates the effect of thrombin cleavage on MT binding and bundling activities of MT-bound TrxNT proteins. Panel b, left column indicates MT binding and bundling activities of cleaved NT proteins. ND: not determined.

LITERATURE CITED

1. Endow, S. A., Henikoff, S., & Soler-Niedziela, L. (1990) *Nature* 345, 81-83.
2. McDonald, H. B., & Goldstein, L. S. B. (1990) *Cell* 61, 991-1000.
3. Hatsumi, M., & Endow, S. A. (1992) *J. Cell Sci.* 103, 1013-1020.
4. Endow, S. A. (1993) *TIG* 9, 52-55.
5. Matthies, H. J. G., McDonald, H. B., Goldstein, L. S. B., & Theurkauf, W. E. (1996) *J. Cell Biol.* 134, 455-464.
6. Endow, S. A., & Komma, D. J. (1997) *J. Cell. Biol.* 137, 1321-1336.
7. Walker, R. A., Salmon, E. D., & Endow, S. A. (1990) *Nature* 347, 780-782.
8. McDonald, H. B., Stewart, R. J., & Goldstein S. B. (1990) *Cell* 63, 1159-1165.
9. Chandra, R., Salmon, E. D., Erickson, H. P., Lockhart, A., & Endow, S. A. (1993) *J. Biol. Chem.* 268, 9005-9013.
10. Schagger, H., & Jagow, G. V. (1987) *Anal. Biochem.* 166, 368-379.
11. Walker, R. A., O'Brien, E. T., Pryer, N. K., Soboeiro, M. F., Voter, W. A., Erickson, H. P., & Salmon, E.D. (1988) *J. Cell Biol.* 107, 1437-1448.
12. Boucher, D., Larcher, J-C., Gros, F., & Denoulet, P. (1994) *Biochemistry* 33, 12471-12477.
13. Larcher, J-C., Boucher, D., Lazereg, S., Gros, F., & Denoulet, P. (1996) *J. Biol. Chem.* 271, 22117-22124.
14. Walker, R. A. (1995) *Proc. Natl. Acad. Sci. USA* 92, 5960-5964.
15. Siegel, L. M., & Monty, K. J. (1965) *Biochim. Biophys. Acta* 112, 346-362.
16. Crevel, I. M.-T., Lockhart, A., & Cross, R. A. (1996) *J. Mol. Biol.* 257, 66-76
17. Moore, J. D., Song, H., & Endow, S. (1996) *The EMBO Journal* 15 (13), 3306-3314
18. Goode, B., & Feinstein, S. C. (1994) *J. Cell Biol.* 124 (5), 769-782
19. Gustke, N., Trinczek B., Biernat, J., Mandelkow E.-M., & Mandelkow E. (1994) *Biochemistry* 33 (32), 9511-9522
20. Nogales, E., Wolf, S. G., & Downing K. H. (1998) *Nature* 391, 199-203
21. Sackett, D. L., & Wolff, J. (1986) *J. Biol. Chem.* 261, 9070-9076.
22. Britling, F., & Little, M. (1986) *J. Mol. Biol.* 189, 367-370.
23. Delacourte, A., & Buee L. (1997) *Intl. Rev. Cytol.* 171, 167-210.
24. Goode, B. L., Denis, P. E., Panda, D., Radeke, M. J., Miller, H. P., Wilson, L., & Feinstein, S. C. (1997) *Mol. Biol. Cell* 8, 353-365.
25. Lewis, S. A., Wang, D., & Cowan, N. J. (1988) *Science* 242, 936-939.
26. Ennulat, D. J., Liem, R. K. H., Hashim, G. A., & Shelanski M. L. (1989) *J. Biol. Chem.* 264, 5327-5330.
27. Meluh, P. B., & Rose, M. D. (1990) *Cell* 60, 1029-1041.
28. Scott, C. W., Klika, A. B., Lo, M. M. S., Norris, T.E., & Caputo, C. B. (1992) *J. Neurosci. Res.* 33, 19-29.

29. Brandt, R., & Lee, G. (1993) *J. Cell Biol.* 268, 3414-3419.

CHAPTER 3

THE NCD TAIL DOMAIN PROMOTES MICROTUBULE ASSEMBLY AND STABILITY

This work was previously published as:

A. Karabay and R. A. Walker* (1999)

Biochemical and Biophysical Research Communications, 258, 39-43

Department of Biology, Virginia Polytechnic Institute and State University, Blacksburg, VA,
USA

* Corresponding author: Dr. Richard A. Walker

Department of Biology

Virginia Polytechnic Institute and State University

Blacksburg, VA 24061-0406

Phone: (540) 231-3803

Fax: (540) 231-9307

E-mail: rawalker@vt.edu

ABSTRACT

Non-claret disjunctional (Ncd) is a *Drosophila* kinesin-like motor required for spindle assembly and maintenance in oocytes and early embryos. Ncd has an ATP-independent microtubule binding site in the N-terminal tail domain as well as an ATP-dependent microtubule binding site in the C-terminal motor domain. The Ncd tail domain shares many properties with the microtubule-associated proteins that regulate microtubule assembly, including microtubule binding and bundling activity and an abundance of basic and proline residues. Given these similarities, we examined the ability of Ncd tail domain proteins to promote MT assembly and stability. The results indicate that the Ncd tail domain can promote MT assembly and stabilize MTs against conditions that induce MT disassembly, and suggest that Ncd may influence MT dynamics within the spindle.

INTRODUCTION

Non-claret disjunctional (Ncd) is a *Drosophila* minus end-directed, kinesin-like motor protein required for spindle assembly and maintenance during meiosis in oocytes and early mitosis in embryos (1-6). The C-terminal motor domain (residues 356-700) contains an ATP-dependent microtubule (MT) binding site, and is attached to the N-terminal tail domain (residues 1-200) by an α -helical stalk domain responsible for subunit dimerization (1, 2). The Ncd tail (NT) domain sequence is unique among kinesin superfamily motors and is rich in basic and proline residues (1,2,7). Based on *in vitro* experiments in which Ncd bundled MTs (8), and NT proteins both bound and bundled MTs (7), it has been suggested that the Ncd tail contains an ATP-independent MT binding site (7, 8) that may aid in MT bundling and/or the sliding of a “cargo” MT along a “roadway” MT. *In vivo* analysis of Ncd mutants also supports the presence of an ATP-independent MT binding site in the tail of Ncd (3, 5). Recently, we have shown that Ncd residues 83-100 and 115-187 contain sites that exhibit ATP-independent MT binding with high and low affinity respectively, and have suggested that these MT interaction sites structurally combine in the native protein to form a single MT binding site (9).

The abundance of basic and proline residues in the NT domain is a common feature of many MT-associated proteins (MAPs), such as MAP2 and tau, which promote and stabilize MT assembly (see 10 and 11 for review). Given these similarities, we have examined the ability of the NT domain to promote MT assembly and to stabilize assembled MTs. Two different NT proteins were expressed as thioredoxin (Trx) fusions in *E. coli* and evaluated: TrxNT6, which corresponds to residues 83-187 and contains both the high and low affinity MT binding sites; and TrxNT8, which corresponds to residues 115-187 and contains only the low affinity MT binding site. MT sedimentation, turbidity measurements, video-enhanced differential interference contrast (VE-DIC) microscopy and electron microscopy (EM) were used to determine if TrxNT proteins promote MT assembly. MT sedimentation and turbidity measurements were also used to determine whether the TrxNT proteins stabilized MTs against conditions that induce MT depolymerization. We have found that TrxNT6 but not TrxNT8 can promote tubulin assembly into MTs and can stabilize MTs. These results suggest that the tail of Ncd, in addition to bundling spindle MTs (5-8), may also influence MT dynamics within spindles.

MATERIALS AND METHODS

Protein Preparation

TrxNT6 and TrxNT8 were expressed in *E. coli* and purified as previously described (9). Tubulin was purified from porcine brain (12). Purified proteins were quick frozen in liquid nitrogen and stored at -70°C. Protein concentrations were determined by the Bradford assay (BioRad) using bovine serum albumin (BSA) as a standard.

MT Sedimentation and Turbidity Assays

MT sedimentation assays were performed in AB buffer (20 mM Pipes, pH 6.9, 1 mM MgCl₂, 1 mM EGTA) containing 1 mM MgGTP and 100 µg/ml BSA. In a reaction volume of 100 µl, TrxNT6 or TrxNT8 (typically 5-35 µM final) was mixed with tubulin (5 µM final). After incubation for 15 minutes at 23°C, reactions were centrifuged at 100,000 x g for 15 minutes at 23°C. The resulting supernatants and pellets were then analyzed by SDS-PAGE (9). For MT stability assays, 50 µM tubulin was first polymerized at 37°C for 15 minutes and then diluted 10-fold into a reaction mixture containing TrxNT6 or TrxNT8. After 15 minutes at 23°C, identical reaction mixtures were either placed on ice, diluted a further 5-fold, or supplemented with either CaCl₂ (5 mM final) or NaCl (500 mM final). After 30 minutes, the reactions were centrifuged and processed as described above (except cold samples were centrifuged at 4°C).

MT assembly and stability were also evaluated by measuring turbidity at 350 nm in a Beckman DU-640 spectrophotometer. Tubulin (5 µM final) was mixed with TrxNT6 or TrxNT8 (1:1 TrxNT:tubulin), and A₃₅₀ was measured for 30 minutes at 23°C. At 30 minutes, samples were either diluted 5-fold or supplemented with CaCl₂ (5 mM final), and A₃₅₀ was measured for an additional 30 minutes.

Microscopy

Tubulin (5 µM final) was mixed with either TrxNT6 or TrxNT8 (2:1 or 4:1 TrxNT:tubulin), incubated for 15 minutes at 23°C, and observed with VE-DIC as described previously (12). Alternatively, the effect of TrxNT proteins on seeded MT assembly was examined in experiments in which tubulin was mixed with either TrxNT protein and immediately perfused into a slide-coverslip flow cell containing sea urchin (*Lytechinus pictus*) axonemes affixed to the glass surfaces (12).

For visualization by negative stain EM, tubulin (5 µM final) was mixed with either TrxNT6 or TrxNT8 (4:1 TrxNT:tubulin), incubated for 15 minutes at 23°C, adsorbed to carbon-coated 200 mesh grids, and stained with 2% uranyl acetate. In some cases taxol-

stabilized MTs (TMTs) were substituted for tubulin. Stained samples were observed on a JEOL JEM-100CXII electron microscope.

RESULTS

To evaluate the ability of TrxNT6 or TrxNT8 to promote MT assembly, various concentrations of each TrxNT protein (5-35 μ M final) were mixed with tubulin (5 μ M final) and incubated at 23°C for 15 minutes. At this tubulin concentration and temperature, no MT nucleation or elongation is expected since 5 μ M is well below the critical concentration for both nucleation and elongation of purified tubulin (12, 13). Samples were then subjected to centrifugation at 100,000 x g to pellet any polymer that formed, and supernatant and pellet fractions were analyzed by SDS-PAGE. In control reactions that contained tubulin, TrxNT6 or TrxNT8 individually, almost no protein was found in the pellet fraction (Figure 1a). However, when TrxNT6 was combined with tubulin, there was a concentration-dependent increase in the amount of tubulin (and TrxNT6) found in the pellet fraction as the TrxNT6:tubulin molar ratio was increased to 3:1. Above 3:1, the amount of tubulin and TrxNT6 in the pellet fraction remained constant (Figure 1b). In contrast, addition of TrxNT8 did not increase the amount of tubulin that pelleted even at a 7-fold molar excess of TrxNT8 over tubulin (Figure 1c). The ability of TrxNT6 but not TrxNT8 to promote tubulin assembly was confirmed by measurements of sample turbidity at A_{350} (Figure 2). Neither tubulin, TrxNT6, nor TrxNT8 produced a significant change in sample turbidity compared to the buffer only control. However, addition of TrxNT6 to tubulin caused a rapid and significant increase in turbidity (Figure 2a and c), while addition of TrxNT8 to tubulin had no effect (Figure 2b and d).

To examine the structures that pelleted in the sedimentation assay and caused turbidity at A_{350} , TrxNT-tubulin samples were observed by VE-DIC microscopy (Figure 3). TrxNT6 or TrxNT8 was mixed with tubulin (5 μ M final) at 2:1 and 4:1 TrxNT:tubulin ratios and then observed after 15 minutes at 23°C. Consistent with the results of the sedimentation and turbidity experiments described above, no MTs were observed in reactions that contained only tubulin or tubulin and TrxNT8 (data not shown). However, TrxNT6 at both ratios induced polymerization of tubulin into MTs and generated bundling of the resulting MTs (Figure 3a and b). To determine if TrxNT6 or TrxNT8 promoted seeded tubulin assembly onto sea urchin axoneme fragments, each TrxNT protein was mixed with tubulin (4:1 TrxNT:tubulin ratio) and immediately perfused into a flow cell containing axonemes attached to the coverslip surface. No assembly onto axoneme ends was observed for samples that contained either tubulin alone or tubulin and TrxNT8 (data not shown). However, MT assembly was observed at axoneme ends for samples containing tubulin and TrxNT6 (Figure 3c), although these seeded MTs were subsequently obscured by multiple, short, thick MT bundles that assembled de novo (Figure 3d-f).

In order to obtain a higher resolution view of the polymers assembled in the presence of TrxNT6, TrxNT6-tubulin samples were observed by negative stain EM (Figure 4a). The

polymers and bundles generated in samples containing 4:1 TrxNT6:tubulin appeared identical to those observed in samples of TrxNT6 and TMTs (Figure 4b). Further, the polymers present in the TrxNT6-tubulin samples were identical to polymers observed in samples of TMTs (Figure 4c), indicating that TrxNT6 promoted assembly of MTs rather than simply generating tubulin aggregates.

To evaluate the ability of TrxNT6 and TrxNT8 to stabilize MTs under conditions that induce MT disassembly, a modified MT sedimentation assay was used (Figure 5). In initial experiments, 50 μM tubulin was polymerized at 37°C to form MTs and then diluted 10-fold into AB buffer containing TrxNT6 or TrxNT8 (20 μM final to give a 4:1 TrxNT:tubulin molar ratio). After incubation at 23°C for 15 minutes, reaction mixtures were subjected to centrifugation to determine the ability of each TrxNT protein to stabilize MTs following dilution below the critical concentration for elongation. In the absence of TrxNT protein, tubulin was found in the supernatant fraction indicating that the MTs had disassembled following dilution (see Figure 1). Dilution of MTs into a solution containing TrxNT8 resulted in the majority of tubulin partitioning to the supernatant fraction, indicating that TrxNT8 did not stabilize MTs under these conditions (Figure 5). In comparison, dilution of MTs into a solution containing TrxNT6 resulted in the majority of tubulin partitioning to the pellet fraction, suggesting that TrxNT6 was able to stabilize MTs. To characterize further the MT stabilizing ability of TrxNT proteins, MTs were diluted into a solution containing TrxNT6 or TrxNT8 as described above, and then subsequently exposed to additional MT-destabilizing conditions (cold, further dilution to 1 μM tubulin, Ca^{++}) or to 500 mM NaCl for 30 minutes before centrifugation. Consistent with the failure of TrxNT8 to stabilize polymerized MTs against dilution to 5 μM tubulin, TrxNT8 had no stabilizing effect on MTs subjected to cold, dilution to 1 μM tubulin, Ca^{++} , or NaCl (data not shown). However, for MTs stabilized by TrxNT6, incubation on ice (Figure 5: cold), dilution to 1 μM tubulin (data not shown), or addition of CaCl_2 to 5 mM (Figure 5: CaCl_2) did not alter the relative distribution of tubulin into supernatant and pellet fractions, indicating that TrxNT6 also stabilized MTs against the effects of these disassembly-inducing conditions. Turbidity measurements of TrxNT6-tubulin samples either diluted 5-fold (Figure 2a) or supplemented with 5 mM CaCl_2 yielded results (Figure 2c) consistent with those observed in the sedimentation assay. Upon 5-fold dilution, sample turbidity also decreased 5-fold, while addition of CaCl_2 actually caused an increase in turbidity. The only agent that was effective at disassembling TrxNT6-MT complexes was 500 mM NaCl, which caused tubulin to redistribute to the supernatant fraction in the sedimentation assay (Figure 5).

DISCUSSION

Like tau and MAP2, the Ncd tail domain binds and bundles MTs and contains an abundance of basic and proline residues (1, 2, 10). These similarities suggest that the Ncd tail may be capable of influencing MT assembly. To address this possibility, two proteins that correspond to different portions of the Ncd tail domain were assayed for the ability to promote tubulin assembly and stabilize MTs. Both TrxNT6 (thioredoxin linked to Ncd residues 83-187) and TrxNT8 (thioredoxin linked to Ncd residues 115-187) have previously been shown to bind and bundle MTs (9). TrxNT6 contains two sites that interact with MTs, a high affinity site within residues 83-100 and a low affinity site within residues 115-187, while TrxNT8 contains only the low affinity site (9).

Promotion of tubulin assembly was analyzed by sedimentation and turbidity assays. In these assays, TrxNT8 did not increase the amount of tubulin that pelleted in the sedimentation assay (even at 7:1 molar excess over tubulin (Figure 1)) or the A_{350} value in the turbidity assay (Figure 2). In addition, when mixtures of TrxNT8 and tubulin were observed by VE-DIC or negative stain EM, no MTs were ever observed. Taken together, these results indicate that even though TrxNT8 can bind TMTs (9), this protein, which contains only the low affinity MT interaction site, cannot promote tubulin assembly. Further, TrxNT8 was incapable of stabilizing MTs that were subjected to MT depolymerizing conditions such as dilution, cold, or Ca^{++} ions. In comparison, TrxNT6 increased the amount of tubulin that pelleted in the sedimentation assay as well as increasing sample turbidity at A_{350} . TrxNT6 was able to assemble tubulin at a 1:1 TrxNT6:tubulin ratio (Figure 1 and 2), and was maximally effective at a 3:1 ratio (Figure 1), which corresponds to the maximal binding stoichiometry of TrxNT6:tubulin (9). In addition to promoting tubulin assembly, TrxNT6 was able to stabilize MTs under conditions that induce MT depolymerization. In fact, $CaCl_2$ caused an unexpected increase in turbidity. The reason for this increase is unclear but may be due to increased MT bundling. The only condition that resulting in depolymerization of TrxNT6-stabilized MTs was 500 mM NaCl, which previously was shown to cause complete release of TrxNT6 from MTs (9). Although both the sedimentation and turbidity results support the hypothesis that TrxNT6 promotes tubulin assembly, neither assay provided information concerning the structures assembled. However, direct observation of the assembled products by VE-DIC and EM demonstrated that tubulin did in fact assemble into MTs in the presence of TrxNT6 (Figure 4).

The finding that TrxNT6 but not TrxNT8 promotes the assembly of tubulin into MTs and stabilizes MTs provides further evidence that the two previously identified MT-interaction sites in the Ncd tail (9) may combine to form a single MT binding site in the native protein, and suggests that the Ncd tail may be involved in regulation of MT assembly as well as attachment to a cargo MT. This is the first demonstration that the tail domain of a kinesin family motor may influence the dynamics of a cargo MT.

FIGURE 1: Effects of TrxNT6 and TrxNT8 on tubulin assembly as measured by a sedimentation assay.

MT sedimentation assays were performed as described under Material and Methods, and supernatant (S) and pellet (P) fractions were separated by SDS-PAGE and proteins stained with Coomassie Blue. Results for tubulin (T), TrxNT6 (6), and TrxNT8 (8) individually are shown in (a), and results for the indicated molar ratios of TrxNT6:tubulin and TrxNT8:tubulin are shown in (b) and (c) respectively.

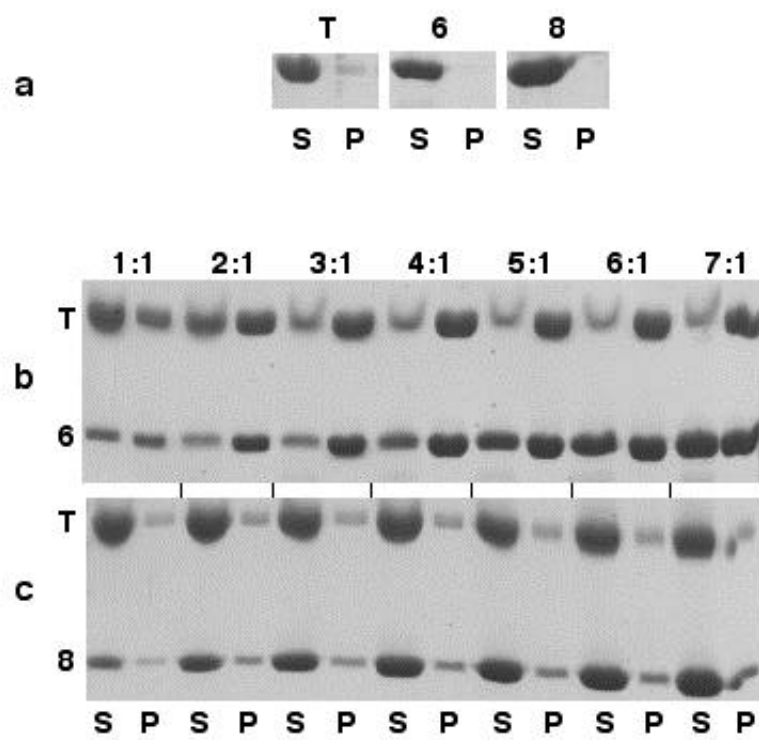


FIGURE 2: Effects of TrxNT6 and TrxNT8 on tubulin assembly as measured by a turbidity assay.

Tubulin (5 μ M) was mixed with 5 μ M TrxNT6 (a and c) or TrxNT8 (b and d), and A_{350} was measured for 30 minutes then samples were either diluted 5-fold (a and b) or supplemented with CaCl_2 to 5 mM (c and d), and A_{350} was measured for an additional 30 minutes. Tubulin only samples are indicated by the dotted line, TrxNT only samples are indicated by the dashed line, and TrxNT and tubulin samples are indicated by the solid line.

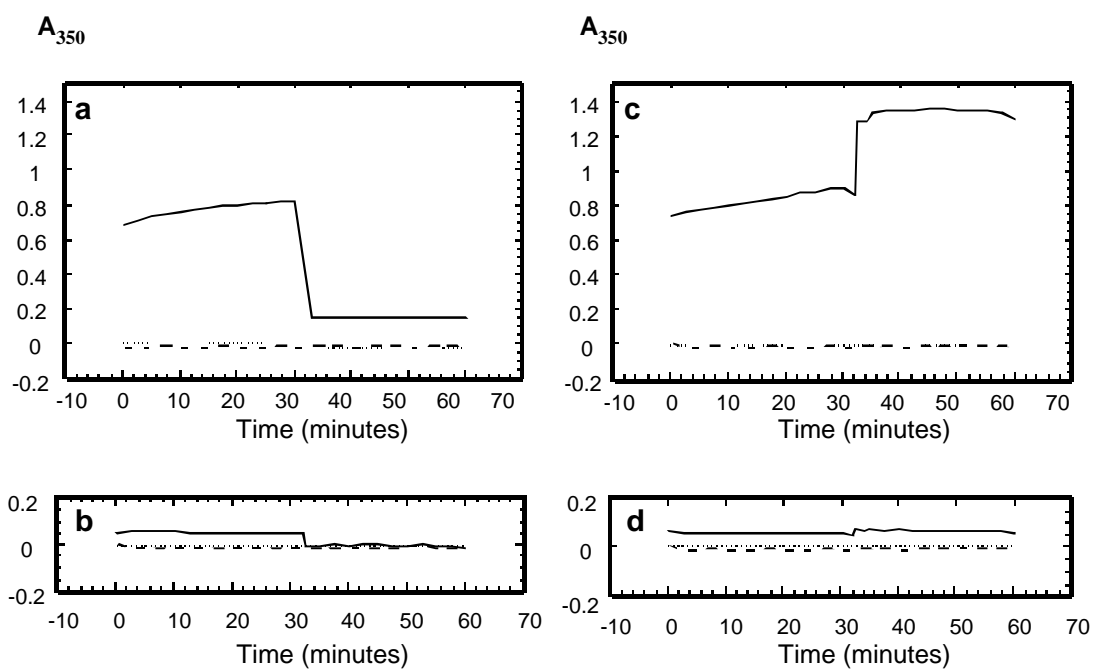


FIGURE 3: TrxNT6-promoted MT assembly observed by VE-DIC microscopy.

Samples were prepared to observe TrxNT6 promotion of MT self-assembly and seeded assembly as described under Materials and Methods. Two example fields of MTs and MT bundles resulting from TrxNT6-promoted MT self-assembly (TrxNT6:tubulin = 4:1) are shown (a, b). To determine effects on seeded assembly, a 4:1 TrxNT6:tubulin mixture was perfused into a flow cell containing axonemes. Assembly of MTs at 1 (c), 5 (d) and 15 (e) minutes post-perfusion is shown. The arrow in (c) indicates MTs assembling onto the end of an axoneme and the asterisk indicates a self-assembled MT. MT assembly in a different field at 20 minutes post-perfusion is also shown (f). The width of each image is equivalent to 25 μm .

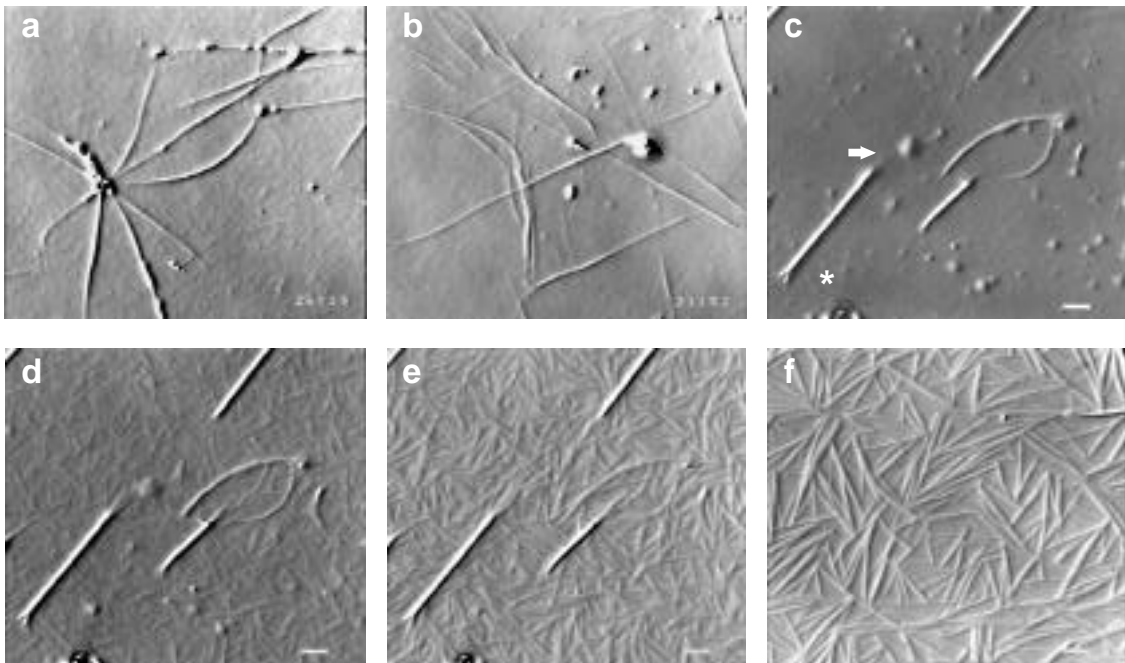


FIGURE 4: EM images of TrxNT6 with tubulin and TMTs.

Samples containing 4:1 TrxNT6:tubulin (a) or TrxNT6 and TMTs at a 4: 1 TrxNT6:tubulin ratio (b) were prepared and processed for negative stain EM as described under Materials and Methods. TMTs (c) are shown for comparison. Magnification 130,000.

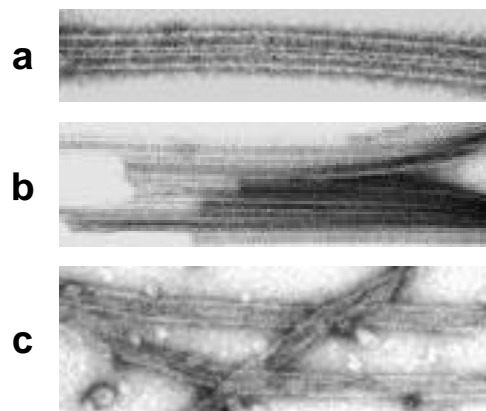
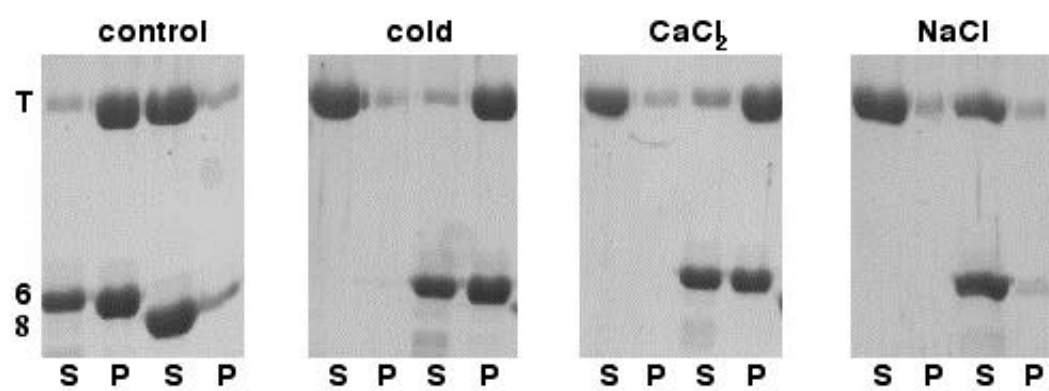


FIGURE 5: The effects of TrxNT6 and TrxNT8 on MT stability.

MT stability assays were performed as described under Material and Methods, and supernatant (S) and pellet (P) fractions were separated by SDS-PAGE and proteins stained with Coomassie Blue. The results for dilution of MTs to 5 μ M tubulin in the presence of either TrxNT6 or TrxNT8 are shown (control), and the effects of additional MT destabilizing conditions (cold, CaCl_2 , NaCl) on MTs (left 2 lanes) and TrxNT6-stabilized MTs (right 2 lanes) are also shown. The positions of tubulin (T), TrxNT6 (6), and TrxNT8 (8) are indicated.



LITERATURE CITED

1. Endow, S. A., Henikoff, S., and Soler-Niedziela, L. (1990) *Nature*. **345**, 81-83.
2. McDonald, H. B., and Goldstein, L. S. B. (1990) *Cell*. **61**, 991-1000.
3. Hatsumi, M., and Endow, S. A. (1992) *J. Cell Sci.* **103**, 1013-1020.
4. Endow, S. A. (1993) *Trends Genet.* **9**, 52-55.
5. Matthies, H. J. G., McDonald, H. B., Goldstein, L. S. B., and Theurkauf, W. E. (1996) *J. Cell Biol.* **134**, 455-464.
6. Endow, S. A., and Komma, D. J. (1997) *J. Cell. Biol.* **137**, 1321-1336.
7. Chandra, R., Salmon, E. D., Erickson, H. P., Lockhart, A., and Endow, S. A. (1993) *J. Biol. Chem.* **268**, 9005-9013.
8. McDonald, H. B., Stewart, R. J., and Goldstein S. B. (1990) *Cell*. **63**, 1159-1165.
9. Karabay, A., and Walker, R. A. (1999) *Biochemistry*. **38**, 1838-1849
10. Delacourte, A., and Buee L. (1997) *Intl. Rev. Cytol.* **171**, 167-210.
11. Goode, B. L., Denis, P. E., Panda, D., Radeke, M. J., Miller, H. P., Wilson, L., and Feinstein, S. C. (1997) *Mol. Biol. Cell.* **8**, 353-365.
12. Walker, R. A., O'Brien, E. T., Pryer, N. K., Soboeiro, M. F., Voter, W. A., Erickson, H. P., and Salmon, E. D. (1988) *J. Cell Biol.* **107**, 1437-1448.
13. Walker, R. A., Inoue, S., and Salmon, E. D. (1989) *J. Cell Biol.* **108**, 931-937.

CHAPTER 4
THE NCD TAIL DOMAIN INTERACTS WITH BOTH
 α - AND β -TUBULIN

ABSTRACT

Non-claret disjunctional (Ncd) is a minus end-directed kinesin-like *Drosophila* motor protein that is required for spindle assembly in oocytes and spindle maintenance in early embryos. Through the action of ATP-dependent and ATP-independent MT binding sites in the head and tail domains, respectively, Ncd is thought to bundle and perhaps slide MTs relative to each other. The Ncd motor domain has a high homology to the kinesin motor domain, whereas the tail domain is unique among kinesin superfamily members. Instead, the tail domain shares structural and functional similarities with microtubule-associated proteins (MAPs), such as MAP2 and tau. Like tau MT-binding motifs, the ATP-independent MT binding sites of the Ncd tail domain contain basic residues flanked by prolines, and can also promote MT assembly and stability. Given these similarities, we analyzed the Ncd tail binding sites on tubulin by chemical cross-linking and MT co-sedimentation assays using an Ncd tail protein (NT6 comprising Ncd residues 83-187) and subtilisin-digested-MTs. Ncd tail binding sites on tubulin correspond to sites which tau binds. The results indicate that there are four potential Ncd tail binding sites on a tubulin dimer: one within 15 amino acids at the extreme C-terminus and the other within 20 amino acids in the H11-H12 loop / H12 helix of each tubulin monomer.

INTRODUCTION

The *Drosophila* nonclaret disjunctional (Ncd) motor protein is involved in spindle assembly during meiosis in oocytes and spindle maintenance during mitosis in early embryos (1-6). Ncd binds to “roadway” and “cargo” microtubules (MTs) via an ATP-dependent MT binding site in the C-terminal motor domain (residues 356-700) and an ATP-independent MT binding site in the N-terminal tail domain (residues 1-200), respectively. Through the action of these binding sites, Ncd cross-links and bundles MTs, and may slide MTs relative to each other (7, 8, 9). The ability of Ncd to bundle and perhaps slide MTs is likely to be important for Ncd function in spindle assembly and maintenance, and several observations are consistent with this hypothesis (3, 5, 6, 8).

The Ncd motor domain is 41% identical to the kinesin motor domain, but the tail domain is unique among kinesin superfamily motors (1, 2). Instead, the tail domain shares structural and functional similarities with microtubule-associated proteins (MAPs), such as tau and MAP2. Recently, we have identified ATP-independent MT binding sites in the Ncd tail domain. These sites, like the MT binding motifs of tau and MAP2, contain clusters of basic residues flanked by proline residues (9, 10). We have also demonstrated that the Ncd tail, like tau and MAP2, is capable of promoting MT assembly and stability (11). Together, these results suggest that in addition to bundling spindle MTs, the Ncd tail may also influence spindle MT dynamics.

Based on the 4:1 binding ratio of Ncd tail proteins to tubulin, we previously proposed that the tubulin dimer contains four potential binding sites for the Ncd tail (9). Given the ionic nature of binding (9) and the large number of acidic residues in the exposed C-terminal domains of α - and β -tubulin, we suggested that the Ncd tail binds to two acidic clusters, one at the extreme C-terminus and the other in the H11-H12 loop / H12 helix of each tubulin monomer. These proposed Ncd tail interaction sites correspond to sites to which tau has recently been shown to bind (12). Chau et al. showed that tau can interact with two sites on each tubulin monomer: the C-terminal tau interaction site is located within the 12 C-terminal amino acids of both α - and β -tubulin, and the internal tau interaction site is located within the C-terminal one third of α - and β -tubulin.

Given the structural and functional similarities of tau and Ncd tail region (9, 11), we have investigated the Ncd tail binding sites on tubulin using subtilisin-digestion of MTs, the same approach used historically in many MAP-MT binding studies (13, 14, 15, 16, 17). The interactions of an Ncd tail protein (NT6 comprised of Ncd residues 83-187) with subtilisin-digested MTs were analyzed in cross-linking and MT co-sedimentation assays. Results of these assays indicate that the extreme C-terminal regions (each containing 15 amino acids) on both α - and β -tubulin monomers contain two of the four Ncd tail binding sites, and

suggest that the other two Ncd tail binding sites are likely to be located in the H11-H12 loop / H12 helix sequence (each containing 20 amino acids) of both α - and β -tubulin monomers.

MATERIALS AND METHODS

Purification of NT6 Protein

A pET32a (Novagen) plasmid containing the cDNA encoding Ncd residues 83-187 (termed NT6) (9) was transformed into BL21 (DE3) pLysS cells for expression. The induced protein, which was fused to thioredoxin (Trx), was purified by ion exchange chromatography (S-Sepharose (Pharmacia)). Briefly, frozen cells were thawed and lysed in AB buffer (20 mM Pipes, pH 6.9, 1 mM $MgCl_2$, 1mM EGTA, 1 mM DTT) containing 100 mM NaCl and 1 mM PMSF. The cell lysate was then supplemented with 10 mM $MgCl_2$ and 40 μ g/ml DNase I (Boehringer Mannheim), incubated for 30 minutes on ice, and clarified (9). The high-speed supernatant containing TrxNT6 fusion protein was loaded onto an S-Sepharose column, and TrxNT6 protein was eluted with AB buffer containing 250 mM NaCl. The eluted protein was dialyzed against AB buffer containing 1 mM DTT, and then digested with 1 U thrombin (Sigma) per mg of fusion protein to cleave the Trx fusion partner from the NT6 protein. Thrombin was inactivated by the addition of PMSF to 1 mM final concentration, and Trx and NT6 were separated by S-Sepharose ion exchange chromatography. After dialysis against AB buffer containing 1 mM DTT, aliquots of the NT6 protein were quick frozen in liquid nitrogen and stored at -70°C .

Preparation of Subtilisin-digested-MTs

To prepare taxol-stabilized MTs (α -MTs), 10 mg/ml purified bovine tubulin (Cytoskeleton) was assembled at 37°C for 30 minutes, and then an equal volume of AB buffer containing 100 μ M taxol (Calbiochem) was added. α -MTs were treated with 1% (w/w) subtilisin (Boehringer Mannheim) at 37°C for 15 minutes to generate α -digested-MTs (α_s -MTs) or 10 hours to generate α - and β -digested-MTs ($\alpha_s \beta_s$ -MTs) (12). Subtilisin was inactivated with 3 mM PMSF and the digested MTs were centrifuged at $100,000 \times g$ for 30 minutes to remove the cleaved C-termini of α - and β -tubulin. The supernatants were removed for use in cross-linking experiments (see below), and the pellets were resuspended in AB buffer.

MT Binding Assay

A MT co-sedimentation assay was used to determine the affinity (K_d) and stoichiometry (B_{\max}) of NT6 binding to α -, α_s - and $\alpha_s \beta_s$ -MTs. In each set of experiments, the tubulin concentration was kept constant and the NT6 protein concentration was varied to produce different molar ratios (from 1:1 to 10:1) of NT6 to α -, α_s - or $\alpha_s \beta_s$ -MTs. For α -MTs, the tubulin concentration was kept constant at 5 μ M. For α_s -MTs, one set of experiments was performed at 2.9 μ M tubulin, and a second set at 5 μ M tubulin. For $\alpha_s \beta_s$ -

MTs, one set of experiments was performed at 2.63 μ M tubulin, and a second set at 5 μ M tubulin. The reactions were performed in AB buffer containing 40 μ M taxol and 100 μ g/ml bovine serum albumin (BSA), and incubated for 30 minutes at 22°C, then subjected to centrifugation as described above. The supernatant and pellet fractions were processed (9), and analyzed by tricine-PAGE (18). For quantitative analysis, the amount of supernatant and pellet samples loaded onto the gels was optimized to ensure a linear relationship between the amount of NT6 protein and the intensity of the Coomassie blue stained protein bands. The amount of NT6 protein in the supernatant and pellet fractions was quantified by measuring the protein band intensities relative to standards (known amounts of NT6 protein) with AlphaImager™ 2000 Documentation and Analysis System controlled by AlphaEase™ version 3.3 software (Alpha Innotech Corporation). Since experiments were performed at two different tubulin concentrations for α - and β -MTs, K_d and B_{max} values were obtained by fitting bound NT6/tubulin (μ M/ μ M) versus unbound NT6 (μ M) data with a rectangular hyperbola. Curve fits were calculated with Prism version 3.0 software (Graph-Pad).

MT Cross-linking Assay

To analyze the interactions of the Ncd tail domain with α -, β - or γ -MTs by chemical cross-linking approach, the zero-length covalent cross-linker, EDC (1-ethyl-3-(3-dimethylaminopropylcarbodiimide)) was used. To stabilize the intermediates, S-NHS (Sulfo- N-Hydroxysulfosuccinimide) was added to reactions.

To generate cross-linked products, α -, β - or γ -MTs (5 μ M tubulin) were mixed with NT6 (5-20 μ M) in AB buffer, EDC (2 mM) and S-NHS (5 mM) were added, and the reactions were incubated for 30 minutes at 22°C. Control reactions included either MTs or NT6 alone with/without EDC and S-NHS, and a mixture of MTs and NT6 without EDC and S-NHS. The reactions were terminated after 30 minutes by the addition of 2X sample buffer (125 mM Tris-HCl, pH 6.8, 4% SDS, 20% glycerol, 10% β -mercaptoethanol, 0.05% Pyronin-Y, 0.05% Bromophenol blue).

To determine if NT6 could be cross-linked to C-terminal fragments generated from subtilisin digestion of α - and β -tubulin, supernatants from α - or β -MTs digestions (see tubulin preparation section) were mixed with NT6 (50 μ M) in AB buffer including EDC (2 mM) and S-NHS (5 mM). After 30 minutes of incubation, reactions were stopped by the addition of 2X sample buffer.

In order to determine the composition of the cross-linked products, samples were separated by SDS-PAGE using low grade SDS (Sigma L-5750) to enhance separation of α - and β -tubulin. For C-terminal fragment cross-linking reactions, the samples were separated on 15% tricine gels. Separated proteins were transferred to nitrocellulose membranes and probed with antibodies against α -tubulin (DM1A, mouse, Sigma), β -tubulin (18D6, mouse,

Theodorakis and Cleveland, 1992 (19)) or NT6 (rabbit). Goat anti mouse / anti-rabbit HRP-conjugated secondary antibodies were used to detect the primary antibodies. The membranes were further processed for ECL using the SuperSignal West Dura chemiluminescent kit (Pierce).

RESULTS

Cross-linking of NT6 Protein to α - and β -tubulin

To investigate the involvement of the acidic residues in the C-terminal domains of α - and β -tubulin (Figure 1) in Ncd tail interactions, the zero-length covalent cross-linker EDC, which forms covalent bonds between amino and carboxyl groups that interact, was used to generate NT6-tubulin cross-linked products. NT6 and MTs were combined at different molar ratios (from 1:1 to 4:1 NT6:tubulin) in AB buffer in the presence of EDC and S-NHS. The cross-linked products were analyzed by SDS-PAGE (Figure 2). The yield of the cross-linked products increased with the increasing molar ratios of NT6 to tubulin. Although the cross-linked products at the 1:1 molar ratio of NT6 to α -MTs could not be observed on the gel (Figure 2), western blot analysis confirmed the presence of the cross-linked products (data not shown). At each molar ratio, the major cross-linked products appeared identical and resolved into three bands with the middle band more intense than either the upper or lower band (Figure 2). In control reactions, EDC treatment of NT6 in the absence of α -MTs did not generate any cross-linked products (Figure 2), and western blot analysis with an antibody against NT6 did not reveal any cross-linked bands (data not shown). EDC treatment of β -MTs generated only a major cross-linked product with a higher molecular weight equivalent to cross-linked α -dimer. To determine the relative mobility (M_r) of the cross-linked products, samples were fractionated on an 11.5% low grade SDS-polyacrylamide gel (so that the NT6 protein was also retained on the gel) (data not shown). Under these gel conditions, α - and β -tubulin were estimated to have M_r of 52 and 55 kDa, respectively, while the M_r of NT6 was 18 kDa. The M_r of the cross-linked products ranged from 69 to 74 kDa.

To investigate if the Ncd tail formed cross-links to both α - and β -tubulin, the composition of the cross-linked products was identified using samples of the 4:1 molar ratio (giving the maximum yield of the cross-linked products) of NT6 to tubulin by western blot analysis. To enhance the resolution of the cross-linked products, samples were separated on 7 % low grade SDS-polyacrylamide gels, and then were transferred to nitrocellulose membranes for western blot analysis. Probing with α -tubulin (DM1A) and β -tubulin (18D6) antibodies revealed two bands containing α -tubulin and two bands containing β -tubulin (Figure 3). Probing with the NT6 antibody revealed three bands including one more intense band in the middle, which aligned with the lower α -tubulin and upper β -tubulin bands (Figure 3). The upper NT6 band aligned with the upper β -tubulin band and the lower NT6 band aligned with the lower α -tubulin band (Figure 3). These results indicated that there are

two interaction sites for the Ncd tail on each tubulin monomer and this observation is consistent with the 4:1 binding stoichiometry of Ncd tail proteins to tubulin (9).

Binding of NT6 Protein to Subtilisin-digested-MTs

To further investigate the roles of extreme C terminal acidic clusters (Figure 1) on α - and β -tubulin as Ncd tail binding sites, we took advantage of the differential susceptibility of α - and β -tubulin to subtilisin. Previous studies have shown that brief treatment of MTs with subtilisin removes a 4 kDa fragment from the C-terminus of α -tubulin, while removal of the C-terminal fragment from β -tubulin requires significantly longer treatment with subtilisin (16, 20, 21). In our study, α -MTs were treated with subtilisin for 15 minutes to remove the C-terminus of α -tubulin (generating α_s -MTs) or 10 hours to remove the C-termini of both α - and β -tubulin (generating $\alpha_s\beta_s$ -MTs).

To obtain a quantitative measure of the binding of NT6 to α_s - or $\alpha_s\beta_s$ -MTs, various concentrations (5-50 μ M) of NT6 protein were mixed with a constant concentration of α_s - or $\alpha_s\beta_s$ -MTs (see Materials and Methods) to generate binding at different molar ratios in MT co-sedimentation assays. After centrifugation to separate the supernatants containing the unbound NT6 from the pellets containing MT-bound NT6, supernatant and pellet samples were analyzed by tricine-PAGE and then densitometry analysis was used to determine the concentrations of NT6 in each fraction. The data for bound NT6/tubulin (α_s or $\alpha_s\beta_s$) versus unbound NT6 were plotted and fit with a rectangular hyperbola to calculate K_d and B_{max} values (Figure 4). For comparison to the previously reported data (9), quantitative MT binding experiments were also performed for β -MTs, and values obtained were essentially identical to our previous measurements (see Figure 4 and reference 9). Based on the calculated K_d values, the affinity of NT6 for β -MTs was 0.1 μ M, and the affinity of NT6 for α_s - and $\alpha_s\beta_s$ -MTs was 0.42 μ M and 0.91 μ M, respectively. The calculated B_{max} values for NT6 indicated that NT6 bound to β -, α_s - and $\alpha_s\beta_s$ -MTs at a maximum stoichiometry of 4:1, 3:1 and 2:1, respectively (Figure 4).

Cross-linking of NT6 Protein to C-terminal fragments of α - and β -tubulin

The decreased B_{max} values for NT6 binding to α_s - and $\alpha_s\beta_s$ -MTs observed in Figure 4 suggested that Ncd tail binding sites were removed along with the C-terminal domains of α - and β -tubulin by subtilisin digestion. To determine if the Ncd tail could interact with C-terminal regions of α - and β -tubulin, NT6 was mixed with supernatants of the subtilisin digestions, containing the C-terminal fragments (produced by subtilisin digestion of α - and β -tubulin), and subjected to EDC cross-linking. The cross-linked samples were separated by 15% tricine-PAGE and then transferred to a nitrocellulose membrane for western blot analysis. Probing the blot with the NT6 antibody revealed a single cross-linked product with

both α - and β -MTs, and as a control reaction, EDC treatment of NT6 in the absence of C-terminal fragments of α - and/or β -tubulin did not generate a comparable band (Figure 5). These results indicate that NT6 can interact with C-terminal fragments of α - and/or β -tubulin.

Cross-linking of NT6 Protein to internal sites on α - and β -tubulin

To determine if NT6 could also cross-link to subtilisin-digested-MTs containing the internal interaction sites, NT6 was mixed with α - or β -MTs in cross-linking reactions at a 4:1 ratio as described above. Cross-linked products of NT6 and α - or β -MTs were separated on low grade SDS-polyacrylamide gels, and transferred to nitrocellulose membranes. Western blot analysis with α -tubulin (DM1A) antibody revealed two major α -tubulin cross-linked bands for both α - and β -tubulin (Figure 6a). Analysis of the same cross-linked products with β -tubulin (18D6) antibody also revealed two β -tubulin cross-linked bands for both α - and β -tubulin (Figure 6b). Probing the cross-linked products with NT6 antibody resulted in a smear (with no discrete bands) in the region corresponding to these cross-linked products (data not shown).

To investigate the production of the two NT6 cross-linked bands observed with α - and β -MTs for each tubulin monomer, the compositions of α - and β -MTs were analyzed. Samples of α - and β -MTs were separated by low grade SDS-polyacrylamide gels and transferred to nitrocellulose membranes for western blot analysis. Probing the α - and β -MTs with an α -tubulin (DM1A) antibody revealed a single band for α -MTs since α -tubulin is still intact, as in the case for undigested α -MTs (data not shown). β -tubulin (DM1A) antibody revealed double bands for β -MTs (Figure 6c); and β -tubulin (18D6) antibody also revealed two bands for both α - and β -MTs (Figure 6c), indicating that there are two forms of α and β present. These results suggest that the two NT6 cross-linked bands observed with α - and β -MTs for each tubulin monomer are due to the presence of two forms of α and β .

DISCUSSION

We previously showed that Ncd tail proteins bind to MTs at a 4:1 stoichiometric ratio and proposed that there are four binding sites for Ncd tail proteins on each tubulin dimer (9). Given the ionic nature of Ncd tail binding to MTs (9) and the large number of acidic residues in the exposed C-terminal domains of α - and β -tubulin, it is likely that the Ncd tail binding sites on α - and β -tubulin represent clusters of acidic residues. Two such clusters are present in each tubulin monomer: one in the H11-H12 loop / H12 helix and the other at the extreme C-terminus (Figure 1). To determine if these acidic clusters are indeed involved in Ncd tail binding, chemical cross-linking and MT co-sedimentation assays were used to analyze the interactions of an Ncd tail protein (NT6) with MTs and subtilisin-digested MTs. The results indicate that the extreme C-terminal regions (15 amino acids) of both α - and β -tubulin contain two of the four Ncd tail binding sites, and that the other two binding sites are internal to the subtilisin digestion sites. Due to the involvement of the acidic residues at the exposed C-terminal domain of tubulin in the Ncd tail interaction, the internal binding sites are likely to be located in an 20 amino acid stretch containing acidic residues of the H11-H12 loop / H12 helix of α - and β -tubulin.

EDC cross-linking of NT6 bound to MTs (Figure 2 and 3) demonstrates that the Ncd tail can interact with both α - and β -tubulin, and supports the hypothesis that acidic residues on each monomer are involved in the interaction of the Ncd tail with MTs. Interestingly, there were two cross-linked products generated for each tubulin monomer (Figure 3). One explanation for this observation is that the lower band represents a single NT6 polypeptide cross-linked to each monomer, while the upper band represents two NT6 polypeptides cross-linked to each monomer. An alternative explanation is that a single NT6 polypeptide may be cross-linked at two different sites on each tubulin monomer, and that each cross-linked product has a slightly different mobility. The M_r (69-74 kDa) of the cross-linked products demonstrates that each cross-linked product contains only one NT6 polypeptide, suggesting that the two cross-linked products observed for each tubulin monomer are due to cross-linking of a single NT6 polypeptide at two different sites on both α - and β -tubulin.

Further evidence for the presence of two binding sites on each tubulin monomer came from MT co-sedimentation assays using subtilisin-digested-MTs. Evidence that the extreme C-terminal acidic clusters of α - and β -tubulin contain Ncd tail binding sites is based on the decreased B_{max} values of NT6 binding to α_s - and β_s -MTs. NT6 binds α -MTs at a 4:1 stoichiometry (Figure 4 and reference 9), but subtilisin digestion of α -tubulin (α_s -MTs) and subsequently β -tubulin (β_s -MTs) decreased the binding stoichiometry to 3:1 and 2:1, respectively (Figure 4). Thus, removal of each C-terminal acidic fragment (see Figure 1) also removes one Ncd tail binding site.

The decrease in the binding stoichiometry of NT6 to α -MTs after removal of α - and β -tubulin C-terminal acidic fragments was accompanied by a decrease in the binding affinity of NT6 to α - and β -MTs (Figure 4). Based on the 2 fold decrease in the affinity of NT6 to β -MTs upon removal of the second interaction site, it may be possible that the two C-terminal fragments of α - and β -tubulin contribute equally to the tight binding affinity for the Ncd tail, and the internal sites might have equal intrinsic binding affinity to NT6. Alternatively, both C-terminal and internal binding sites on each tubulin monomer might have equal binding affinity, but subtilisin digestion might cause loss of critical residues that are part of the internal binding site, and a decrease in the binding affinity for the Ncd tail. The greater decrease in the binding affinity of β -MTs might be explained by the broader subtilisin digestion region, and removal of more critical residues in β -tubulin, compared to α -tubulin, might cause a greater decrease in the binding affinity.

Interpreting the results of NT6 binding to subtilisin-digested-MTs requires knowledge of the subtilisin action sites on α - and β -tubulin. Although there has been disagreement about the exact cleavage sites, it is well accepted that subtilisin cleaves within the extreme C-terminal region of both α - and β -tubulin and removes a fragment of 15-20 amino acids (see Figure 1) (16, 22, 23, 24). Antibody mapping of subtilisin digested MTs (15, 25) showed that the epitopes recognized by DM1A (426-430) (26) and DM1B (416-430) (27) antibodies on α - and β -tubulin were still present on subtilisin-digested tubulin. These results indicate that the subtilisin digestion site(s) is C-terminal to residue 430 on both α - and β -tubulin. For β -tubulin, our result was in agreement with this subtilisin digestion site as observed with the conservation of the DM1A site on β -tubulin (see Figure 6). However for α -tubulin, the 18D6 antibody (recognizes the N-terminal of α -tubulin) used in our cross-linking experiments was not suitable for determination of the subtilisin digestion site on α -tubulin; but again, based on the similar conditions used in other studies (15, 17, 20, 25), the subtilisin action site(s) on α -tubulin was likely to be at the C-terminal of the residue 430. Regardless of the specific cleavage site, all reported major cleavage sites are between the two acidic clusters in each monomer. Therefore, subtilisin digestion should remove the C-terminal binding sites for Ncd tail on both α - and β -tubulin and leave the internal binding sites on each tubulin monomer (see Figure 1).

Cross-linking of NT6 to C-terminal fragments of α - and/or β -tubulin supports the conclusion that these fragments contain Ncd tail binding sites (Figure 5). In the cross-linking reactions of NT6 with the C-terminal fragment released from β -MTs, the cross-linked band observed must be a product of the β -tubulin C-terminal fragment since this was the only C-terminal fragment in the reaction. In the cross-linking reactions of NT6 with the C-terminal fragments released from α -MTs, it could not be directly determined whether NT6 cross-linked to C-terminal fragments of both α - and β -tubulin or only α - or β -tubulin as only a

single band was observed. Attempts to detect the α -tubulin C-terminal fragment in cross-linked products of NT6 and C-terminal fragments released from α - β -MTs with an antibody (YL1/2) that recognizes the terminal Gly-Gly-Tyr of α -tubulin were not successful. Although the YL1/2 antibody was able to recognize α -tubulin (data not shown), it failed to recognize either α - or β - α -tubulin. Since the C-terminal acidic cluster was removed from α -tubulin in α - β -MTs, it is not surprising that YL1/2 did not recognize α -tubulin, but the fact that YL1/2 did not recognize the α -tubulin in α -MTs suggests that at least the terminal Tyr, which is important for YL1/2 recognition, was removed from α -tubulin upon exposure to subtilisin. In the absence of appropriate antibodies, it is not clear to which C-terminal fragments NT6 were cross-linked, but the decreased binding stoichiometry of NT6 to α - and β - α -MT (see Figure 4) suggests that NT6 interacts with both C-terminal fragments.

The 2:1 stoichiometric ratio of NT6 binding to α - β -MTs suggests that there are still two internal binding sites remaining after subtilisin cleavage, possibly one on each monomer. This is supported by the finding that NT6 is able to cross-link to both α - and β -tubulin (Figure 6). Cross-linking of NT6 at the internal binding sites produced two major cross-linked products with both tubulin monomers (Figure 6a and b) for both α - and β - α -MTs. Since α -MTs should contain two intact Ncd tail interaction sites on α -tubulin, the two α -tubulin-NT6 cross-linked products observed were not surprising (Figure 6a). However for β - α -MTs, removal of the extreme C-terminal binding site from α -tubulin would be expected to generate only one α -tubulin cross-linked product. The most likely reason for the two α -tubulin cross-linked products observed with β - α -tubulin came from the analysis of β - α -MTs with an α -tubulin (DM1A) antibody. Probing β - α -MTs with DM1A revealed two α -tubulin bands (Figure 6c), indicating the presence of two different forms of α -tubulin. This result suggests that, rather than the presence of two cross-linking sites internal to subtilisin-cleavage site, each form of α -tubulin may cross-link with NT6, each product having a slightly different mobility. The two α -tubulin-NT6 cross-linked bands (Figure 6b) were also probably due to the presence of two different forms of α -tubulin (Figure 6c), and not because two cross-linking sites were internal to the subtilisin cleavage site on α -tubulin. Although the internal binding sites cannot be narrowed down to more specific regions with the subtilisin digestion approach, based on the involvement of acidic residues of tubulin in the Ncd tail interaction, it is very likely that the acidic clusters in the H11-H12 loop / H12 helix sequence on both monomers represent the other two Ncd tail binding sites.

There appear to be four binding sites on a tubulin dimer, two on each monomer, for Ncd tail proteins. One important consideration about the binding ratio of the Ncd tail proteins to tubulin is that the Ncd tail protein used in this study, NT6, exists as a monomer (9), but the full-length Ncd exists as a dimer. It may be possible for the monomeric Ncd tail proteins to fill all the possible binding sites on a tubulin dimer, but the constraint between the

two tail regions of an Ncd dimer may not allow the Ncd to fill all four sites on tubulin. Alternatively, the tail regions on a dimer may be flexible to allow each tail domain to interact with the C-termini of α - and β -tubulin and maintain 4:1 binding ratio. In the future, MT binding experiments with stalk-tail dimers of Ncd will help to better relate to *in vivo* interactions of Ncd and MTs. One other consideration is that due to intramolecular interactions between basic and proline rich regions, as suggested by the similarities to tau, the tail region of Ncd is likely to have a complex structure; hence, determination of 3D structure of the Ncd tail will help to elucidate the stoichiometric ratio of Ncd tail proteins to tubulin. Finally, site-directed mutations in the binding sites of the Ncd tail and in the C-terminal binding sites on tubulin may reveal critical amino acid residues in Ncd-MT interactions.

FIGURE 1: Amino acid sequences C-terminal domains of α - and β -tubulin.

The acidic residues of α - and β -tubulin are underlined. Possible subtilisin cleavage sites are located in the regions that are indicated by the lines between closed circles. H12 denotes helix 12 of α - and β -tubulin.

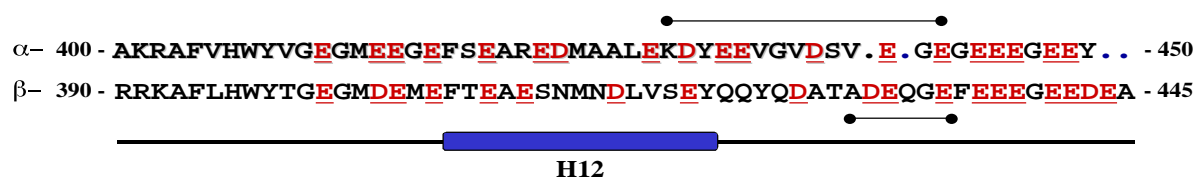


FIGURE 2: Cross-linking of NT6 to α -MTs.

NT6 (5-20 μ M) was mixed with α -MTs (5 μ M tubulin) in AB buffer in the presence of EDC and S-NHS at the indicated molar ratios of NT6 to α -MTs (1:1 - 4:1). After incubation at 22°C for 30 minutes, samples were separated on a 7% low grade SDS-polyacrylamide gel, and then stained with Coomassie blue. Control cross-linking reactions with α -MTs alone () and NT6 alone are shown. denotes the α -tubulin band and denotes the β -tubulin band. The bracket indicates the α -MTs-NT6 cross-linked products. The cross-linked products of α -MTs are shown by an arrowhead.

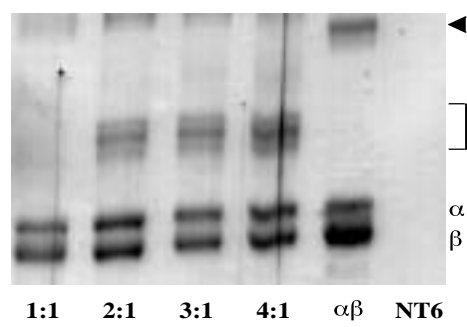


FIGURE 3: Western blot analysis of the α -MTs-NT6 cross-linked products.

Samples of an α -MTs-NT6 cross-linking reaction at 4:1 ratio were separated on a 7% low grade SDS-polyacrylamide gel and transferred to a nitrocellulose membrane for probing with antibodies against α -tubulin (DM1A), β -tubulin (18D6) and NT6. The α -tubulin band is indicated by α and the β -tubulin band is indicated by β . Arrows indicate the cross-linked products observed with α -tubulin, β -tubulin and NT6 antibodies. The more intense middle band (corresponding to the lower α -tubulin and upper β -tubulin bands) recognized by the NT6 antibody is indicated by an arrowhead.

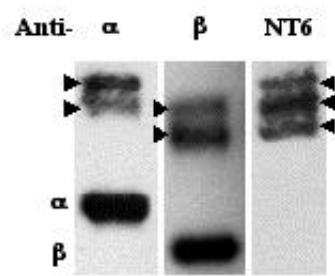


FIGURE 4: Binding affinity and stoichiometry of NT6 protein to MTs and subtilisin-digested-MTs.

NT6 (5-50 μ g) was incubated with α -MTs (5 μ M), β -MTs (2.9 μ M or 5 μ M) or β -s-s-MTs (2.63 μ M or 5 μ M) for 30 minutes at 22°C, then centrifuged to pellet MTs and bound NT6. Supernatant and pellet fractions were analyzed by tricine-PAGE and the amount of NT6 protein in each fraction was determined (see Materials and Methods). The data obtained for bound NT6/tubulin (α , β or β -s-s) and unbound NT6 were plotted and fit with a rectangular hyperbola to determine the affinity (K_d) and stoichiometry (B_{max}) values (see table). For comparison, previously reported data points for α -MTs are indicated by squares in the graph. Data points for β -, β -s- and β -s-s in this study are indicated by circles, diamonds and triangles, respectively. In the table, * represents the previously reported data (reference 9) for NT6 binding to α -MTs.

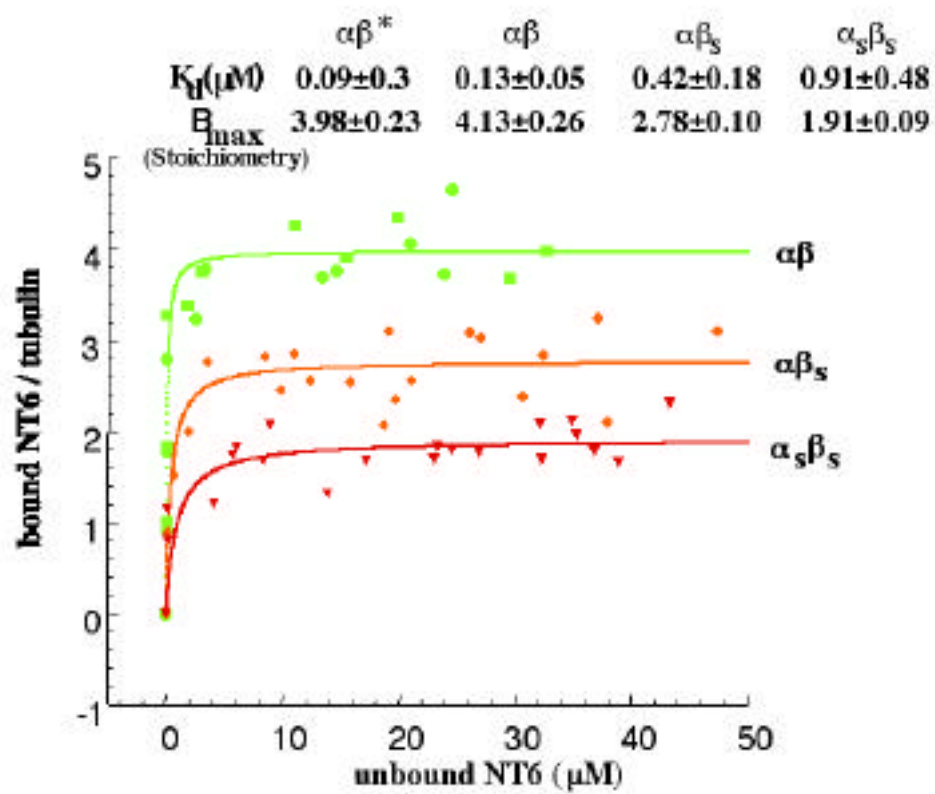


FIGURE 5: Western blot analysis of α - and/or β -tubulin C-terminal fragment-NT6 cross-linked products.

NT6 (50 μ M) was mixed with the subtilisin-produced C-terminal fragments of α - and/or β -tubulin in cross-linking reactions (see Materials and Methods). Samples were separated on a 15% tricine gel and transferred to a nitrocellulose membrane for probing with an antibody against NT6. α_s denotes the C-terminal fragment obtained from subtilisin digestion of α -tubulin and β_s denotes the C-terminal fragments obtained from subtilisin digestion of both α - and β -tubulin. NT6 cross-linking in the absence of C-terminal tubulin fragments (-) is also shown. The cross-linked products are indicated by an arrow.

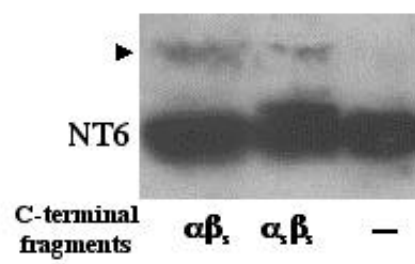
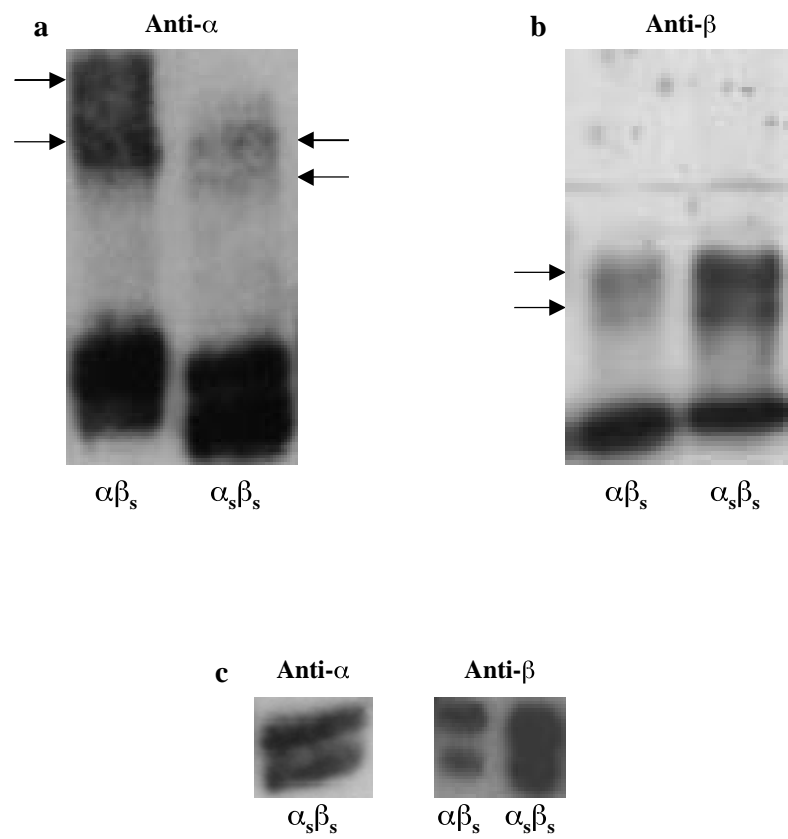


FIGURE 6: Western blot analysis of the subtilisin-digested-MTs and subtilisin-digested-MTs-NT6 cross-linked products.

20 μ M NT6 was mixed with α - or β -MTs (5 μ M tubulin) in AB buffer containing 2 mM EDC and 5 mM S-NHS. After a 30 minute incubation at 22°C, samples were separated on low grade SDS-polyacrylamide gels were mixed with and processed for western blot analysis. Panel a: α - or β -MT-NT6 cross-linked samples (transferred from a 7% low grade SDS-polyacrylamide gel) probed with an anti- α -tubulin antibody (DM1A). Panel b: α - or β -MT-NT6 cross-linked samples (transferred from a 6.5% low grade SDS-polyacrylamide gel) probed with an anti- β -tubulin antibody (18D6). Panel c: α - and β -MT samples (transferred from a 7.5% low grade SDS-polyacrylamide gel) probed with anti- α (DM1A) and/or anti- β (18D6) tubulin antibodies. α - or β -MT-NT6 cross-linked products are indicated by arrows.



LITERATURE CITED

1. Endow, S. A., Henikoff, S., & Soler-Niedziela, L. (1990) *Nature* 345, 81-83.
2. McDonald, H. B., & Goldstein, L. S. B. (1990) *Cell* 61, 991-1000.
3. Hatsumi, M., & Endow, S. A. (1992) *J. Cell Sci.* 103, 1013-1020.
4. Endow, S. A. (1993) *TIG* 9, 52-55.
5. Matthies, H. J. G., McDonald, H. B., Goldstein, L. S. B., & Theurkauf, W. E. (1996) *J. Cell Biol.* 134, 455-464.
6. Endow, S. A., & Komma, D. J. (1997) *J. Cell. Biol.* 137, 1321-1336.
7. Walker, R. A., Salmon, E. D., & Endow, S. A. (1990) *Nature* 347, 780-782.
8. McDonald, H. B., Stewart, R. J., & Goldstein S. B. (1990) *Cell* 63, 1159-1165.
9. Karabay, A., & Walker, R. A. (1999) *Biochemistry* 38, 1838-1849.
10. Goode, B., Denis, P. E., Panda, D., Radeke, M. J., Miller, H. P., Wilson, L., & Feinstein, S. C. (1997) *Mol Cell Biol.* 8, 353-365.
11. Karabay, A., & Walker, R.A. (1999) *Biochem. Biophys. Res. Com.* 258, 39-43.
12. Chau, M-F., Radeke, M. J., Ines, de C., Barasoain, I., Kohlstaedt, L. A. & Feinstein, S. C. (1998) *Biochemistry* 37, 17692-17703.
13. Serrano, L., Avila, J., & Maccioni, R. B. (1984) *Biochemistry* 23, 4675-4681.
14. Serrano, L., Montejo de Garcini, E., Hernandez, M. A., & Avila, J. (1985) *Eur. J. Biochem.* 153, 595-600.
15. Marya, P. K., Syed, Z., Fraylich, P. E., & Eagles, P. A. (1994) *J. Cell Sci.* 107, 339-344.
16. Melki, R., Kerjan, P., Waller, J. P., Carlier, M. F., & Pantoloni, D. (1991) *Biochemistry* 30, 11536-11545.
17. Saoudi, Y., Paintrand, I., Multigner, L., & Didier, J. (1995) *J. Cell Sci.* 108, 357-367.
18. Schagger, H., & Jagow, G. V. (1987) *Anal. Biochem.* 166, 368-379.
19. Theodorakis, N. G., & Cleveland, D. W. (1992) *Mol. Cell Biol.* 12, 791-799.
20. Lobert, S., & Correia, J. J. (1992) *Arch. Biochem. Biophys.* 296, 152-160.
21. Lobert, S., Bettye, S. H., & J. Correia (1993) *Cell Motil. Cytoskeleton* 25, 282-297.
22. Redeker, V., Melki, R., Prome, D., Le Caer, J. P., & Rossier J. (1992) *FEBS Lett.* 313, 185-192.
23. Maccioni, R. B., Serrano, L., Avila, J., & Cann, J. R (1986) *Eur. J. Biochem.* 156, 375-381.
24. De La Vina, S., Andreu, D., Medrano, F. J., Nieto, J. M., and Andreu J. M. (1988) *Biochemistry* 27, 5352-5365.
25. Paschal, B. M., Obar, R. A., & Vallee, R. B. (1989) *Nature* 342, 569-572.
26. Gundersen, G. G., Kalnoski, M. H., & Bulinski, J. C. (1984) *Cell* 38, 779-789.
27. Grimm, M., Breitling, F., & Little, M. (1987) *Biochim. Biophys. Acta* 914, 83-88.

CHAPTER 5

CONCLUSION

CONCLUSION

Based on the high homology to the kinesin head domain, Ncd has been known to contain an ATP-dependent MT binding site (residues 516-668) in the tail domain. Abnormal chromosome distribution in mutant oocytes and embryos and immunolocalization of Ncd to the meiotic and early mitotic spindle implicated a role for the Ncd as a spindle motor. These results suggested that the Ncd motor possess a second MT interaction site that may be involved in bundling of MTs during spindle formation, and perhaps in sliding MTs past each other. Since the tail region of the Ncd motor does not contain an ATP binding site, the MT binding site in tail domain has been thought to function in an ATP-independent manner. In this project, interactions of the Ncd tail domain with cargo MTs were further analyzed and the results indicated that there are two ATP-independent MT interaction sites located in the tail region: one in amino acid region 83-100 and the other in amino acid region 115-187.

Characterization of ATP-independent MT binding sites of the tail region revealed structural and functional similarities of the Ncd tail to MAPs, especially tau and MAP2. Like tau MT-binding motifs, the MT binding sites in the tail domain are rich in basic and proline amino acids. The Ncd tail can also promote MT assembly and stability by binding to acidic clusters located at the extreme C-termini and H11-H12 loop / H12 helix sequences of α - and β -tubulin. These results suggest that in addition to its minus end-directed motor activity, Ncd is involved in maintenance of spindle assembly. Through the action of ATP-dependent and ATP-independent MT binding sites in the head and tail domains, respectively, Ncd has been thought to cross-link MTs as it moves towards the MT minus ends, the focusing activity needed for spindle pole formation. Ncd mutant oocytes displaying spindle pole defects that include diffuse or multiple poles are consistent with the idea that the Ncd motor is required for spindle pole formation.

While there has been considerable advancement made towards the characterization of the Ncd in recent years, there are still many questions waiting to be answered about the regulation of the Ncd functions. What happens to the Ncd motor upon completion of the meiotic and mitotic divisions remains unknown. Is it degraded or regulated by post-translational modifications? Are there light chains associated with the tail domain, as in the case for the conventional kinesin, that regulate the interactions of Ncd with cargo MTs?

Understanding how Ncd performs its cellular functions and how these functions are regulated will be relevant for understanding other motor proteins that are involved in meiosis and mitosis, and ultimately will contribute to our understanding of cell cycle regulation.

ARZU KARABAY

115 Mateer Circle Blacksburg, Virginia-USA 24060
(H): 540-552 8316 (W): 540-231 4828 (F): 540-231 9307
e-mail: akarabay@vt.edu

PERSONAL Birth date: June 19, 1971
Place of birth: Istanbul, Turkey

EDUCATION

August 1995-present Virginia Polytechnic Institute and State University
Biology Department
Molecular Cell Biology and Biotechnology Program
Ph.D. candidate

Spring 1995 University of Iowa College of Medicine
Department of Pathology
Medical Microbiology Division
M.S. program

Summer-Fall 1994 University of Iowa
Microbiology Department
Special study

Fall 1992-Fall 1993 University of Istanbul
Cerrahpasa Medical Faculty, Institute of Health Sciences
Biomedical Sciences Department
M.Sc. program

1988-1992 University of Istanbul
Cerrahpasa Medical Faculty
Biomedical Sciences Department
B.Sc., graduated with the best degree, GPA 94 /100

PROFESSIONAL EXPERIENCE

Teaching Assistant, Virginia Polytechnic Institute and State University

1999 Fall **General Microbiology**

1999 Spring **General Microbiology**

1997 Spring **Principles of Biology**

1997 Spring **General Biology**

Research Assistant, University of Istanbul, Cerrahpasa Medical Faculty

1993 Spring-Fall **Biophysics Department**

PUBLICATIONS

Journal Publications

Identification of Microtubule Binding Sites in the Ncd Tail Domain

A. Karabay and R. A. Walker

Biochemistry, 38 (6), 1838-1849 (1999)

The Ncd Tail Domain Promotes Microtubule Assembly and Stability

A. Karabay and R. A. Walker

Biochemical and Biophysical Research Communications, 258, 39-43 (1999)

Manuscripts in preparation

The Ncd Tail Interacts with both α - and β -tubulin

Karabay and R. A. Walker

will be submitted to **Biochemistry**

Meeting Publications

A Liquid Handling Station to Rapidly Assemble Reagents and Sample Loading for
DNA Amplification by PCR

Werner W. Wilke, **Arzu Karabay**, Ronald N. Jones and Larry D. Sutton

Proceedings of the International Symposium on Laboratory Automation and
Robotics, 664-674 (1995)

Meeting Abstracts

The Ncd Tail Domain Interacts with Both α - and β -Tubulin

A. Karabay and R. A. Walker

Molecular Biology of the Cell, Volume 10, 251a (1999)

Identification of Microtubule Binding Sites in the Ncd Tail Domain

A. Karabay and R. A. Walker

Meeting Booklet, Abstract 28, 1999

15th Annual Research Symposium of the Graduate Student Assembly at Virginia Polytechnic Institute and State University

Identification of Microtubule Binding Sites in the Ncd Tail Domain

A. Karabay and R. A. Walker

Molecular Biology of the Cell, Volume 9, 29a (1998)

Ncd Tail Domain Binding to Microtubules

A. Karabay and R. A. Walker

Meeting Booklet, Abstract 33, 1998

18th Annual Seminar of Cancer Researchers in Virginia

Ncd Tail Domain Binding to Microtubules

A. Karabay and R. A. Walker

Molecular Biology of the Cell, Volume 8, 259a (1997)

Ncd Tail Domain Binding to Microtubules

A. Karabay and R. A. Walker

Virginia Journal of Science, Volume 48 (2), 85 (1997)

Ncd Tail Domain Binding To Microtubules

A. Karabay and R. A. Walker

Meeting Booklet, Abstract 58, 1997

13th Annual Research Symposium of the Graduate Student Assembly at Virginia
Polytechnic Institute and State University

MEETINGS ATTENDED WITH SCIENTIFIC PRESENTATIONS

Platform Presentations

March 1998	18th Annual Meeting of American Cancer Society (Regional) Virginia Chapter March 14, 1998 Blacksburg, VA Ncd Tail Domain Binding To Microtubules
------------	---

Poster Presentations

December 1999	39th American Society for Cell Biology Annual Meeting (International) December 11-15, 1999 Washington, D.C. Identification of Microtubule Binding Sites in the Ncd Tail Domain
March 1999	15th Annual Research Symposium (Local) Graduate Student Assembly at Virginia Polytechnic Institute and State University, March 29, 1999 Blacksburg, VA Identification of Microtubule Binding Sites in the Ncd Tail Domain
December 1998	38th American Society for Cell Biology Annual Meeting (International) December 12-16, 1998 San Francisco, CA Identification of Microtubule Binding Sites in the Ncd Tail Domain
December 1997	37th American Society for Cell Biology Annual Meeting (International) December 13-17, 1997 Washington, D.C. Ncd Tail Domain Binding To Microtubules
May 1997	75th Annual Meeting of the Virginia Academy of Science (Regional) May 21-23, 1997 Blacksburg, VA

Ncd Tail Domain Binding To Microtubules

April 1997 13th Annual Research Symposium (Local)
Graduate Student Assembly at Virginia Polytechnic Institute
and State University, April 28, 1997 Blacksburg, VA
Ncd Tail Domain Binding To Microtubules

MEETINGS ATTENDED WITHOUT PRESENTATIONS

Biotechnology 2001 Conference-2
June 24-26, 1999 Blacksburg, VA

Biotechnology 2001 Conference-1
June 26-27, 1998 Blacksburg, VA

International Symposium on Green-Fluorescent Protein
October 18-22, 1997 New Brunswick, New Jersey

AWARDS

Grant Awards

September 1999 Graduate Research Development Project
Graduate Student Assembly at Virginia Polytechnic Institute
and State University
\$250; Biology Department matched with \$250 (Total \$500)

August 1998 Graduate Research Development Project
Graduate Student Assembly at Virginia Polytechnic Institute
and State University
\$500; Biology Department matched with \$500 (Total \$1000)

July 1998 Grants-in-Aid of Research
Sigma Xi, the Scientific Research Society
\$537; Biology Department matched with \$500 (Total \$1037)

August 1997 Graduate Research Development Project

Graduate Student Assembly at Virginia Polytechnic Institute and State University

\$500; Biology Department matched with \$500 (Total \$1000)

December 1996

Grants-in-Aid of Research

Sigma Xi, the Scientific Research Society

\$495; Biology Department matched with \$500 (Total \$995)

Travel Awards

September 1999

ASCB Predoctoral Travel Award

awarded to attend the 39th American Society of Cell Biology Annual Meeting (International) on December 11-15, 1999
Washington, DC

\$350, Biology Department matched with \$100 (Total \$450)

September 1997

ASCB Predoctoral Travel Award

awarded to attend the 37th American Society of Cell Biology Annual Meeting (International) on December 13-17, 1997
Washington, DC

\$350

SCHOLARSHIPS

1994-1999

Higher Education Council of Turkey
to pursue a Ph.D. degree in Molecular Biology

1988-1993

Higher Education Council of Turkey
undergraduate and master of science scholarships

1988-1993

Alumni Association of Istanbul Kiz Lisesi (High School)
undergraduate and master of science scholarships

1985-1993

Emin Aktar Foundation, Istanbul-Turkey
high school, undergraduate and master of science scholarships

PROFESSIONAL MEMBERSHIPS

December 1998-present

American Physiological Society

August 1997-present	American Society for Cell Biology
May 1997-present	Virginia Academy of Science
May 1997-present	Sigma Xi, The Scientific Research Society

SOCIAL MEMBERSHIPS / ACTIVITIES

July 1998-present	Member, Alumni Association of Biomedical Scientists, University of Istanbul -Cerrahpasa Medical Faculty
May 1997-1998	President of the Turkish Student Association at Virginia Polytechnic Institute and State University
May 1996-1997	Member at large, Turkish Student Association at Virginia Polytechnic Institute and State University

OTHER PROFESSIONAL / SOCIAL ACTIVITIES

Workshop attended

December 13, 1997 “What They Never Taught You in the Graduate School:
Being an Effective Leader In The Laboratory”
American Society for Cell Biology 37th Annual
Meeting, Washington DC

Judge at the 75th Junior Virginia Academy of Science Meeting
May 21-23, 1997, Blacksburg, VA